Supplementary Material

Synthesis of tetramethoxy-(tetra-hydrazinecarboxamide) cyclophanes with unexpected conformation and investigation of their solution-phase recognition of chiral carboxylic guests using time-of-flight and tandem mass spectrometry

Hany F. Nour,*[a] Agnieszka Golon,[b] Tamer El Malah,[a] and Nikolai Kuhnert*[b]

[a] *National Research Centre, Department of Photochemistry, El Behoose Street, PO Box 12622, Cairo, Dokki, Egypt*

[b] *Jacobs University Bremen, School of Engineering and Science, Laboratory of Organic and Analytical Chemistry, D-28759, Bremen, Germany*

E-mail: *hany.nour@daad-alumni.de*, *n.kuhnert@jacobs-university.de*

Table of Contents

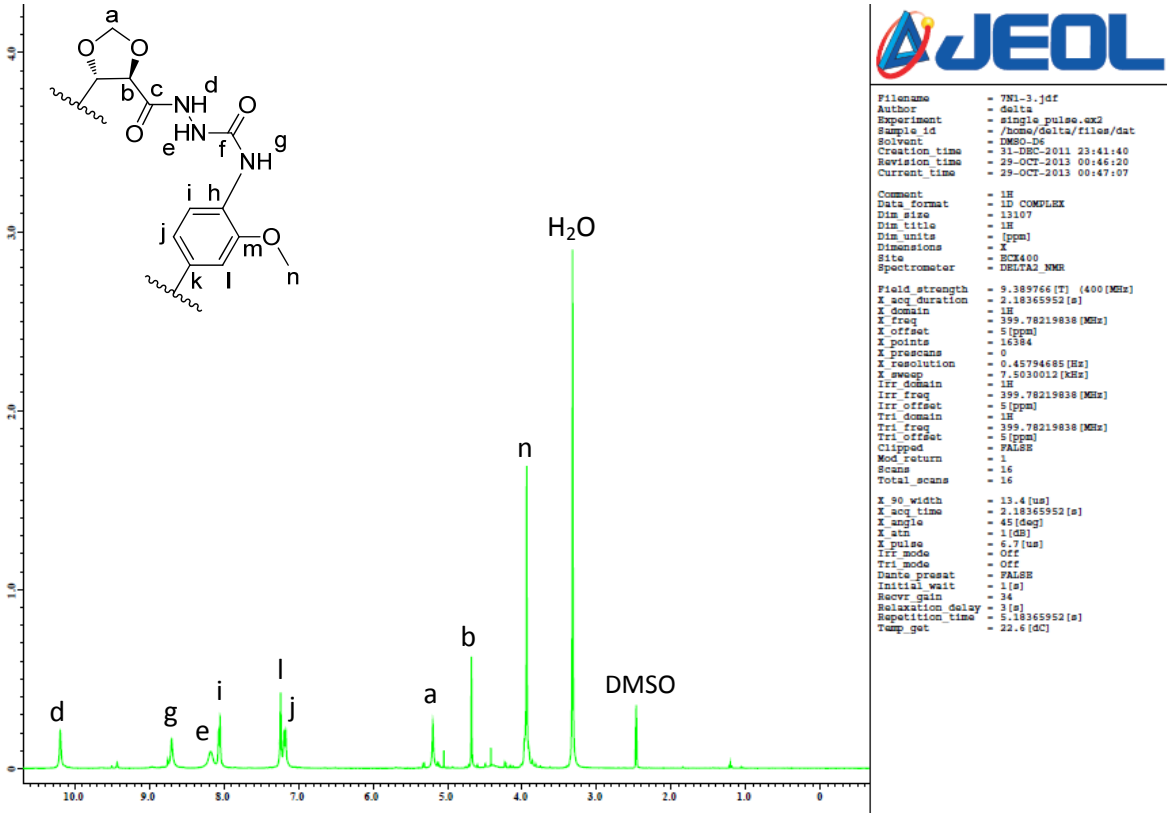

Figure 1. ^{1}H NMR spectrum of macrocycle (**9**) (400 MHz, DMSO-d_6).

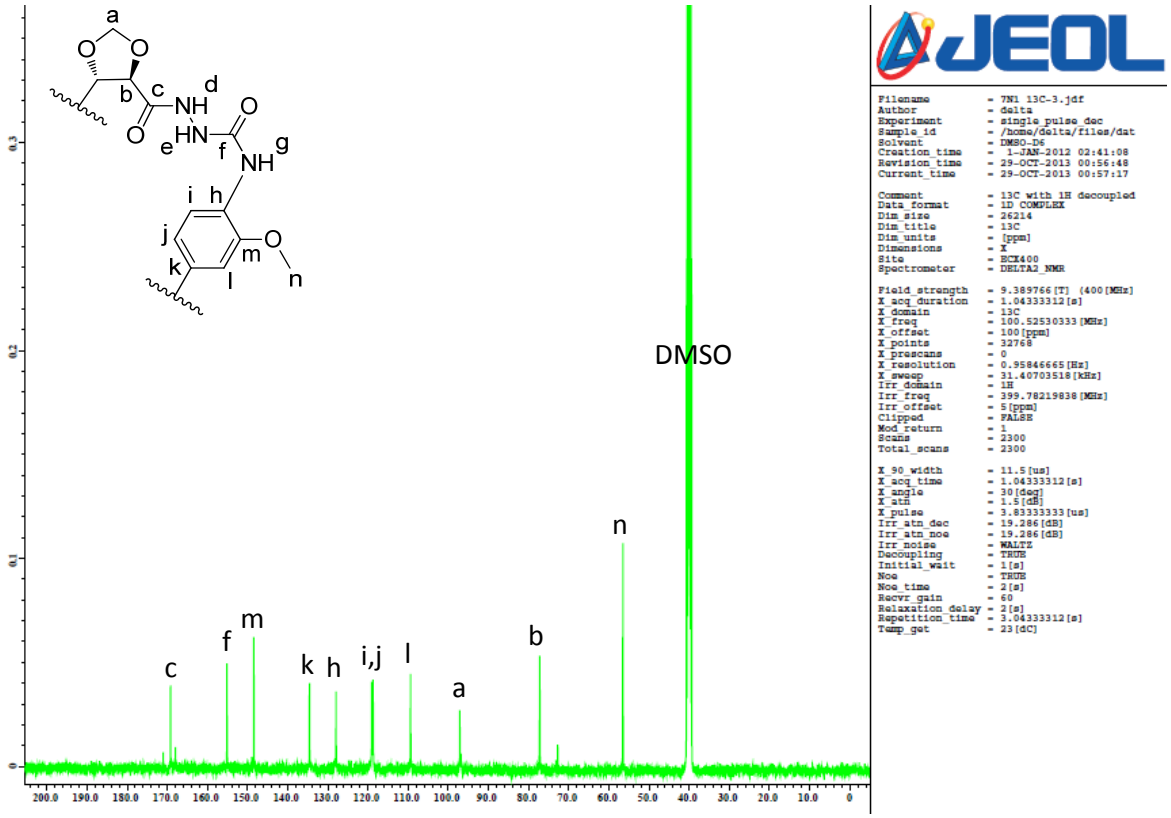

Figure 2. ^{13}C NMR spectrum of macrocycle (**9**) (100 MHz, DMSO-d_6).

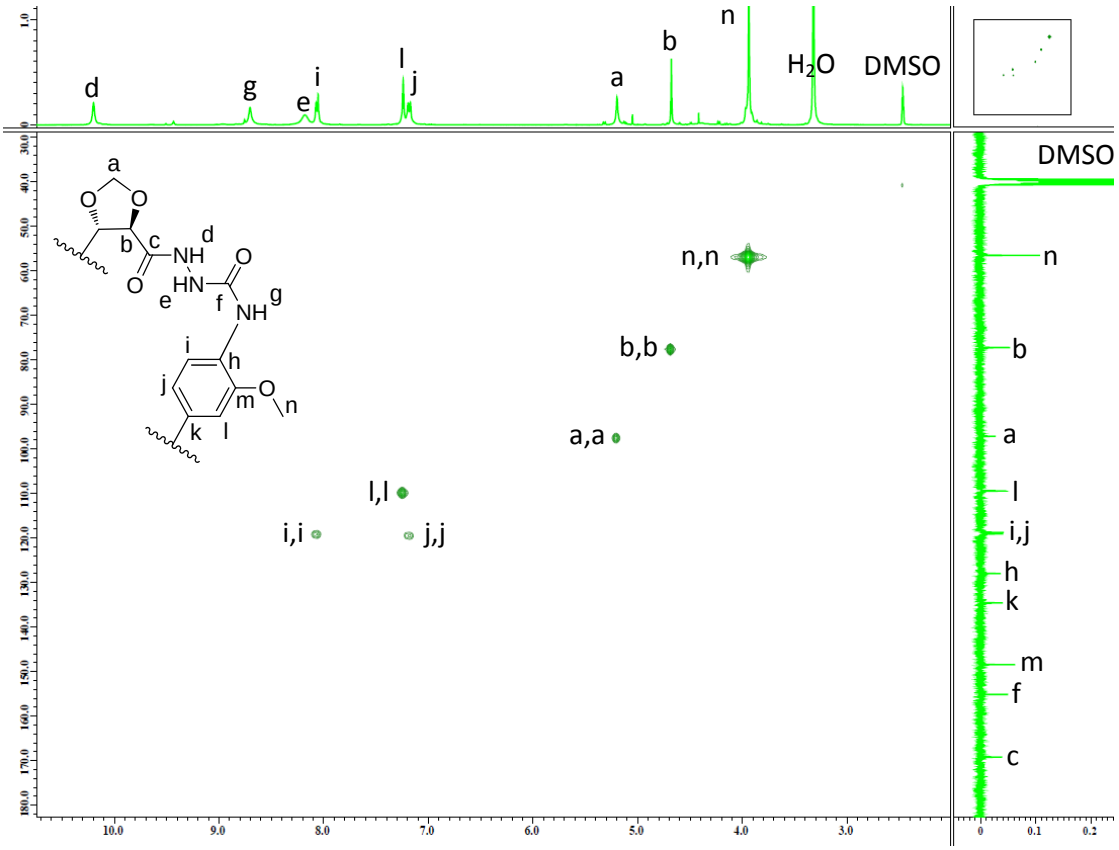

Figure 3. 2D HMQC spectrum of macrocycle (**9**) (DMSO-d_6).

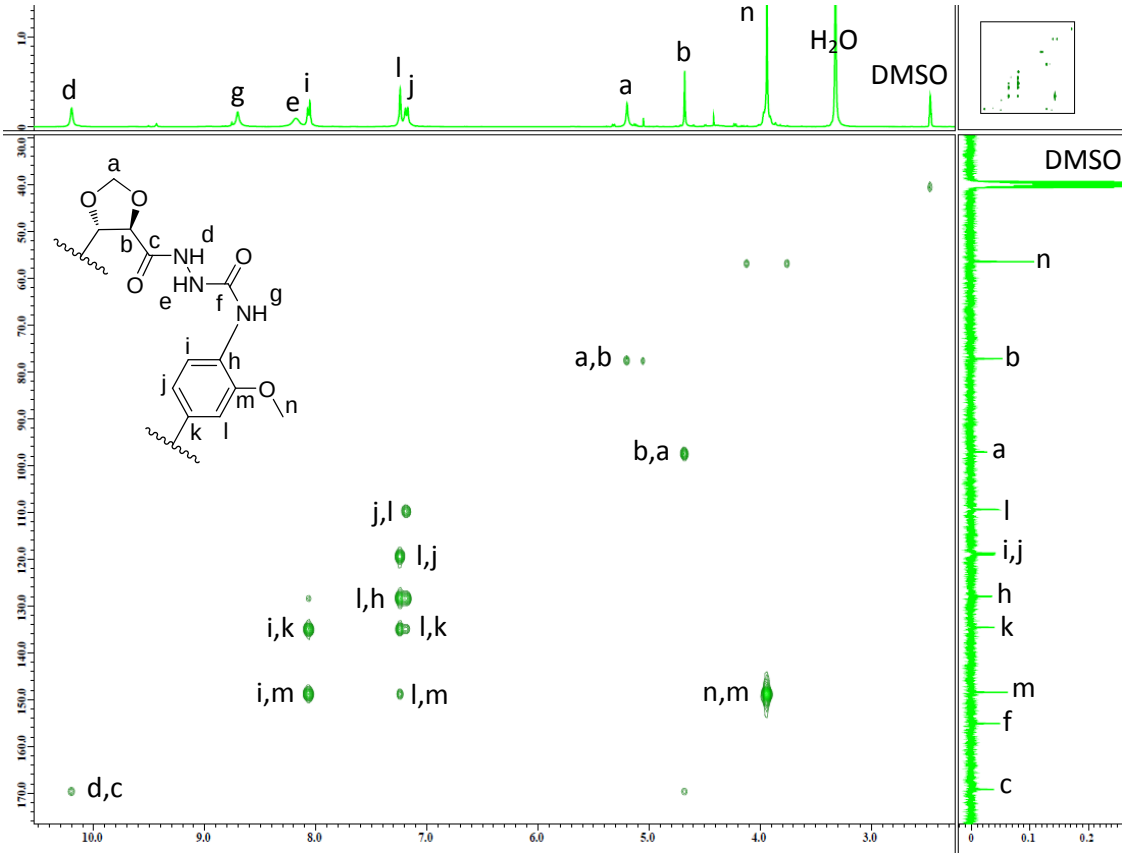

Figure 4. 2D HMBC spectrum of macrocycle (**9**) (DMSO-d_6).

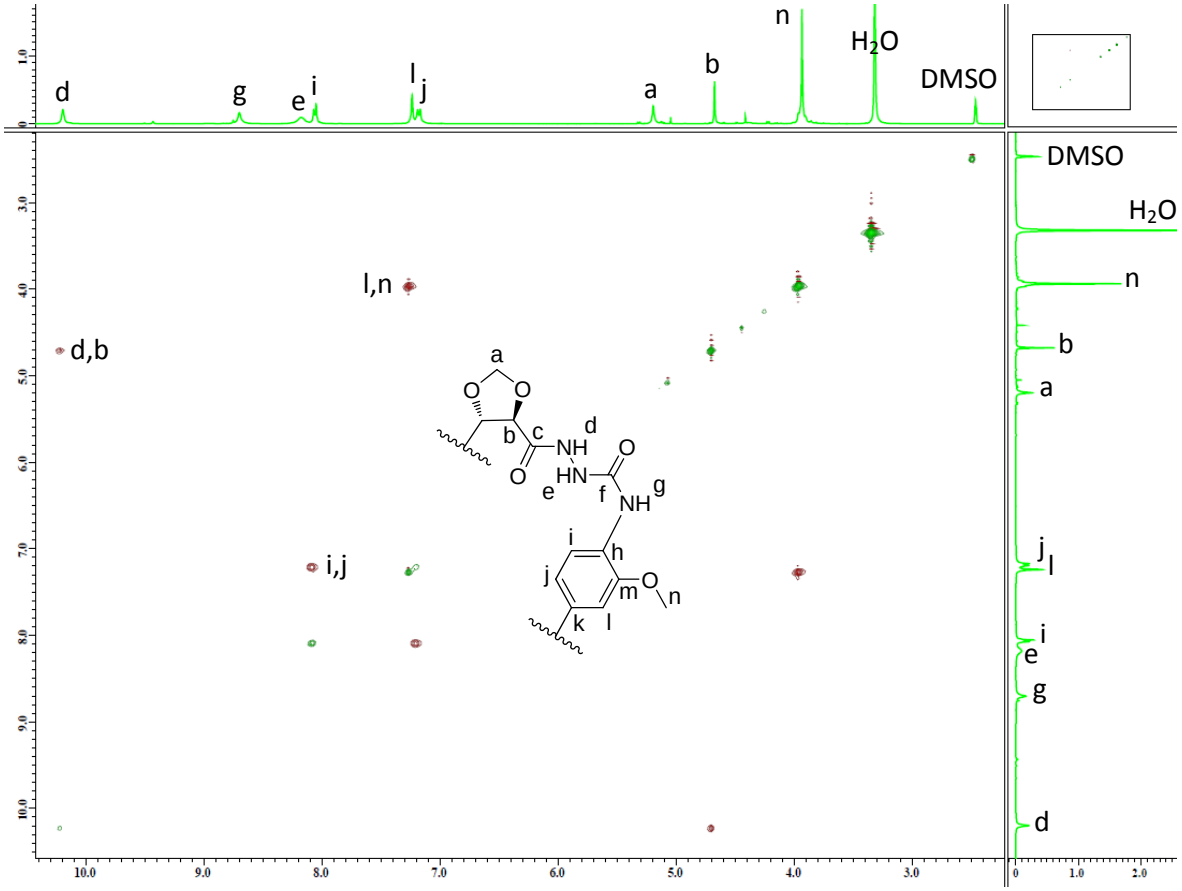

Figure 5. 2D ROESY NMR spectrum of macrocycle (**9**) (DMSO-d_6).

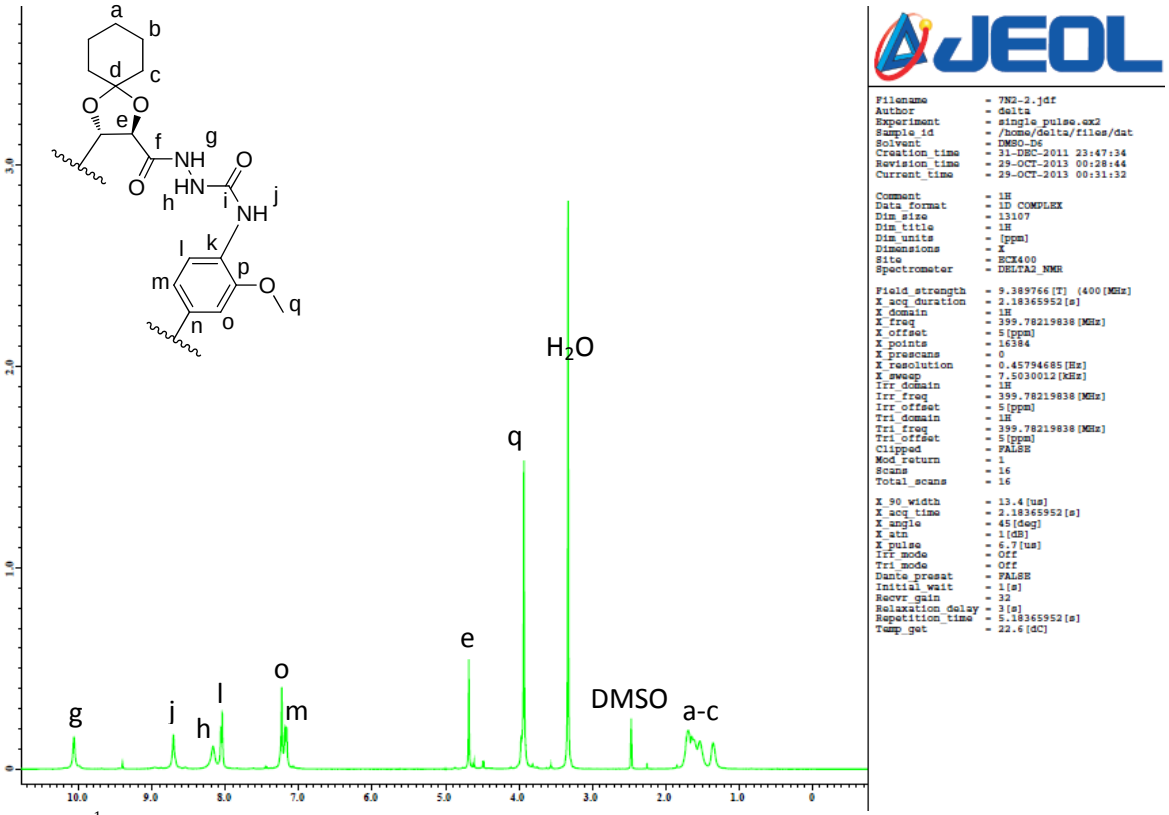

Figure 6. ^{1}H NMR spectrum of macrocycle (**10**) (400 MHz, DMSO-d_6).

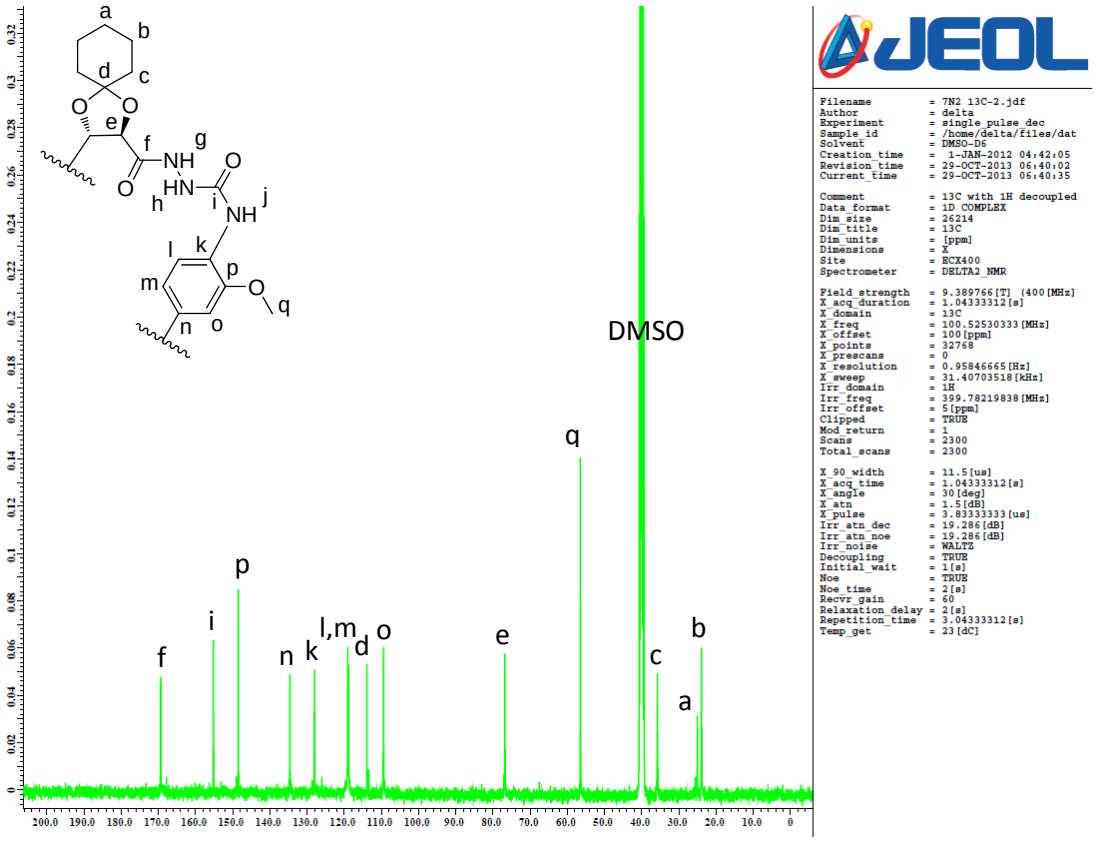

Figure 7. ^{13}C NMR spectrum of macrocycle (**10**) (100 MHz, DMSO-d_6).

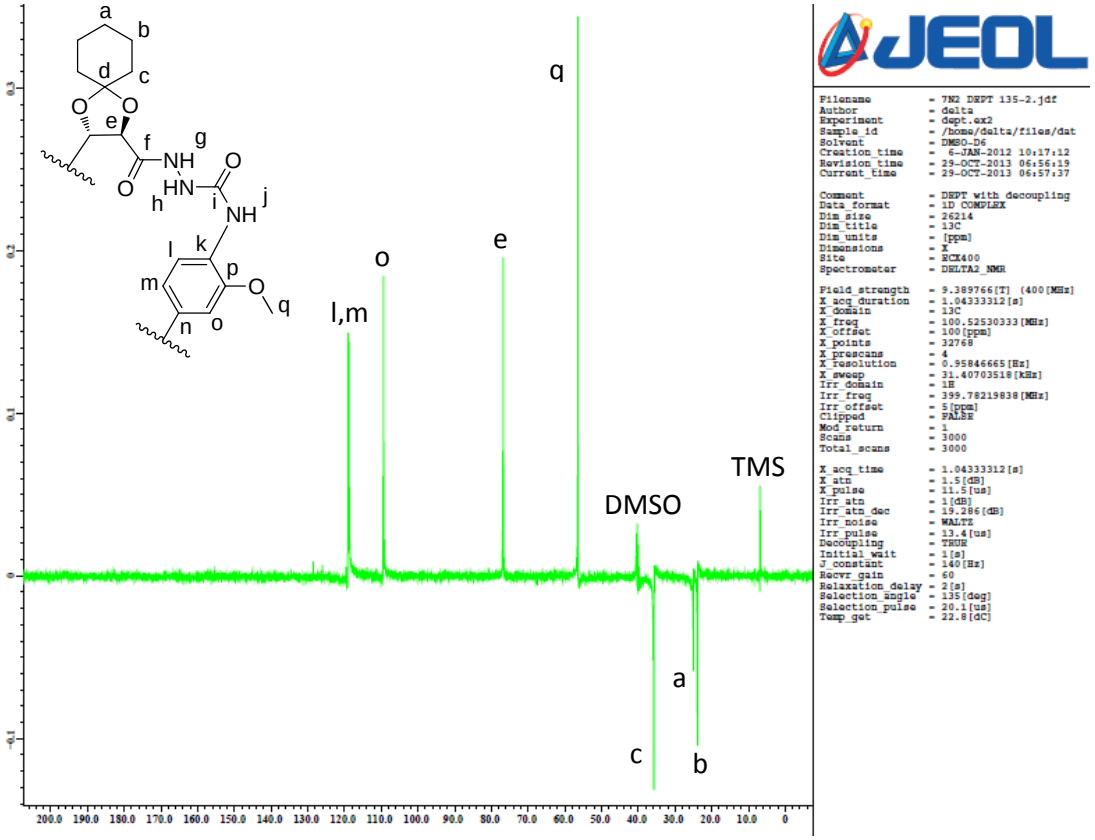

Figure 8. DEPT 135 spectrum of macrocycle (**10**) (DMSO-d_6).

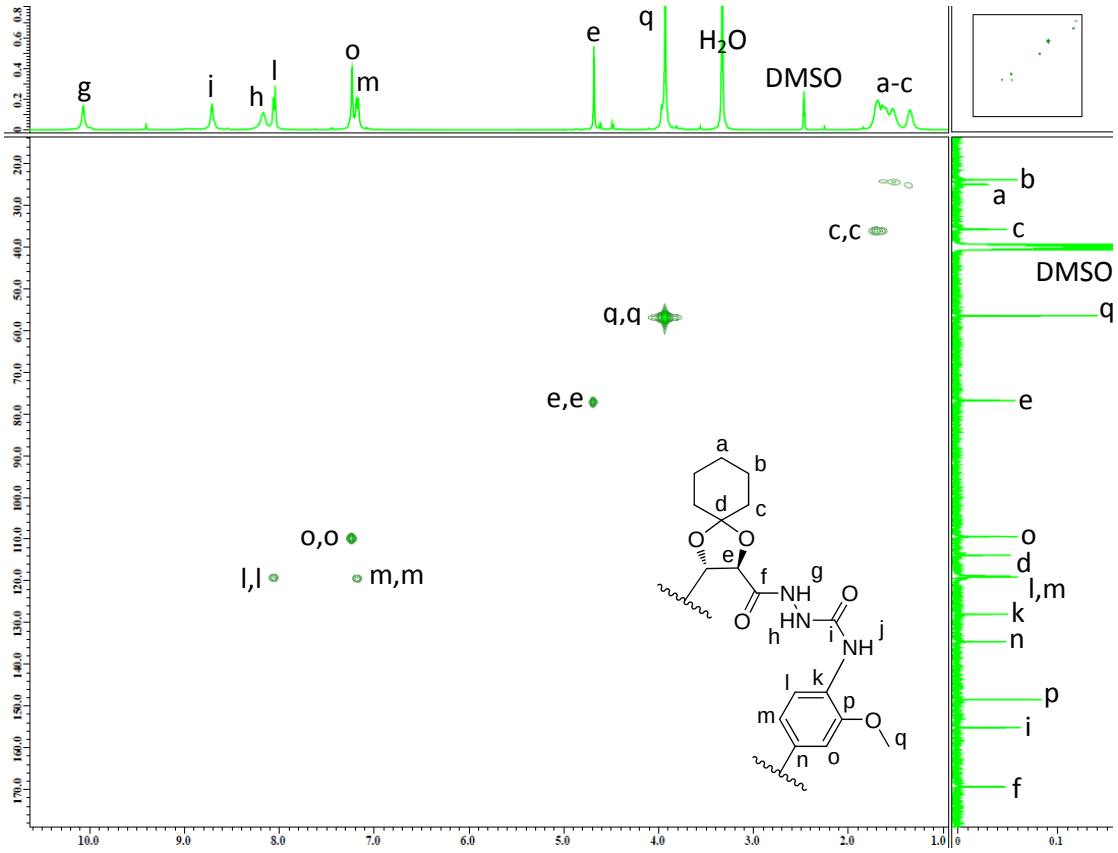

Figure 9. 2D HMQC spectrum of macrocycle (**10**) (DMSO-d_6).

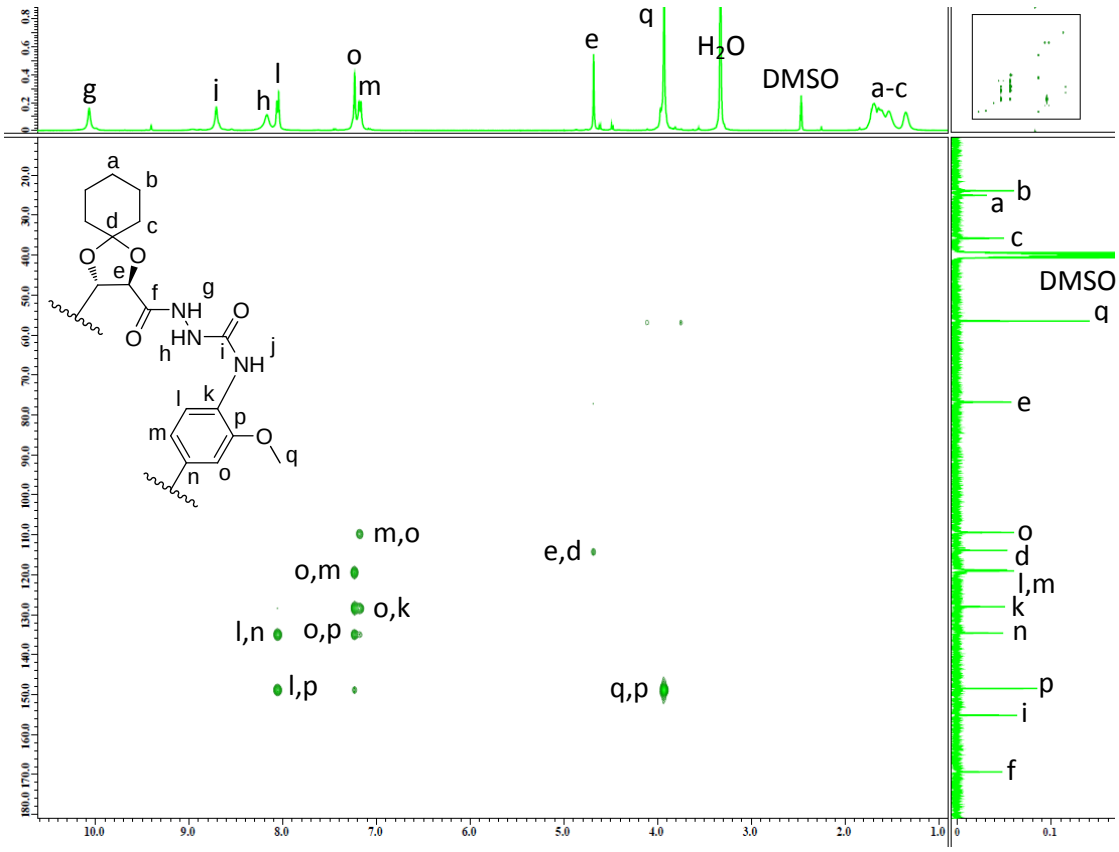

Figure 10. 2D HMBC spectrum of macrocycle (**10**) (DMSO-d_6).

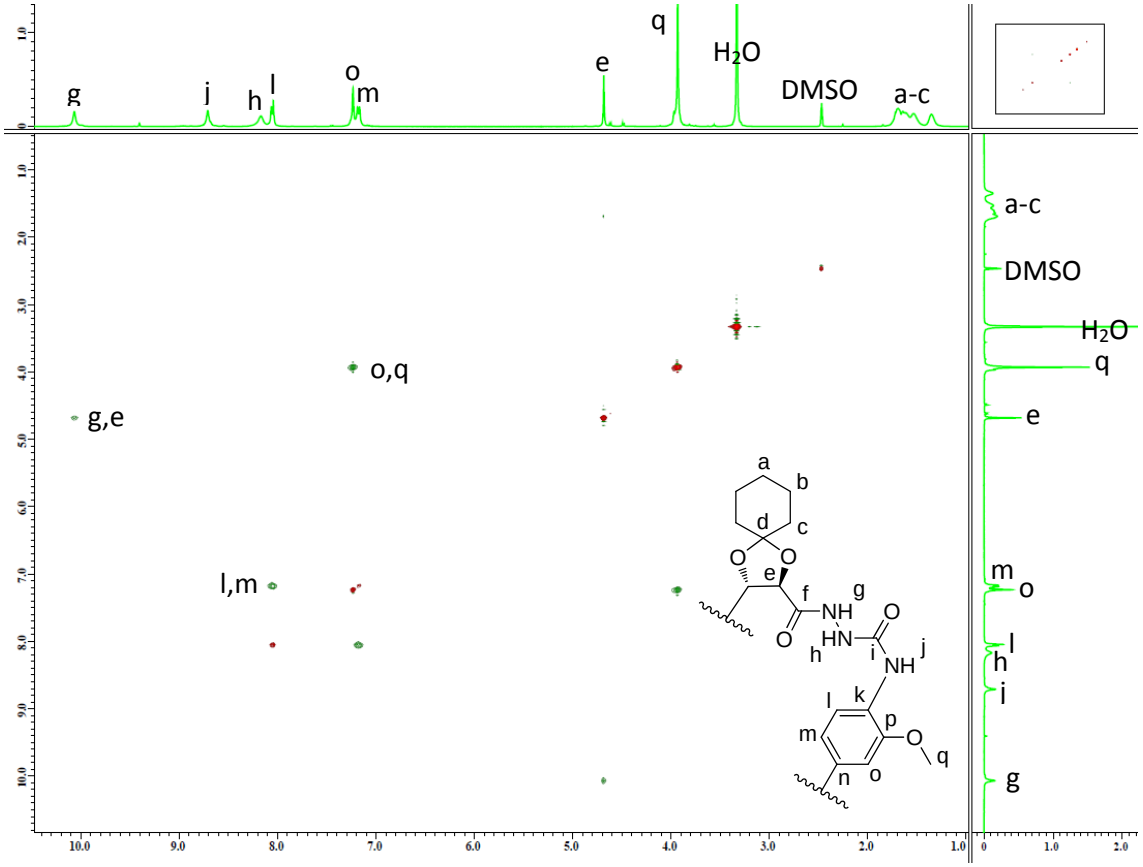

Figure 11. 2D ROESY NMR spectrum of macrocycle (**10**) (DMSO-d_6).

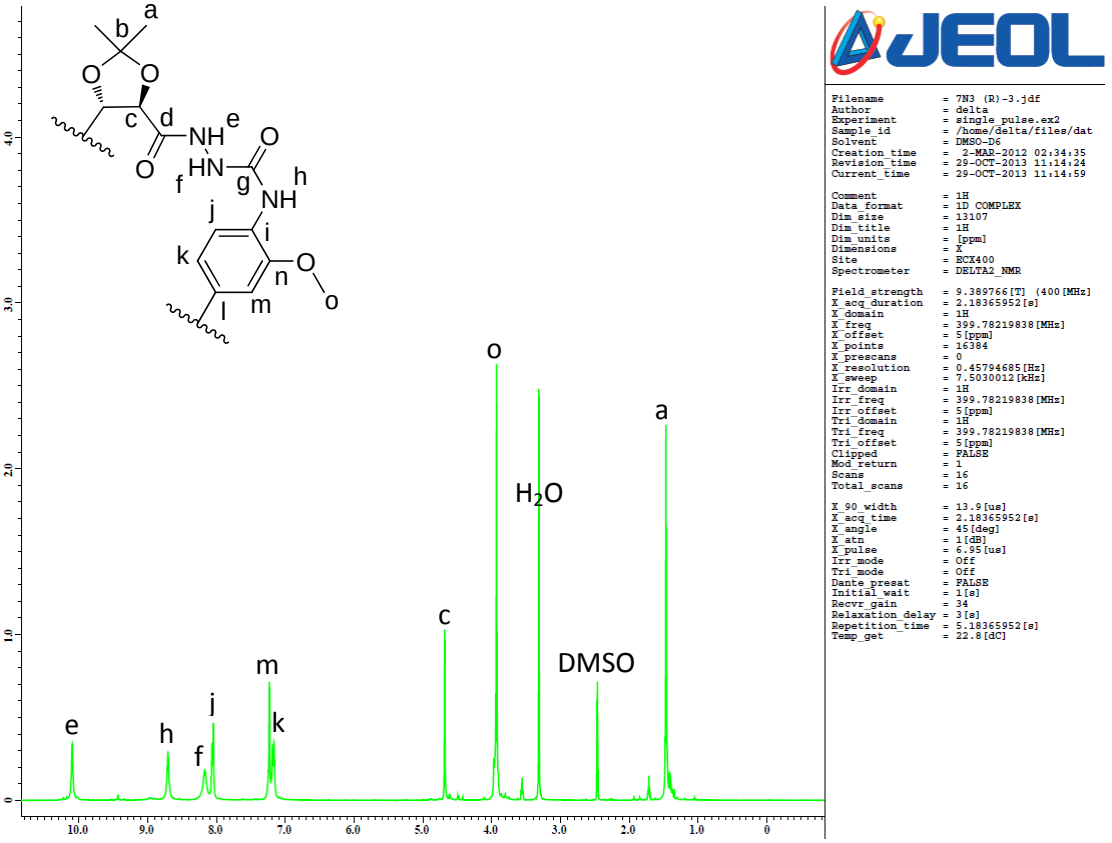

Figure 12. ^{1}H NMR spectrum of macrocycle (**11**) (400 MHz, DMSO-d_6).

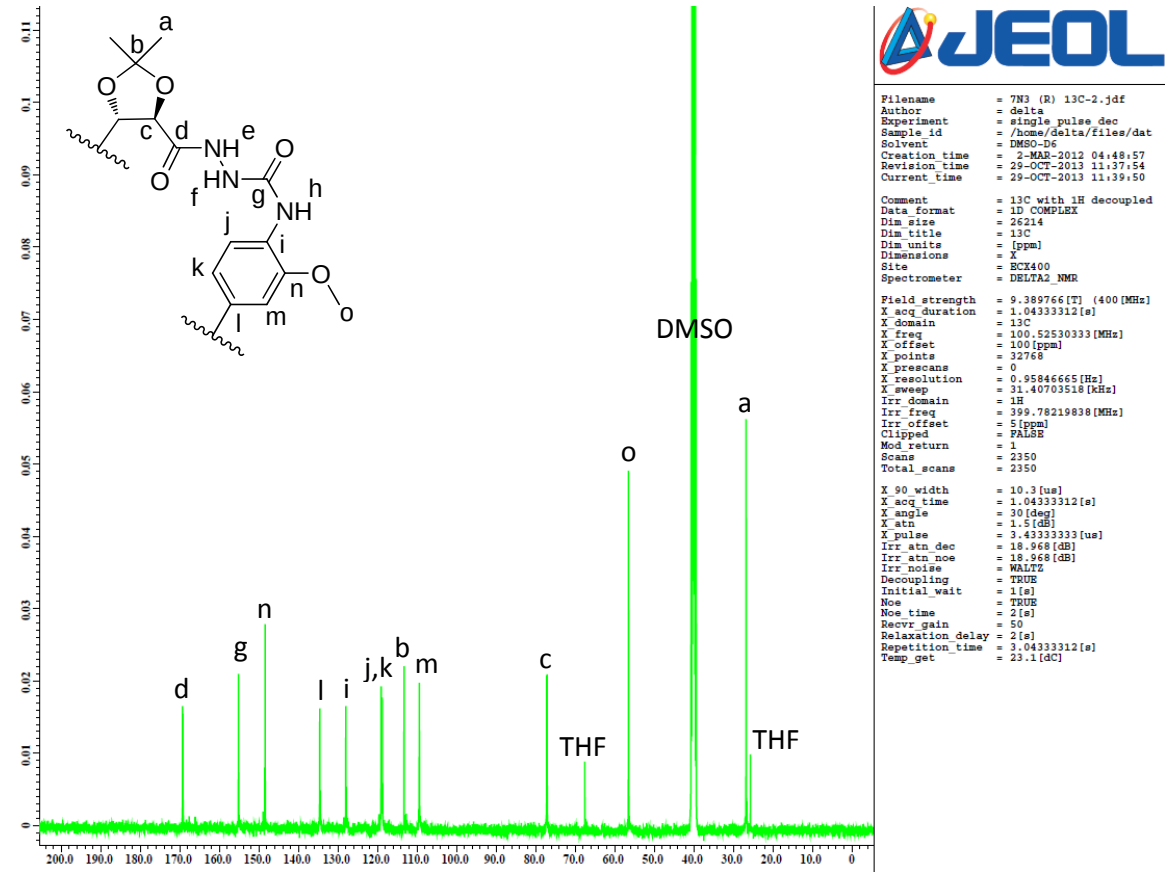

Figure 13. ^{13}C NMR spectrum of macrocycle (**11**) (100 MHz, DMSO-d_6).

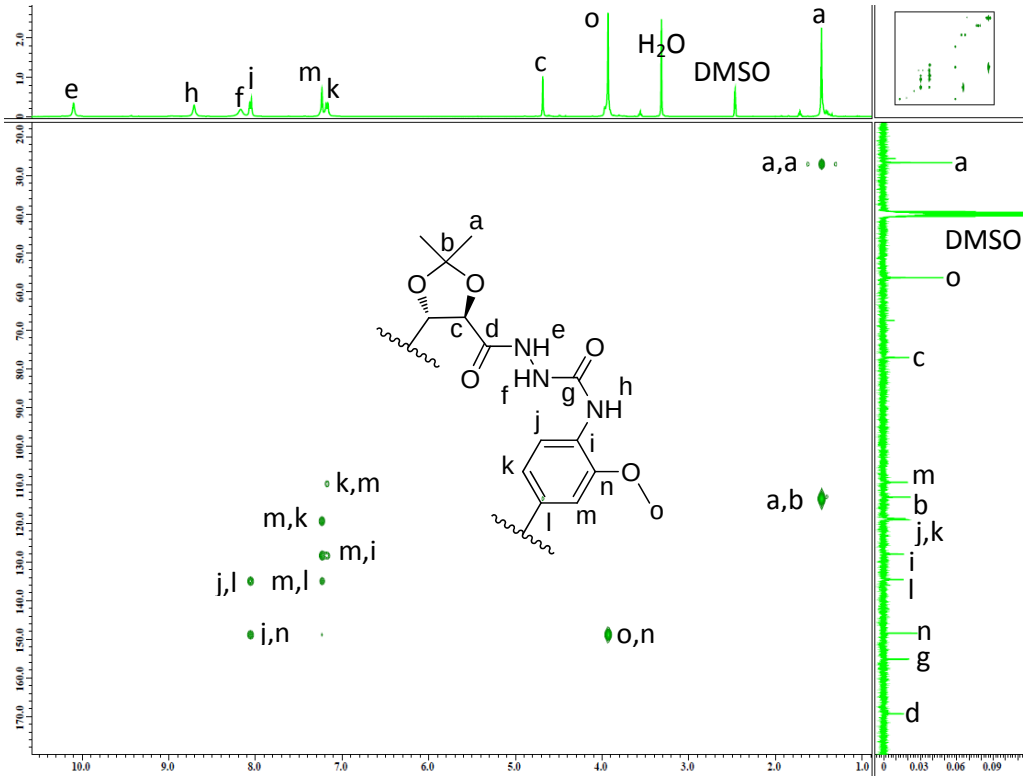

Figure 14. 2D HMBC spectrum of macrocycle (**11**) (DMSO-d_6).

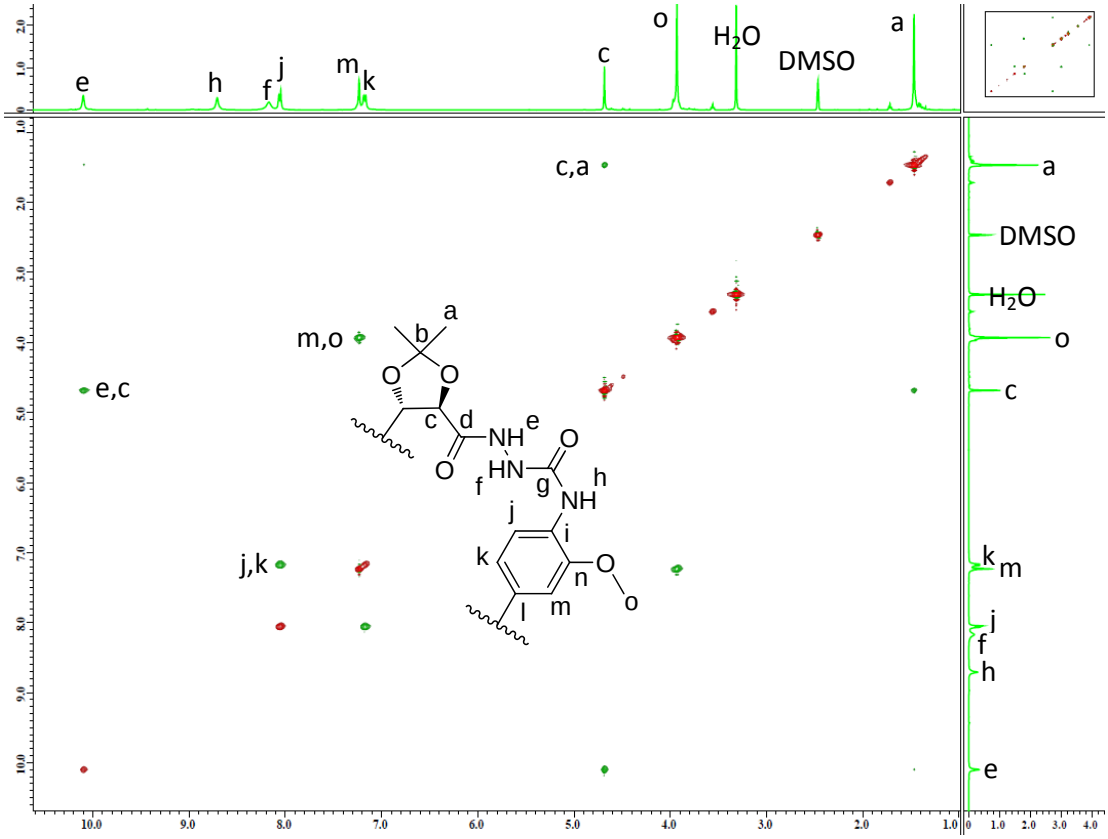

Figure 15. 2D ROESY NMR spectrum of macrocycle (**11**) (DMSO-d_6).

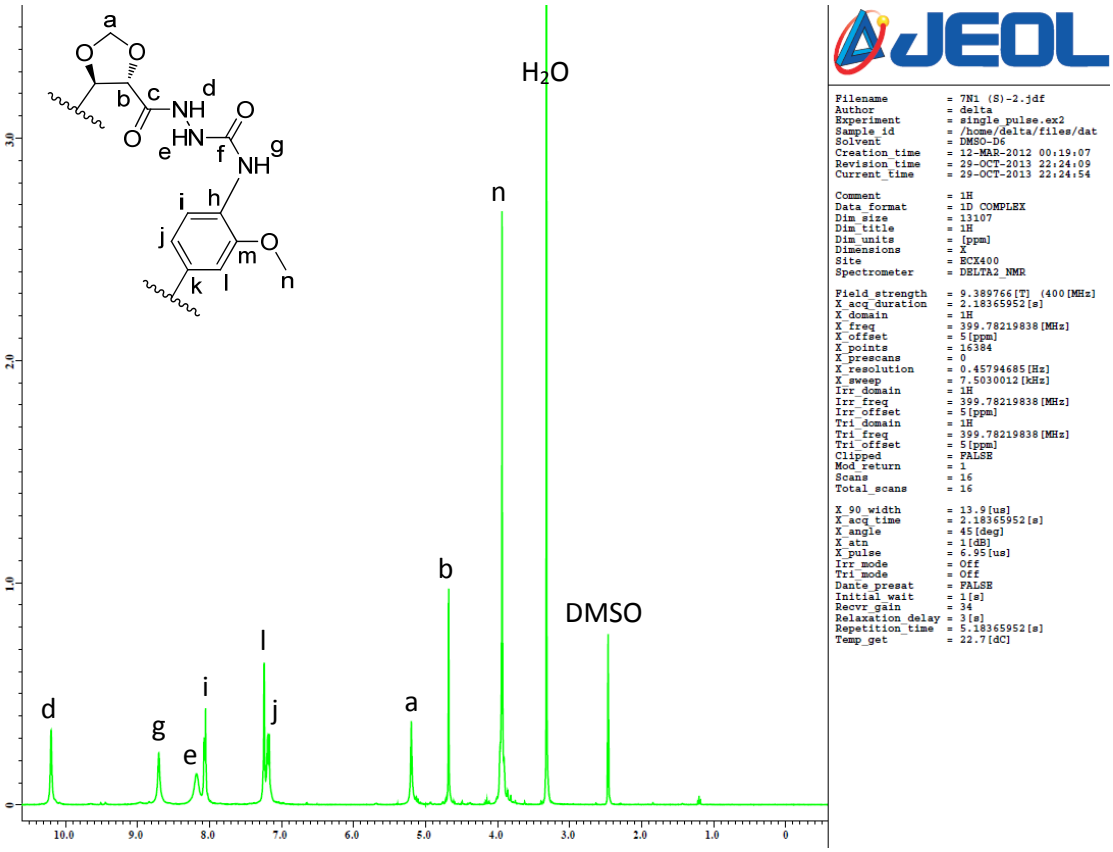

Figure 16. ^{1}H NMR spectrum of macrocycle (**12**) (400 MHz, DMSO-d_6).

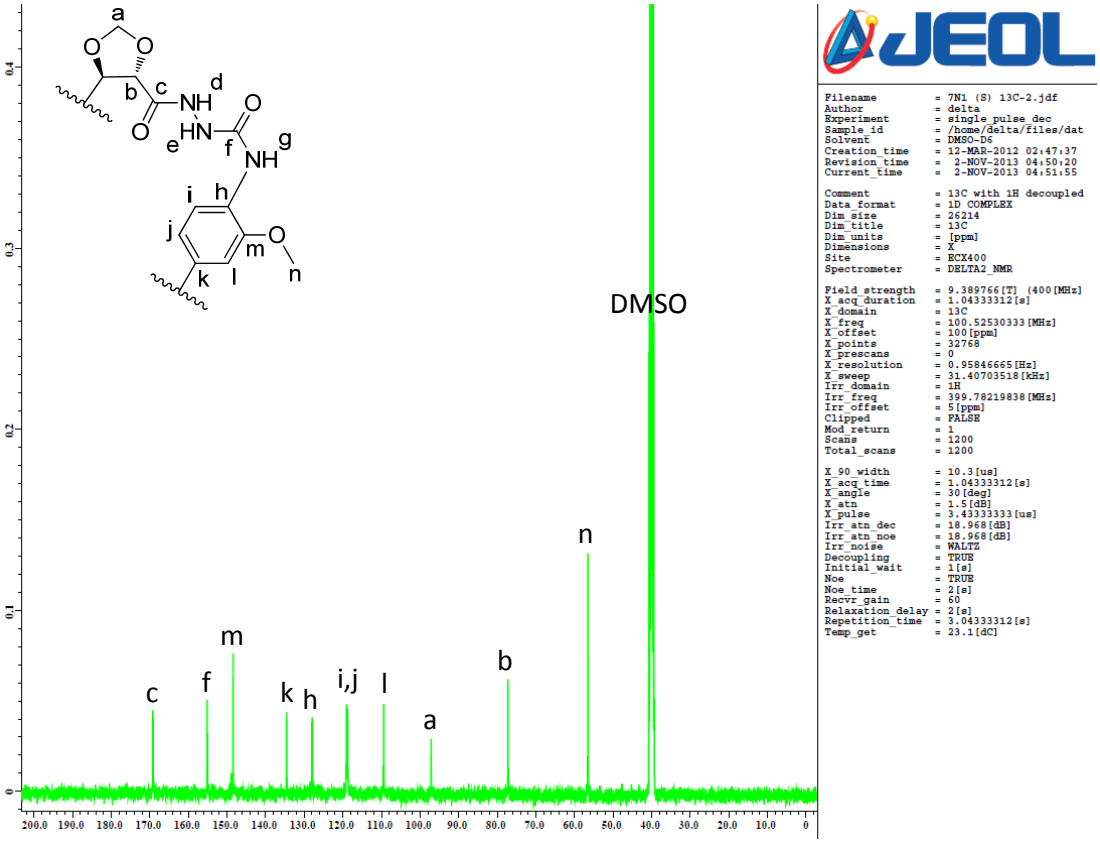

Figure 17. ^{13}C NMR spectrum of macrocycle (**12**) (100 MHz, DMSO-d_6).

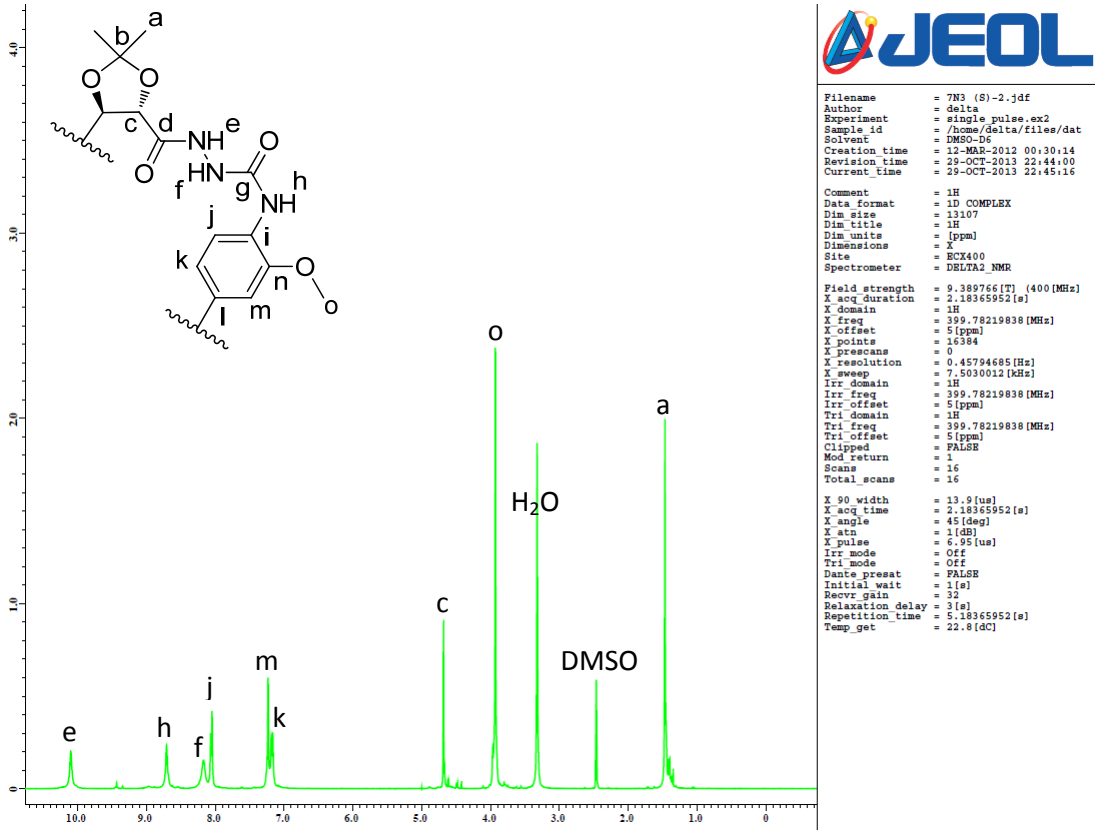

Figure 18. ^{1}H NMR spectrum of macrocycle (**13**) (400 MHz, DMSO-d_6).

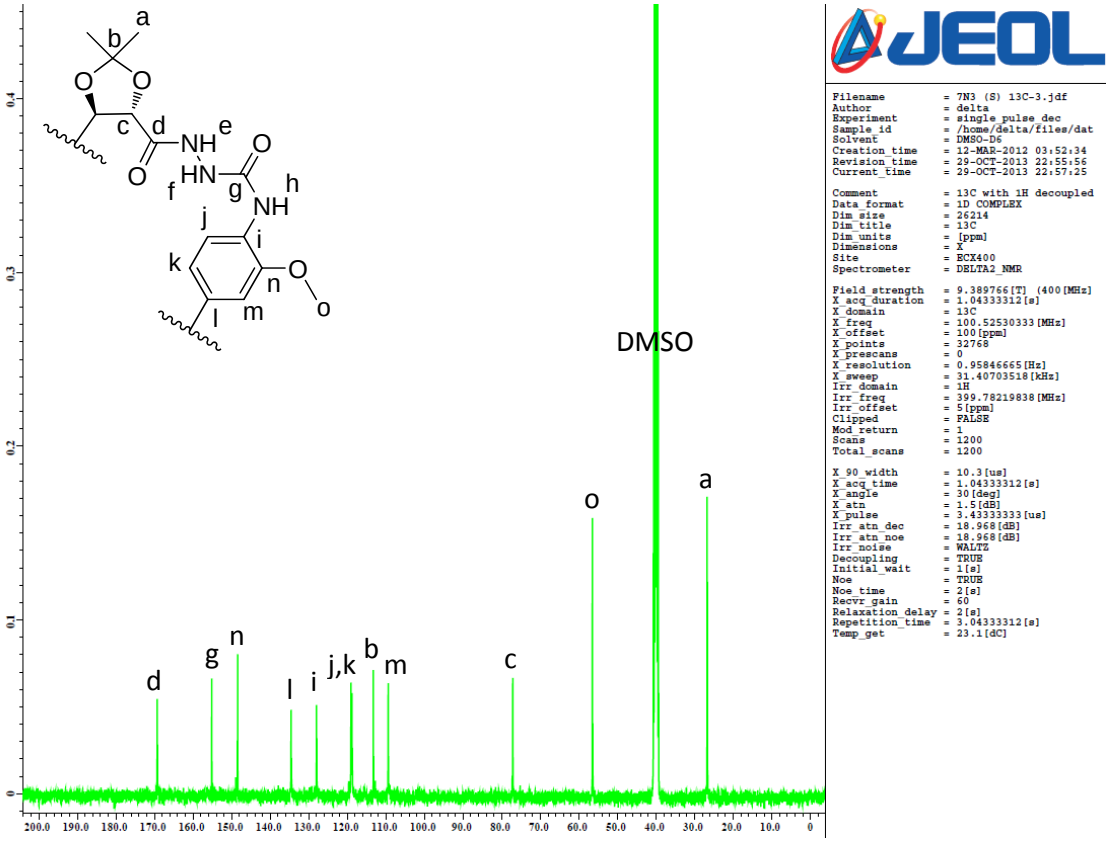

Figure 19. ^{13}C NMR spectrum of macrocycle (**13**) (100 MHz, DMSO-d_6).

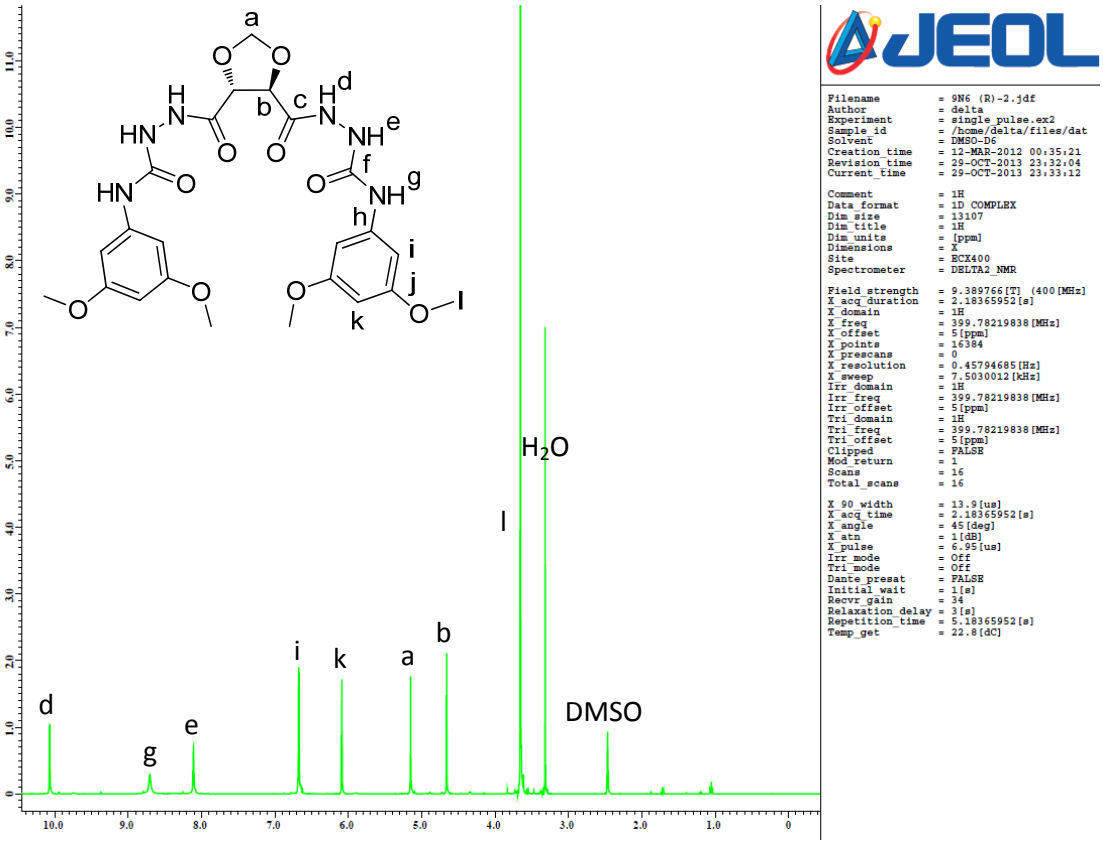

Figure 20. ^{1}H NMR spectrum of compound (**14**) (400 MHz, DMSO-d_6).

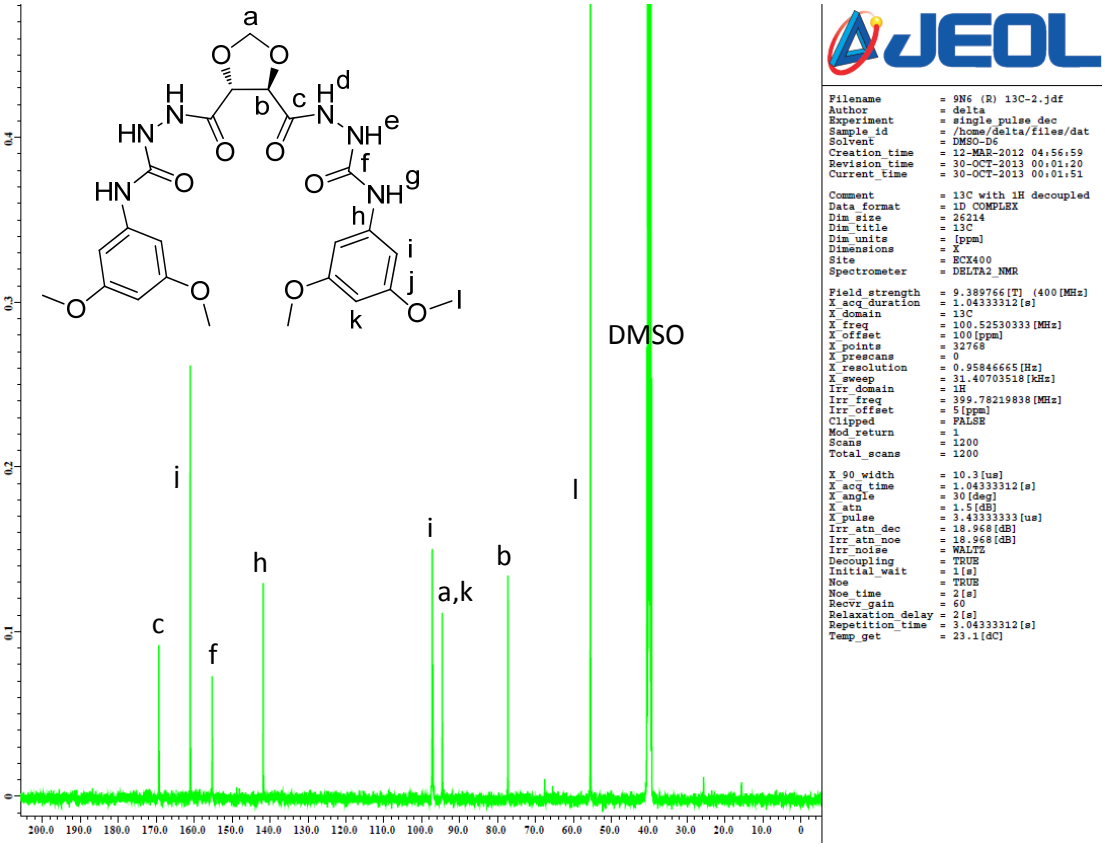

Figure 21. ^{13}C NMR spectrum of compound (**14**) (100 MHz, DMSO-d_6).

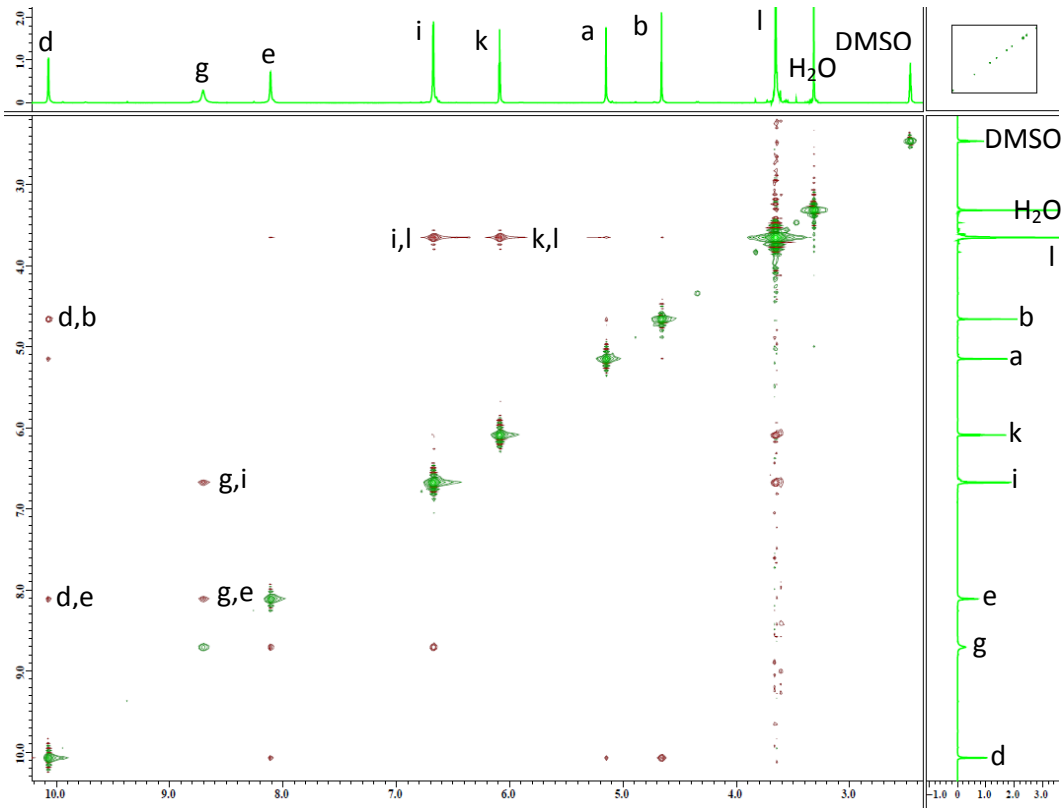

Figure 22. 2D ROESY NMR spectrum of compound (**14**) (DMSO-d_6).

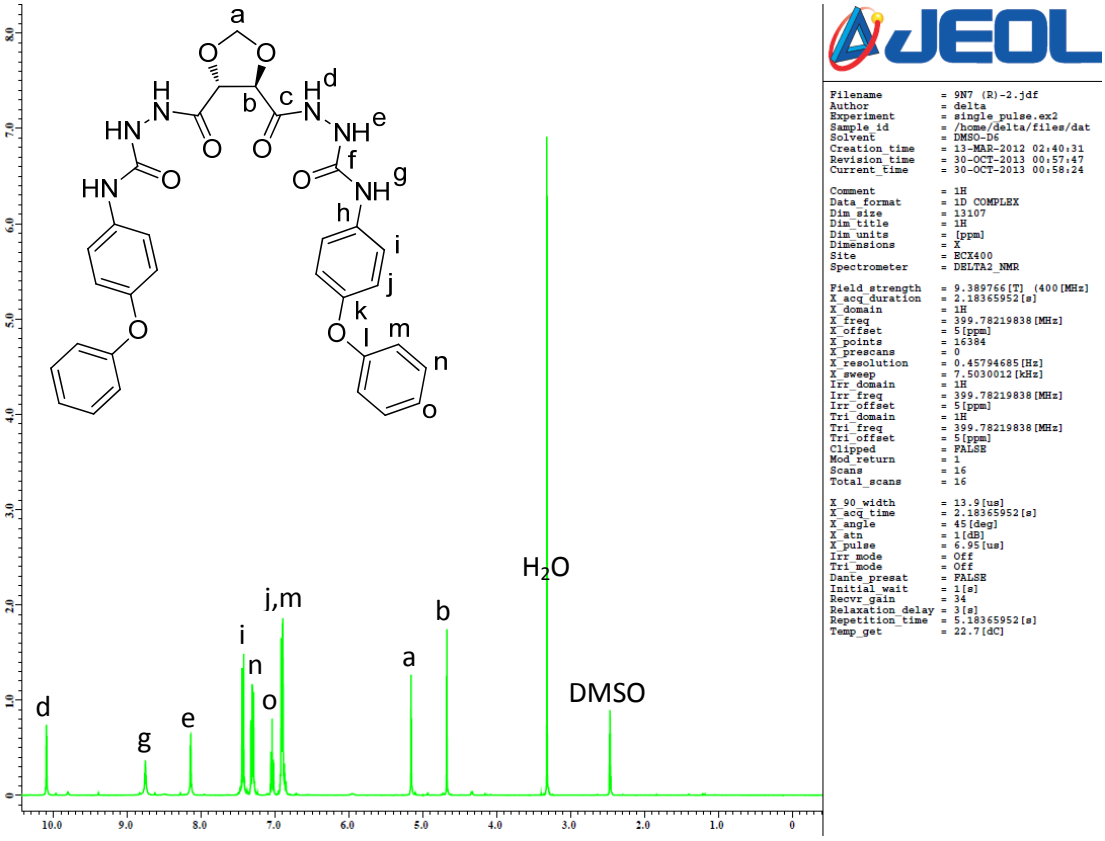

Figure 23. ^{1}H NMR spectrum of compound (**15**) (400 MHz, DMSO-d_6).

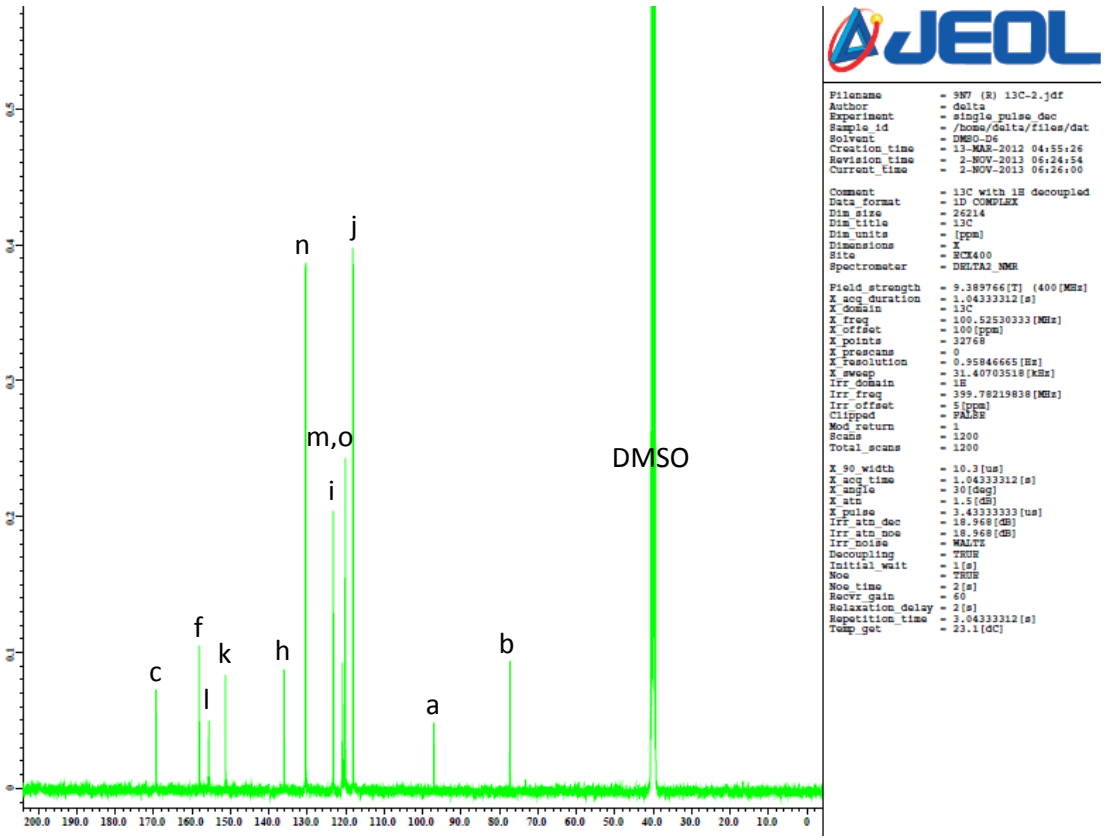

Figure 24. ^{13}C NMR spectrum of compound (**15**) (100 MHz, DMSO-d_6).

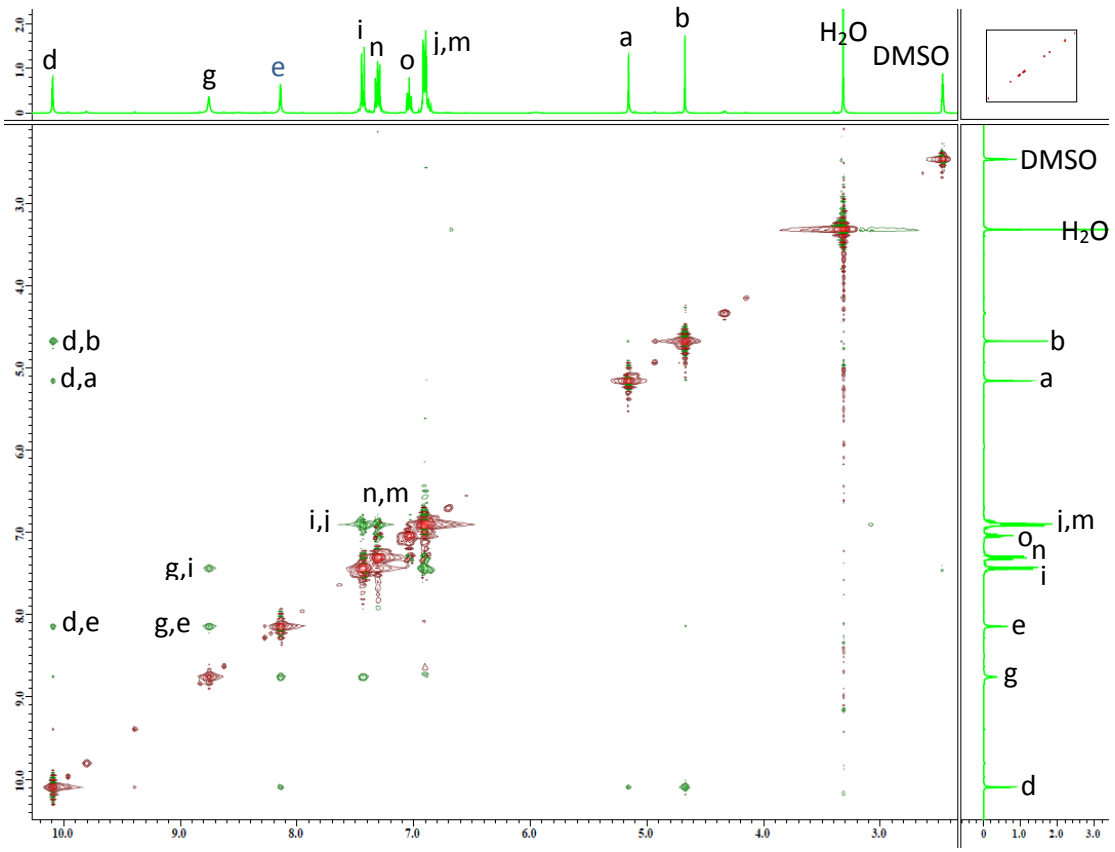

Figure 25. 2D ROESY NMR spectrum of compound (**15**) (DMSO-d_6).

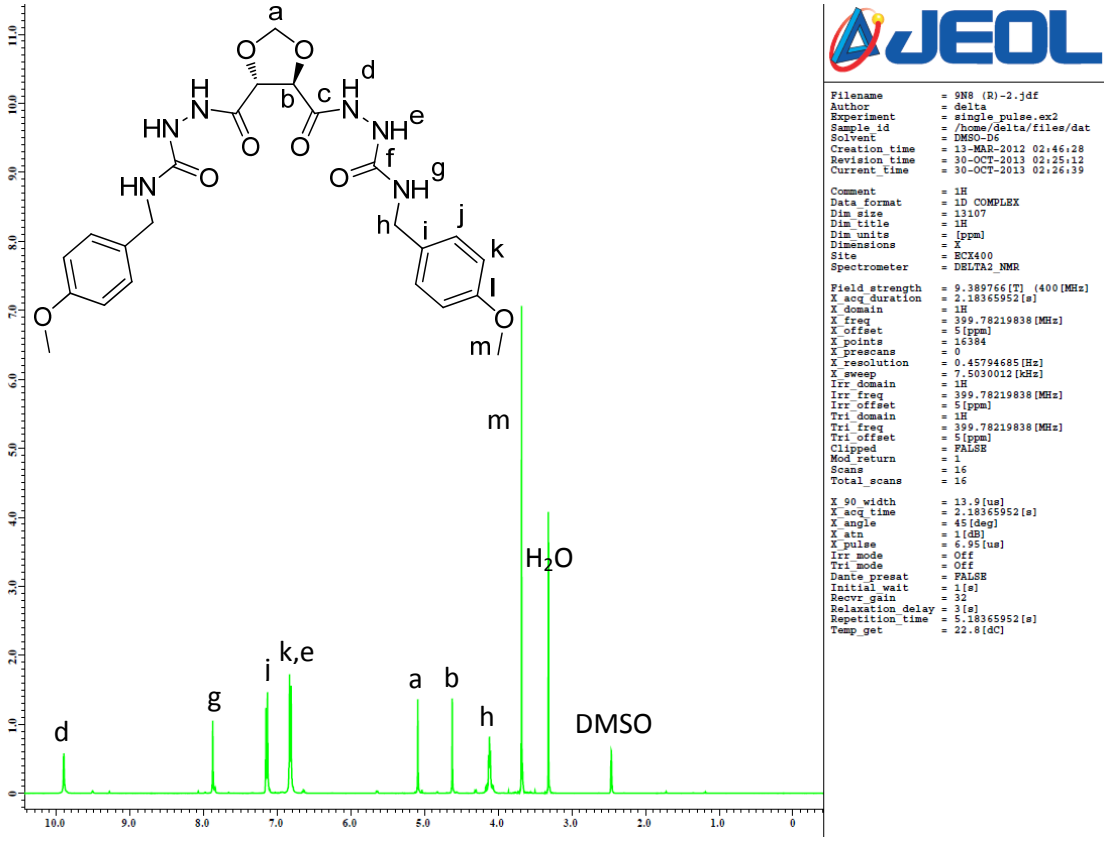

Figure 26. ^{1}H NMR spectrum of compound (**16**) (400 MHz, DMSO-d_6).

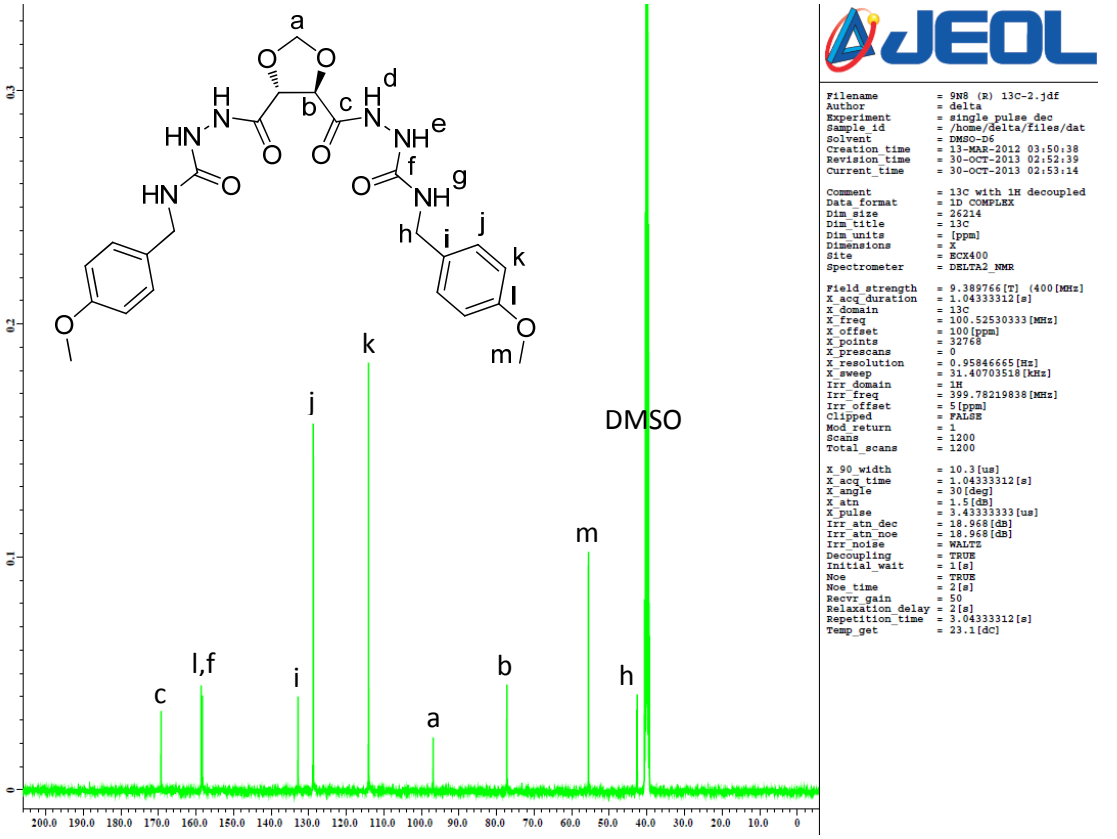

Figure 27. ^{13}C NMR spectrum of compound (**16**) (100 MHz, DMSO-d_6).

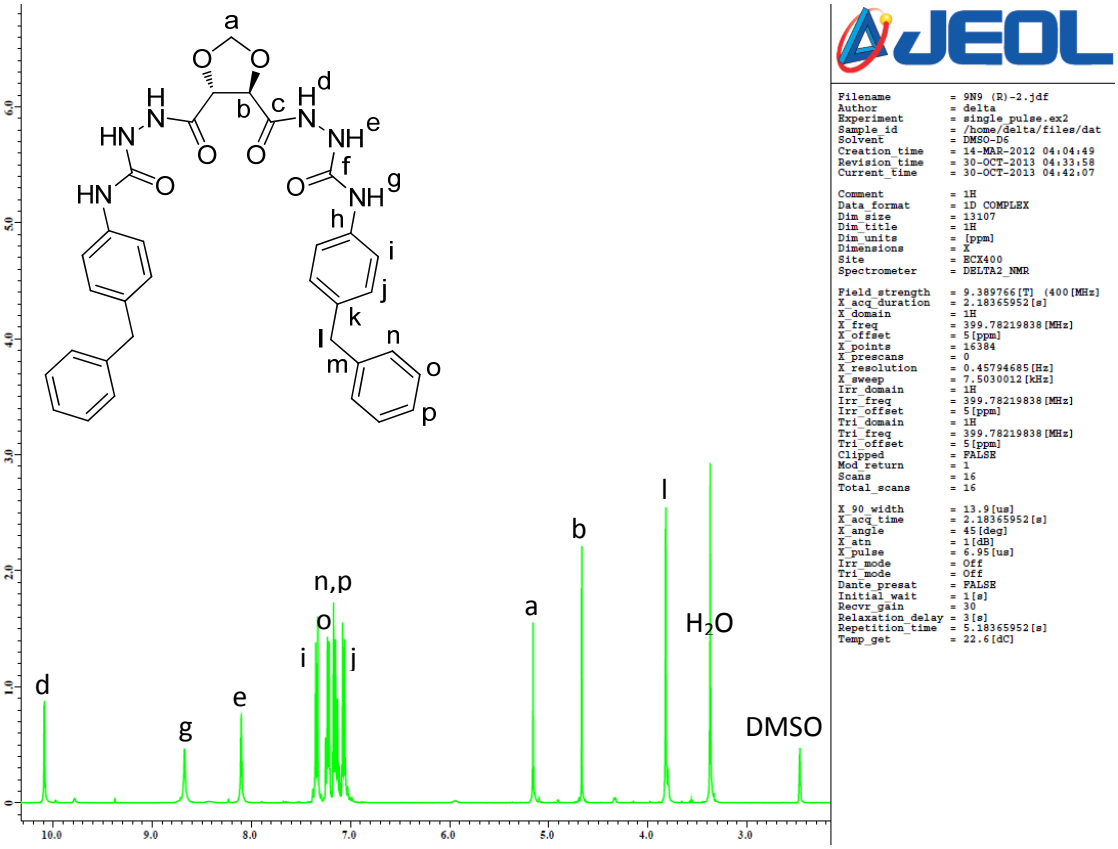

Figure 28. ^{1}H NMR spectrum of compound (**17**) (400 MHz, DMSO-d_6).

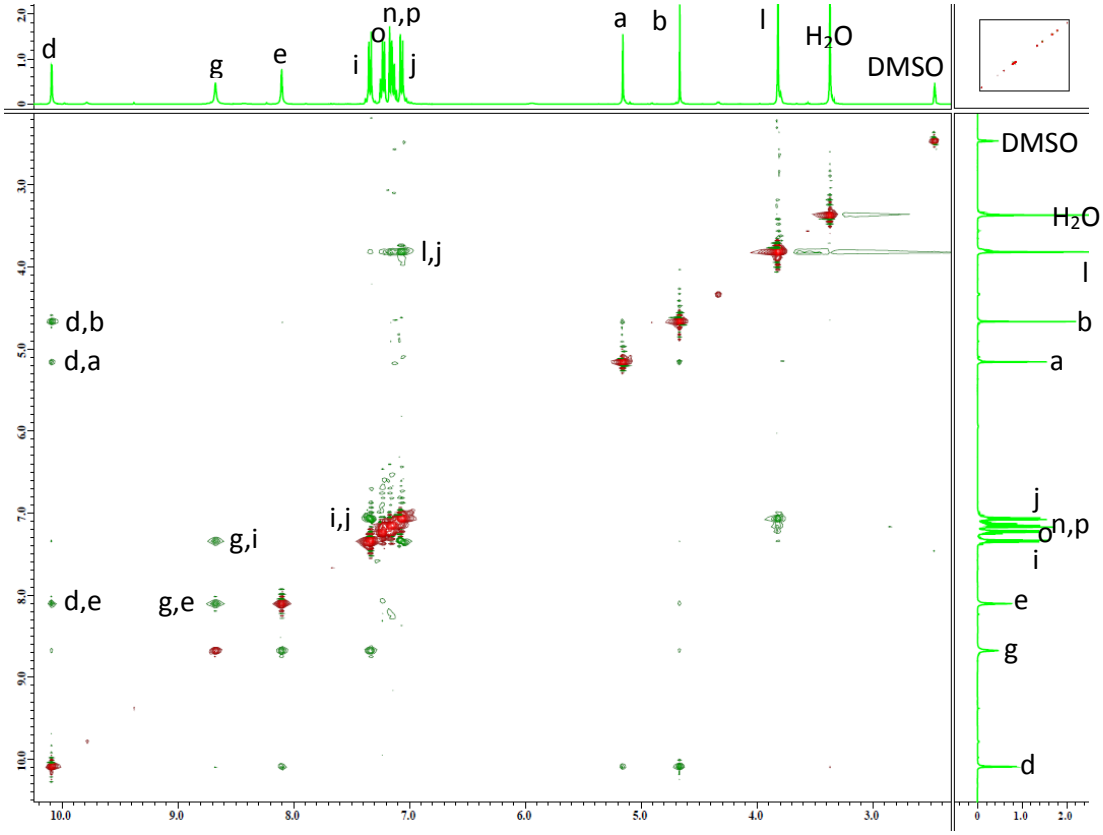

Figure 29. 2D ROESY NMR spectrum of compound (**17**) (DMSO-d_6).

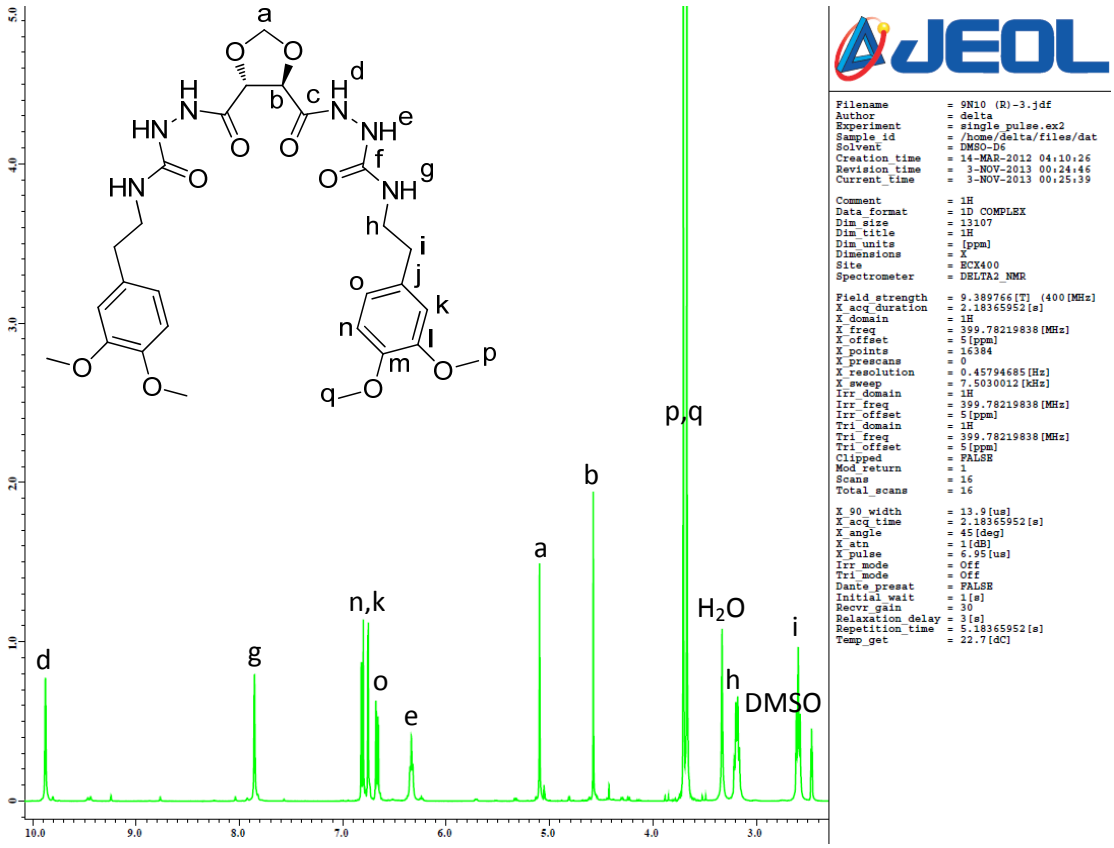

Figure 30. ^{1}H NMR spectrum of compound (**18**) (400 MHz, DMSO-d_6).

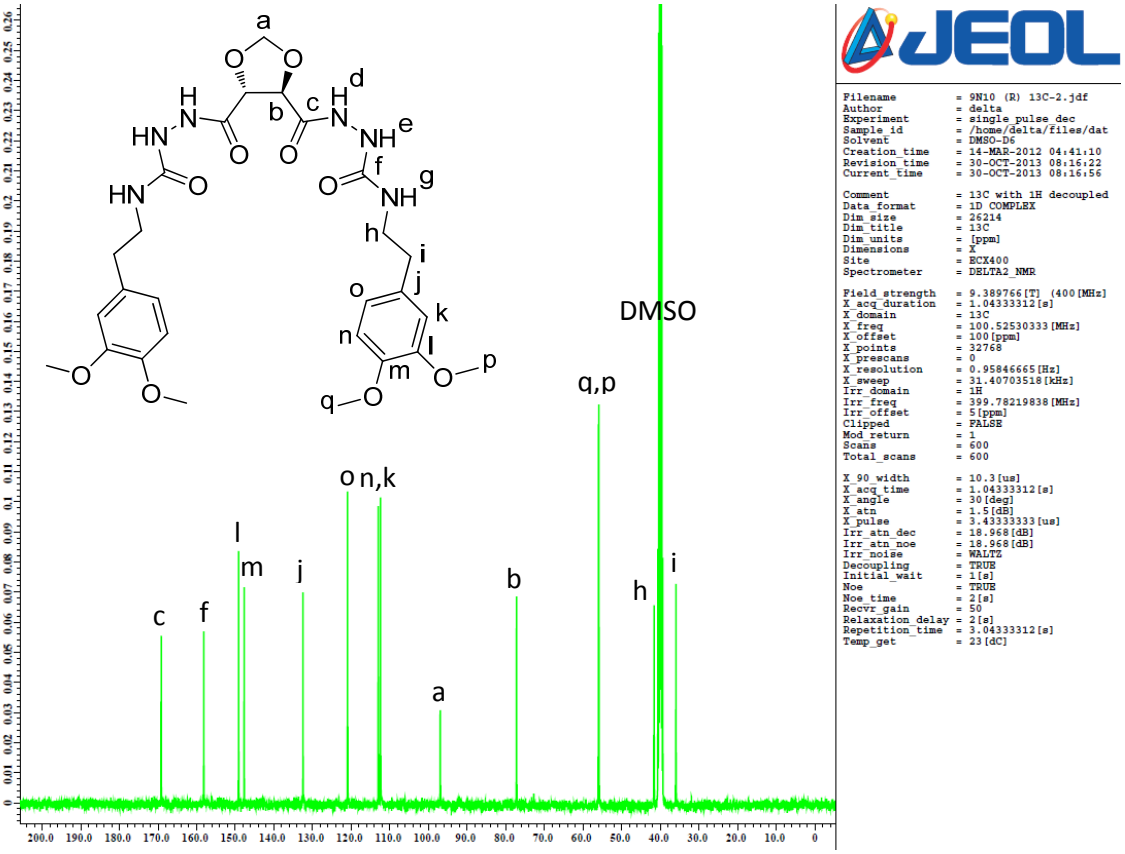

Figure 31. ^{13}C NMR spectrum of compound (**18**) (100 MHz, DMSO-d_6).

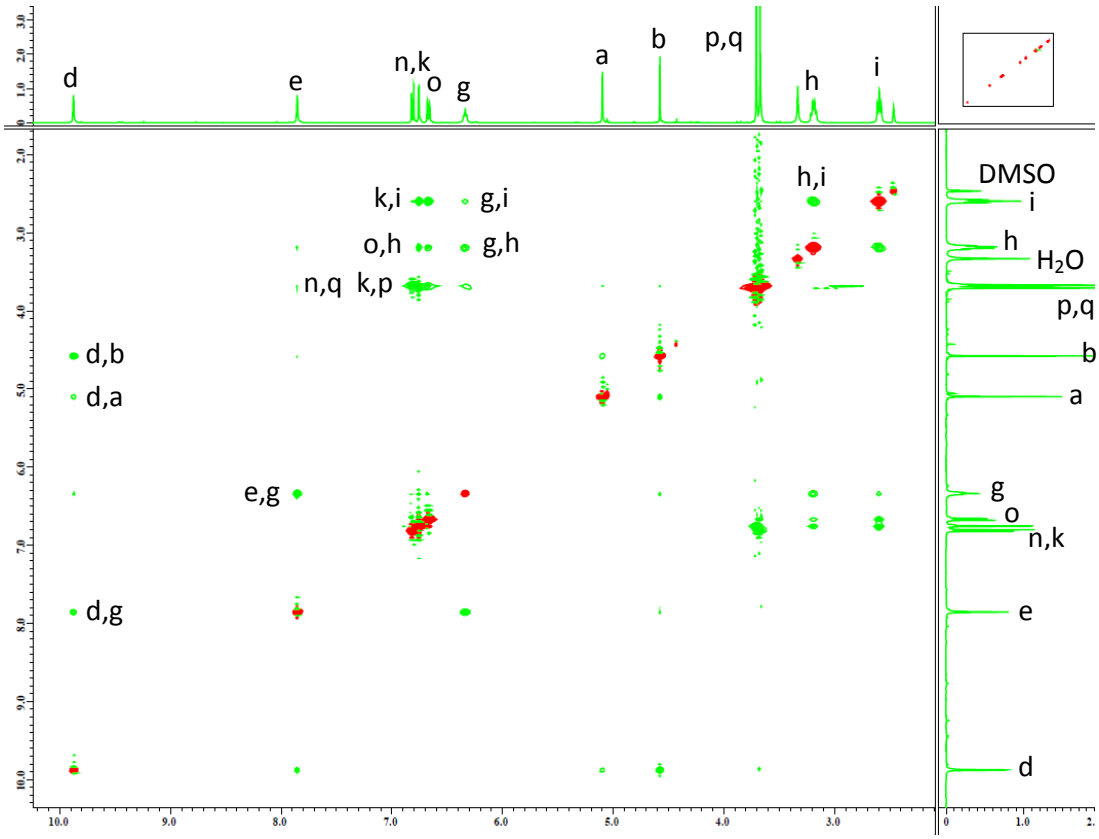

Figure 32. 2D ROESY NMR spectrum of compound (**18**) (DMSO-d_6).

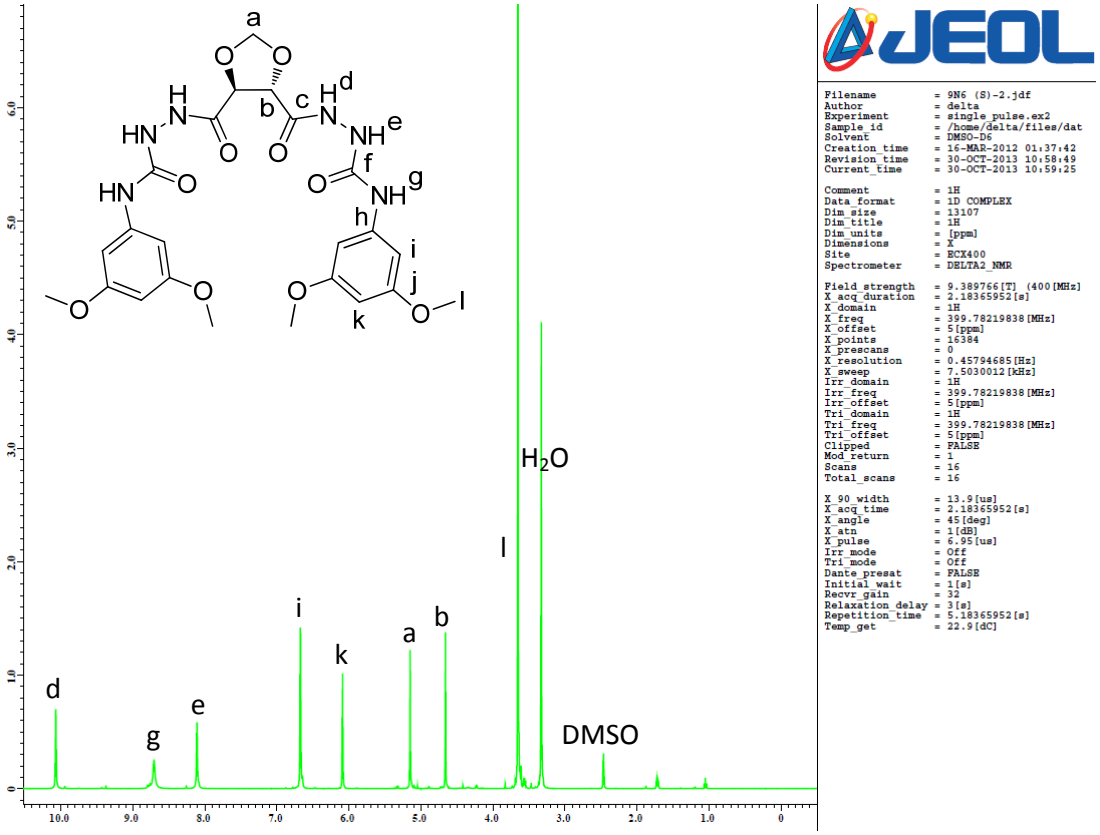

Figure 33. ^{1}H NMR spectrum of compound (**19**) (400 MHz, DMSO-d_6).

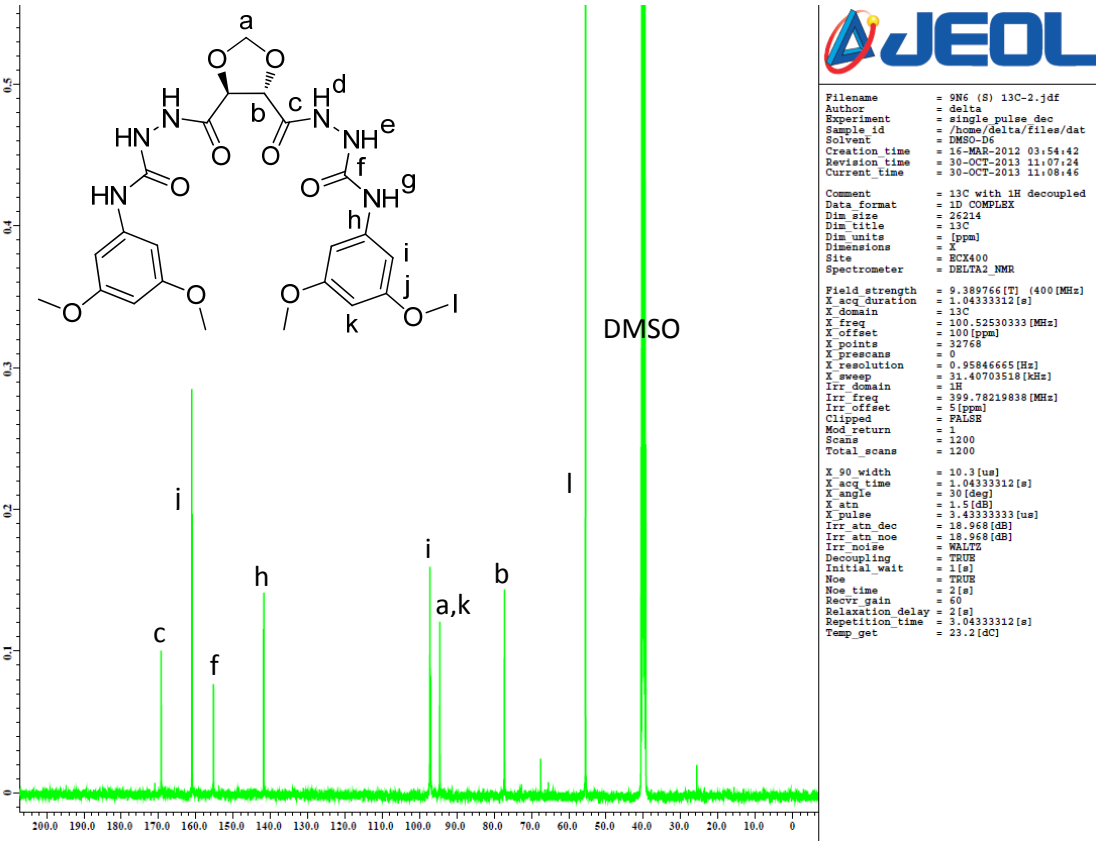

Figure 34. ^{13}C NMR spectrum of compound (**19**) (100 MHz, DMSO-d_6).

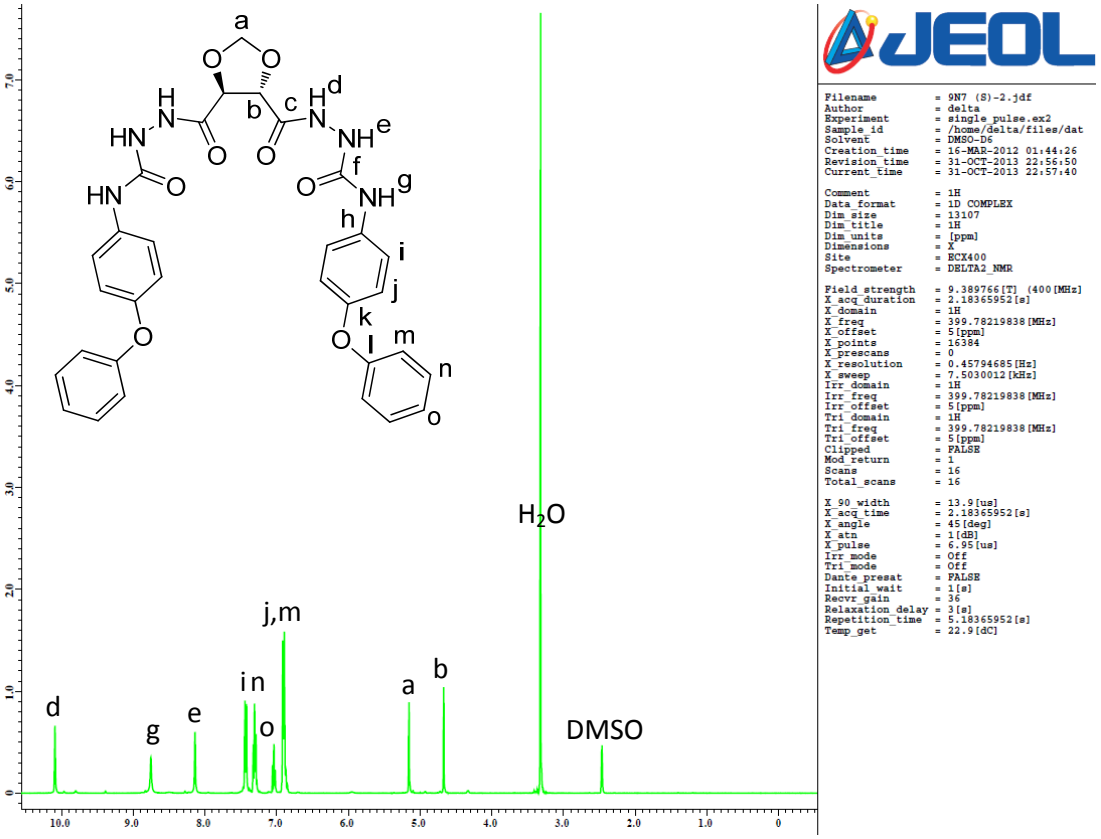

Figure 35. ^{1}H NMR spectrum of compound (**20**) (400 MHz, DMSO-d_6).

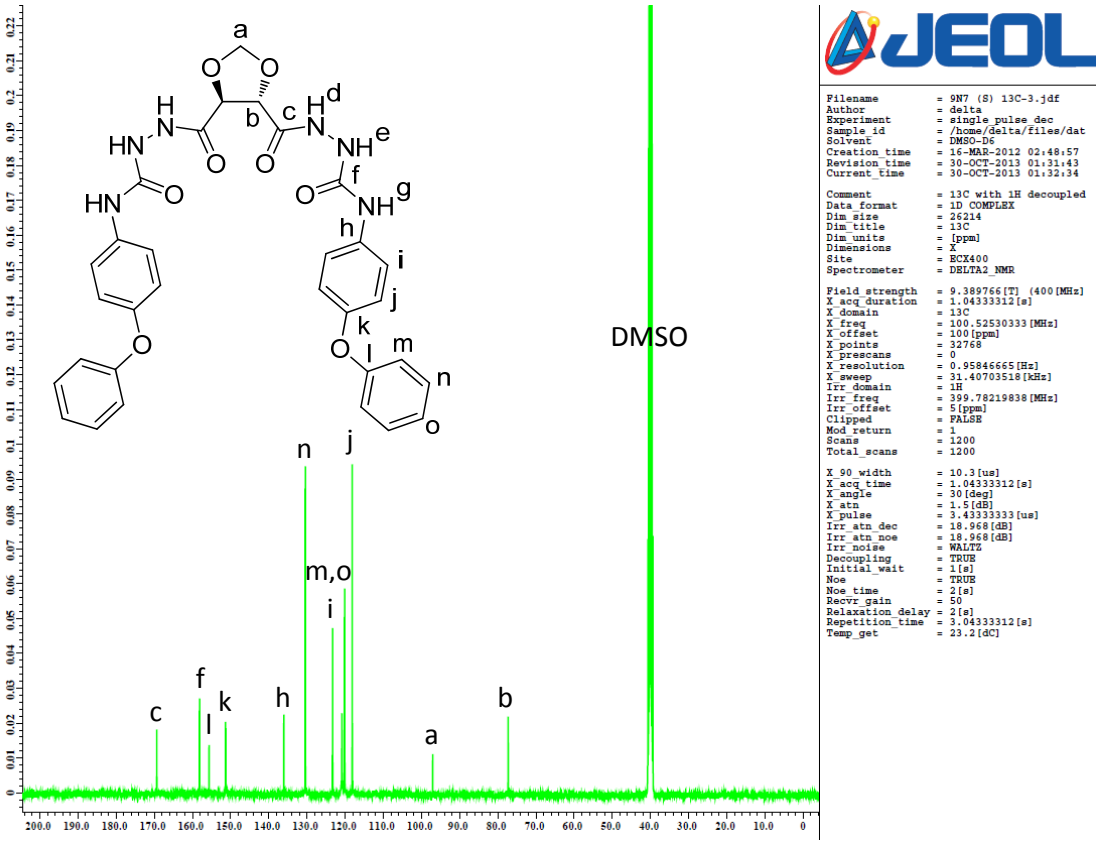

Figure 36. ^{13}C NMR spectrum of compound (**20**) (100 MHz, DMSO-d_6).

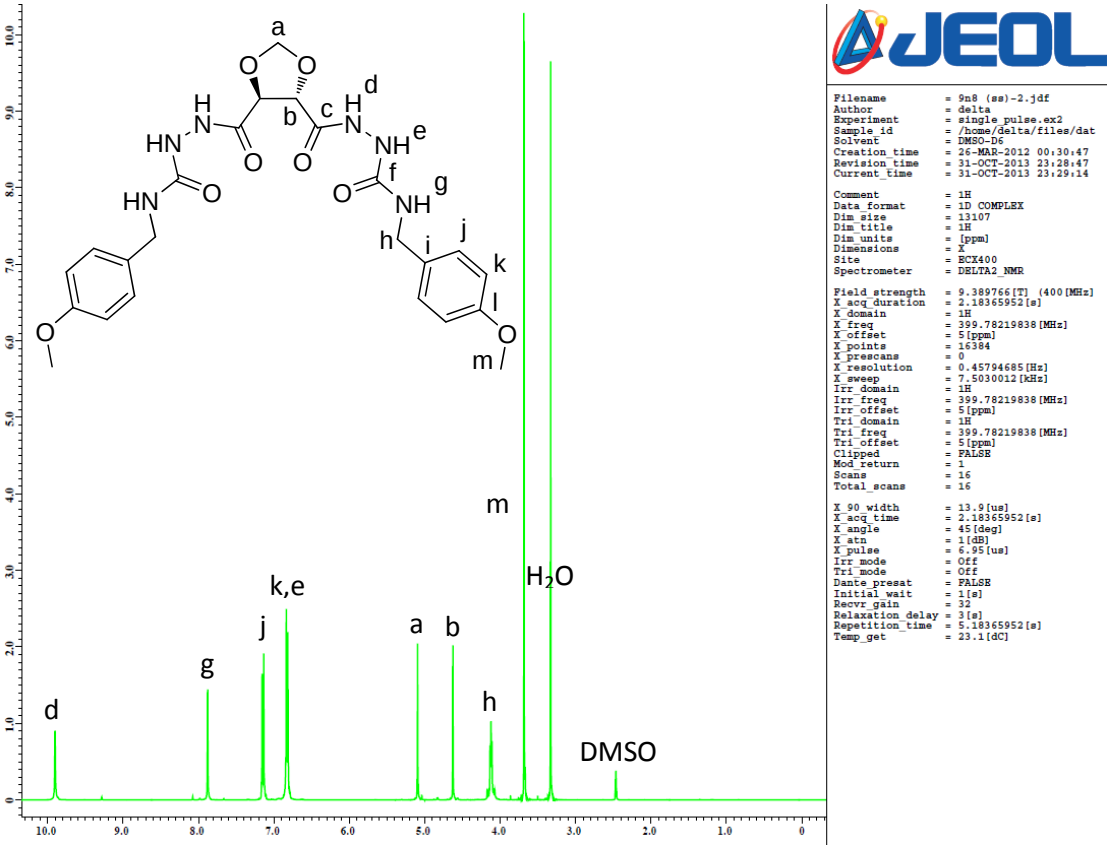

Figure 37. ^{1}H NMR spectrum of compound (**21**) (400 MHz, DMSO-d_6).

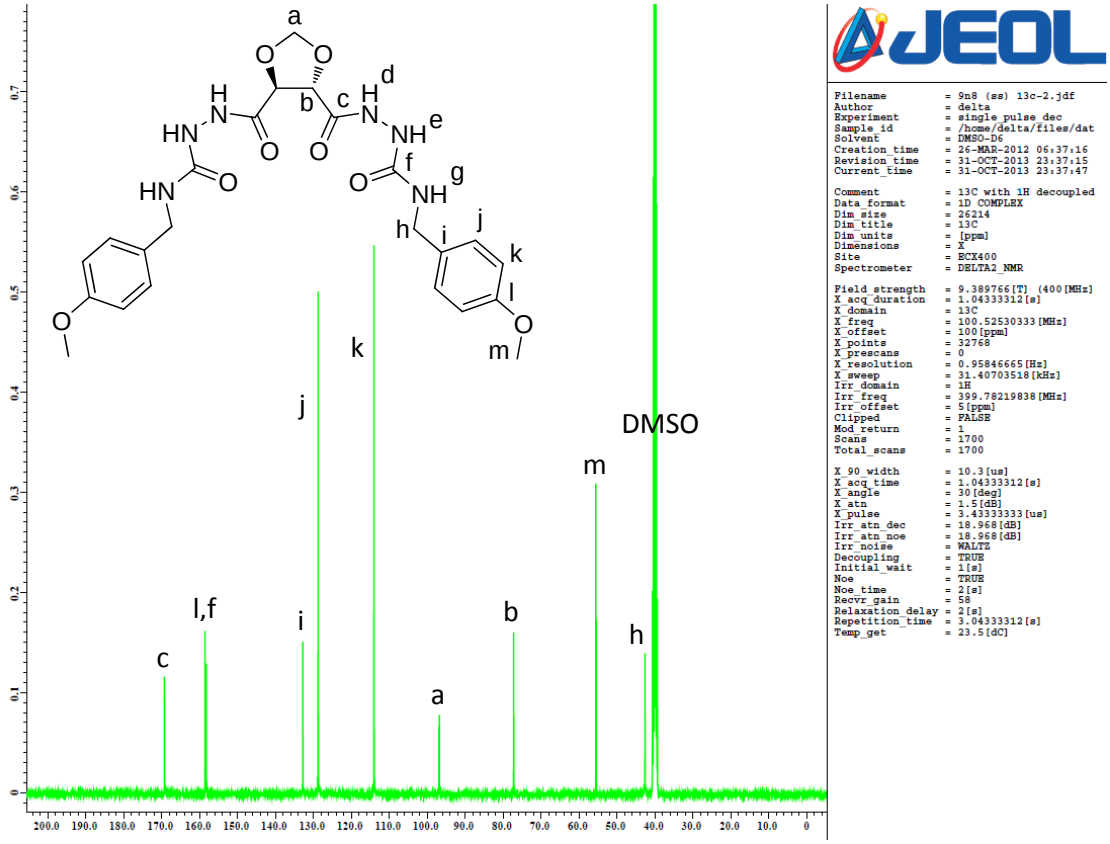

Figure 38. ^{13}C NMR spectrum of compound (**21**) (100 MHz, DMSO-d_6).

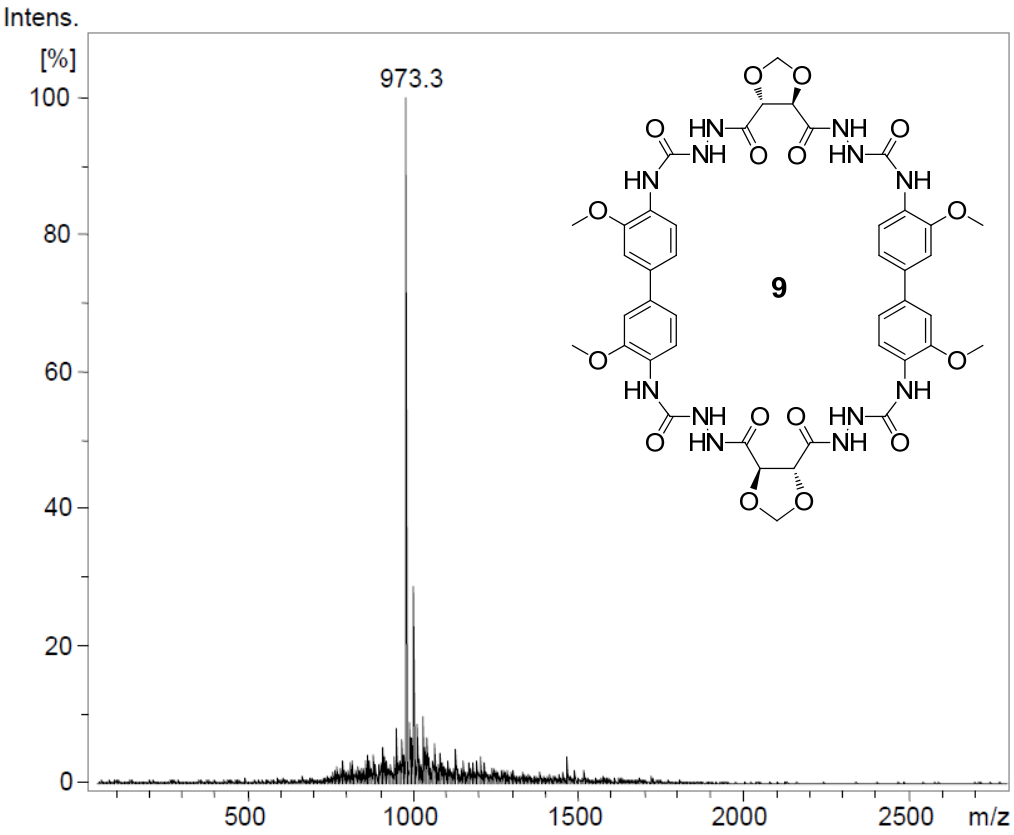

Figure 39. ESI-TOF MS of macrocycle (**9**) (DMF/CH_3CN, positive ion mode, $[M+H]^+$).

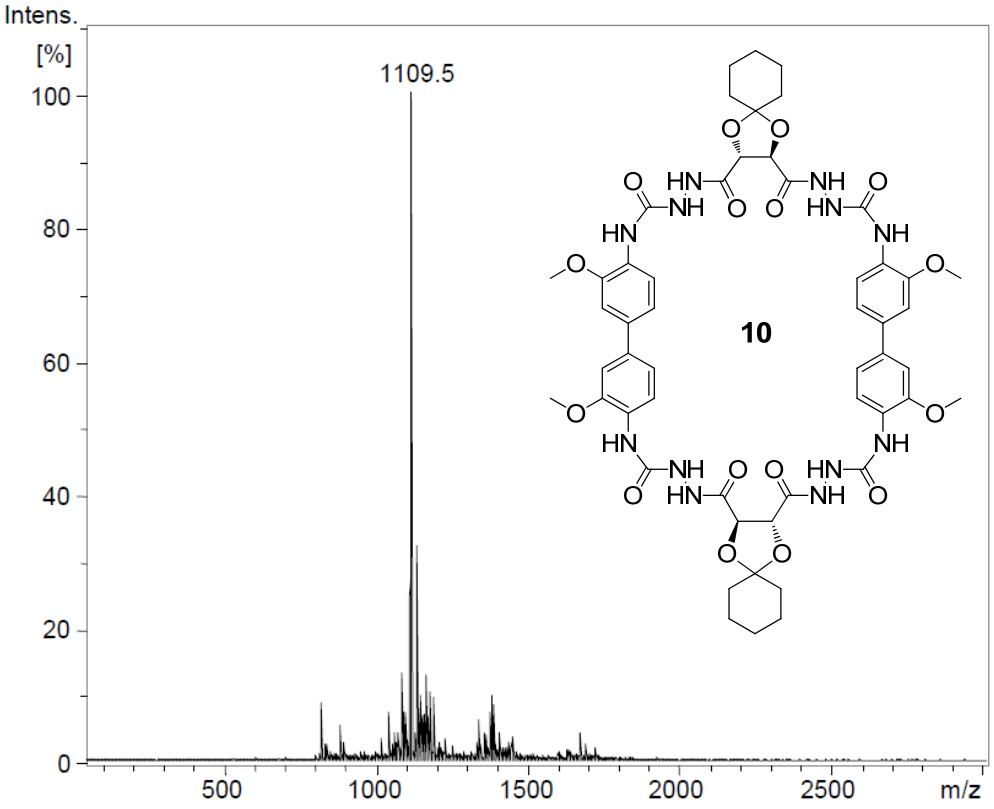

Figure 40. ESI-TOF MS of macrocycle (**10**) (DMF/CH_3CN, positive ion mode, $[M+H]^+$).

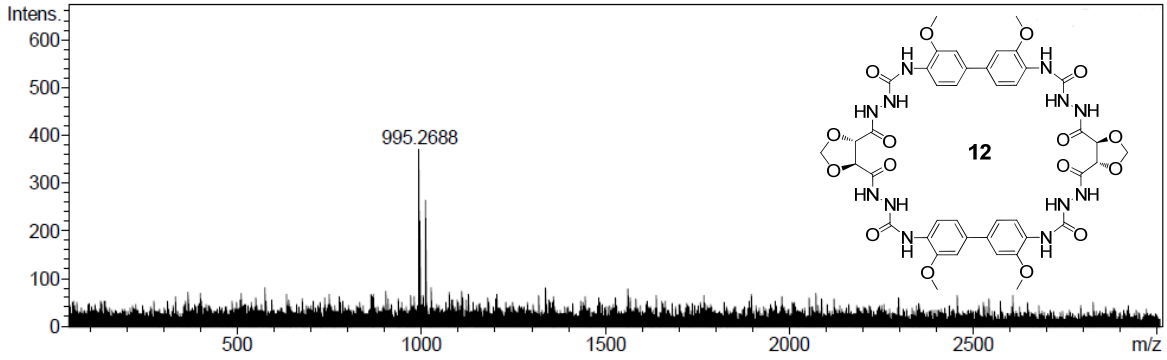

Figure 41. ESI-TOF MS of macrocycle (**12**) (DMF/CH_3CN, positive ion mode, $[M+Na]^+$).

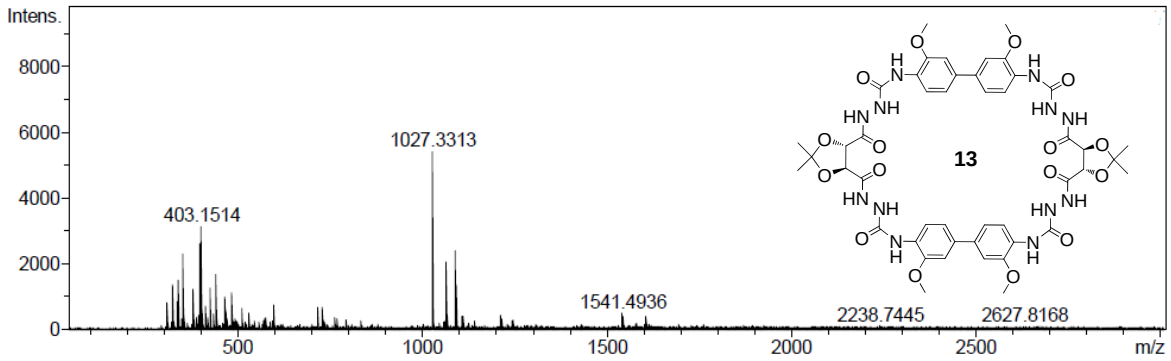

Figure 42. ESI-TOF MS of macrocycle (**13**) (DMF/CH_3CN, negative ion mode, $[M-H]^-$).

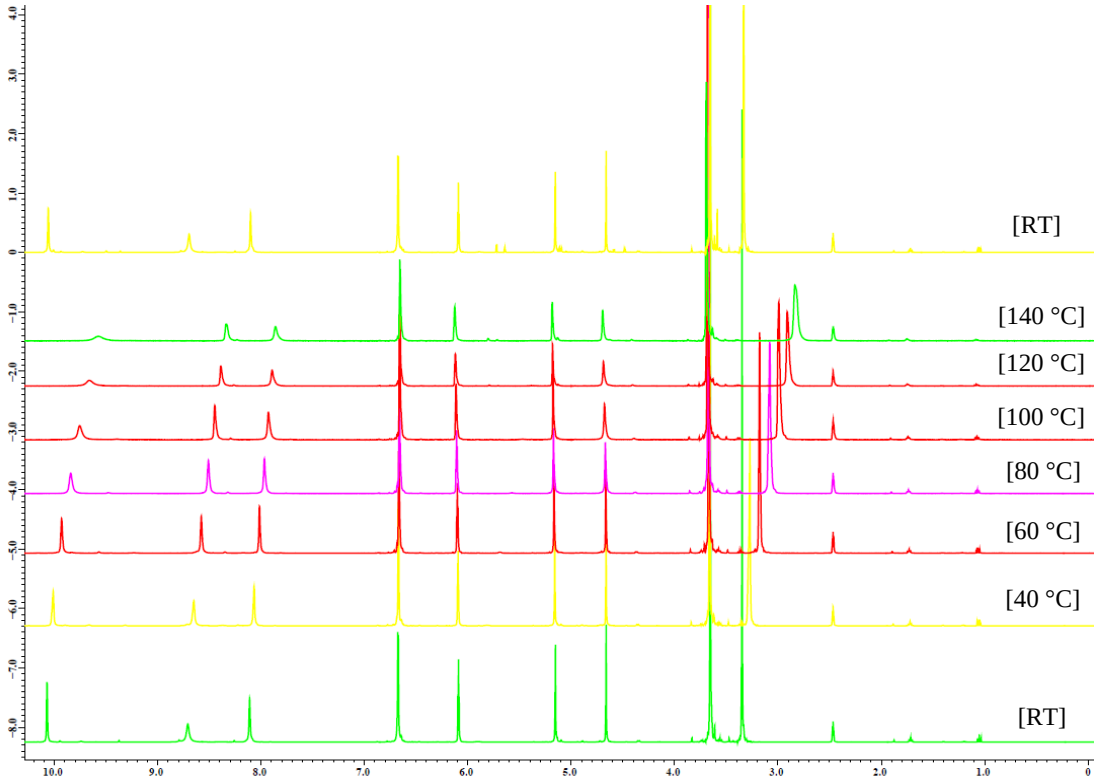

Figure 43. Stacked VT-NMR spectra of compound (**14**) (400 MHz, DMSO-d_6).

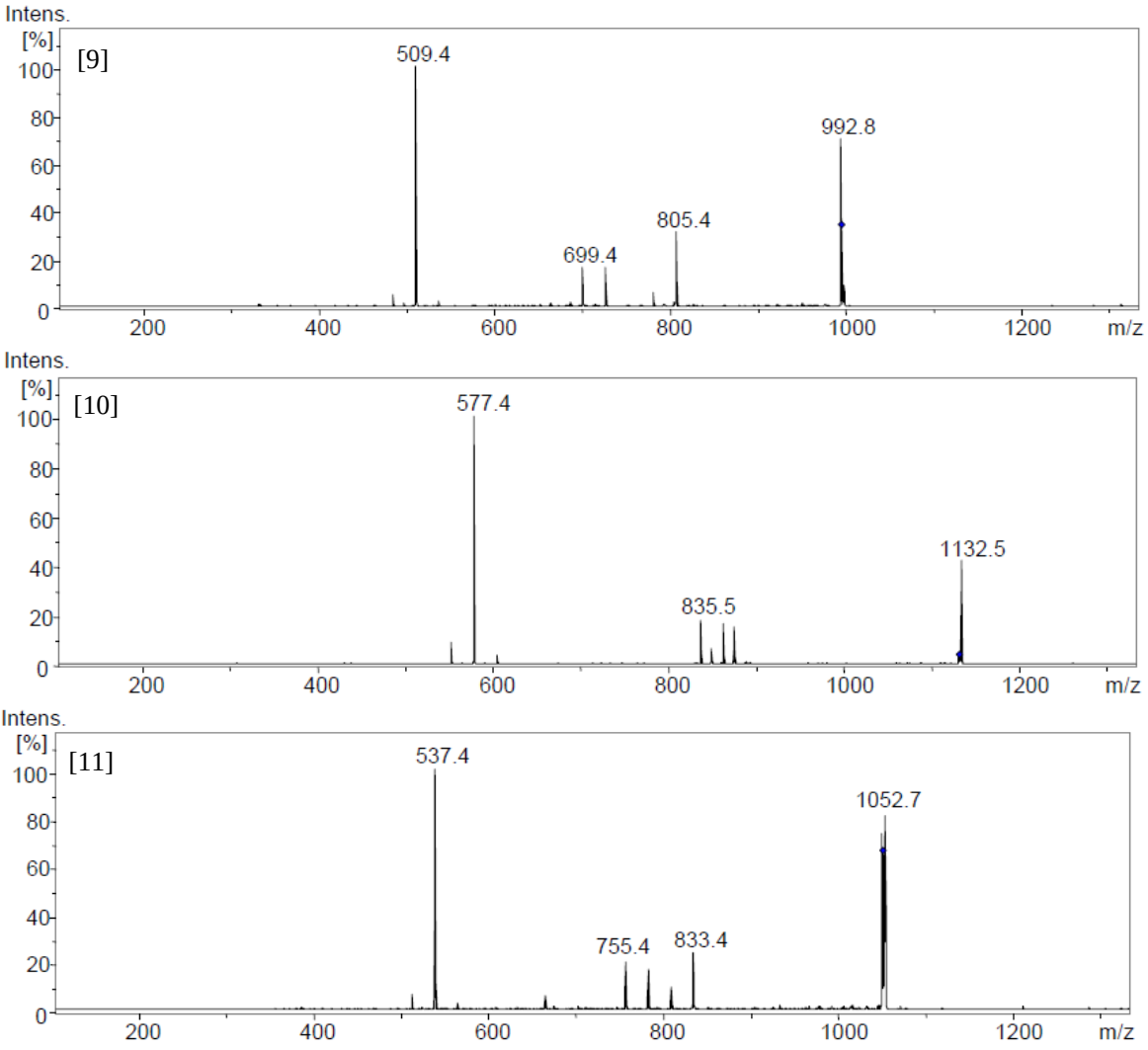

Figure 44. ESI-MS/MS of macrocycles (**9-11**) (DMF/CH_3CN, positive ion mode, $[M+Na]^+$).

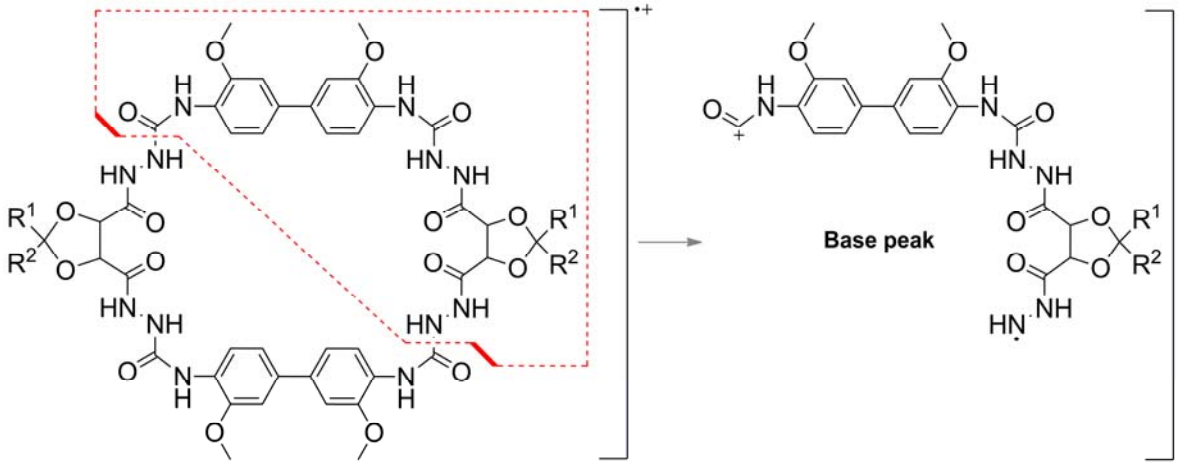

Figure 45. Proposed fragmentation mechanism of macrocycles (**9-13**).

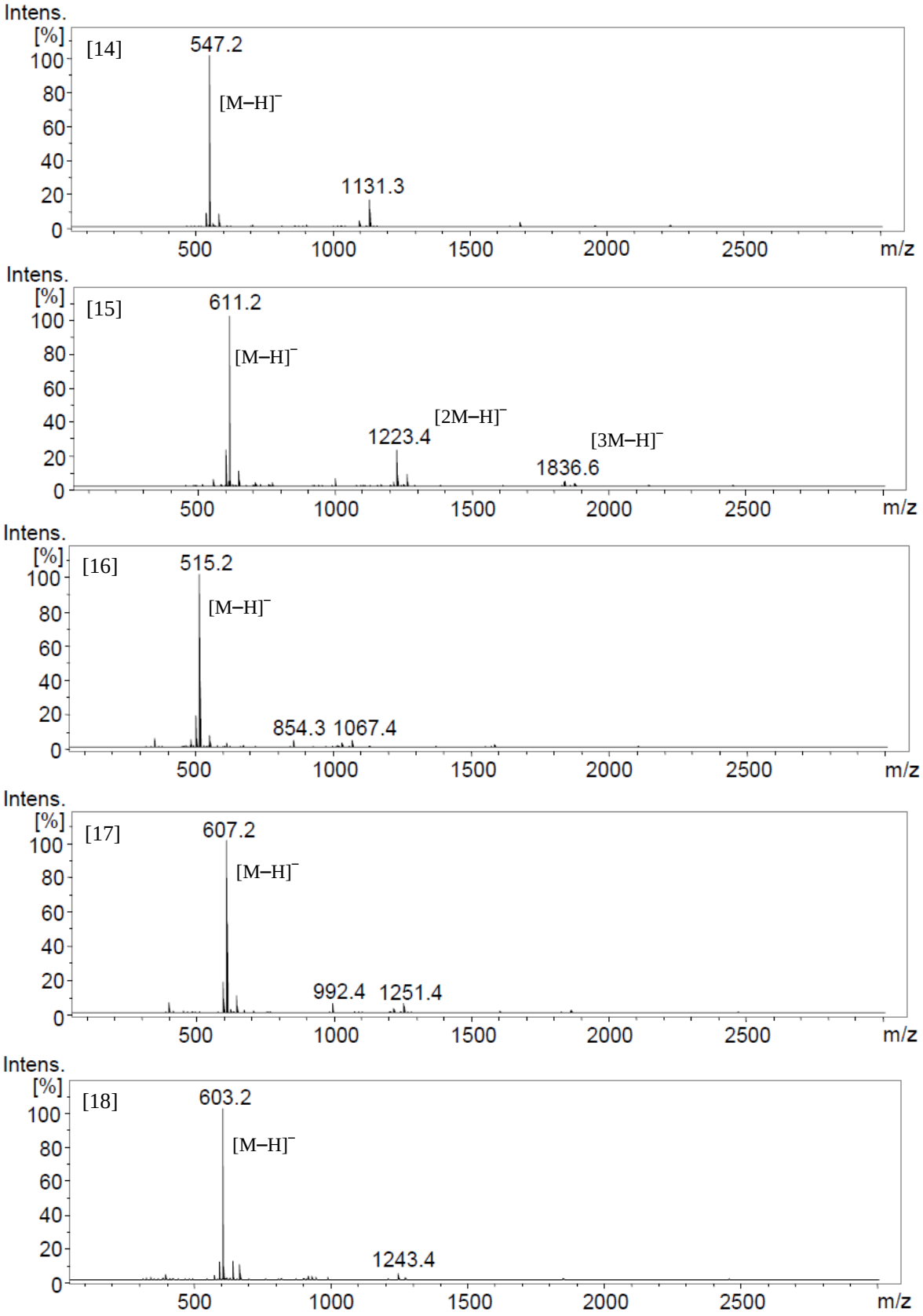

Figure 46. ESI-TOF MS of compounds (**14-18**) (DMF/CH_3CN, negative ion mode, $[M-H]^-$).

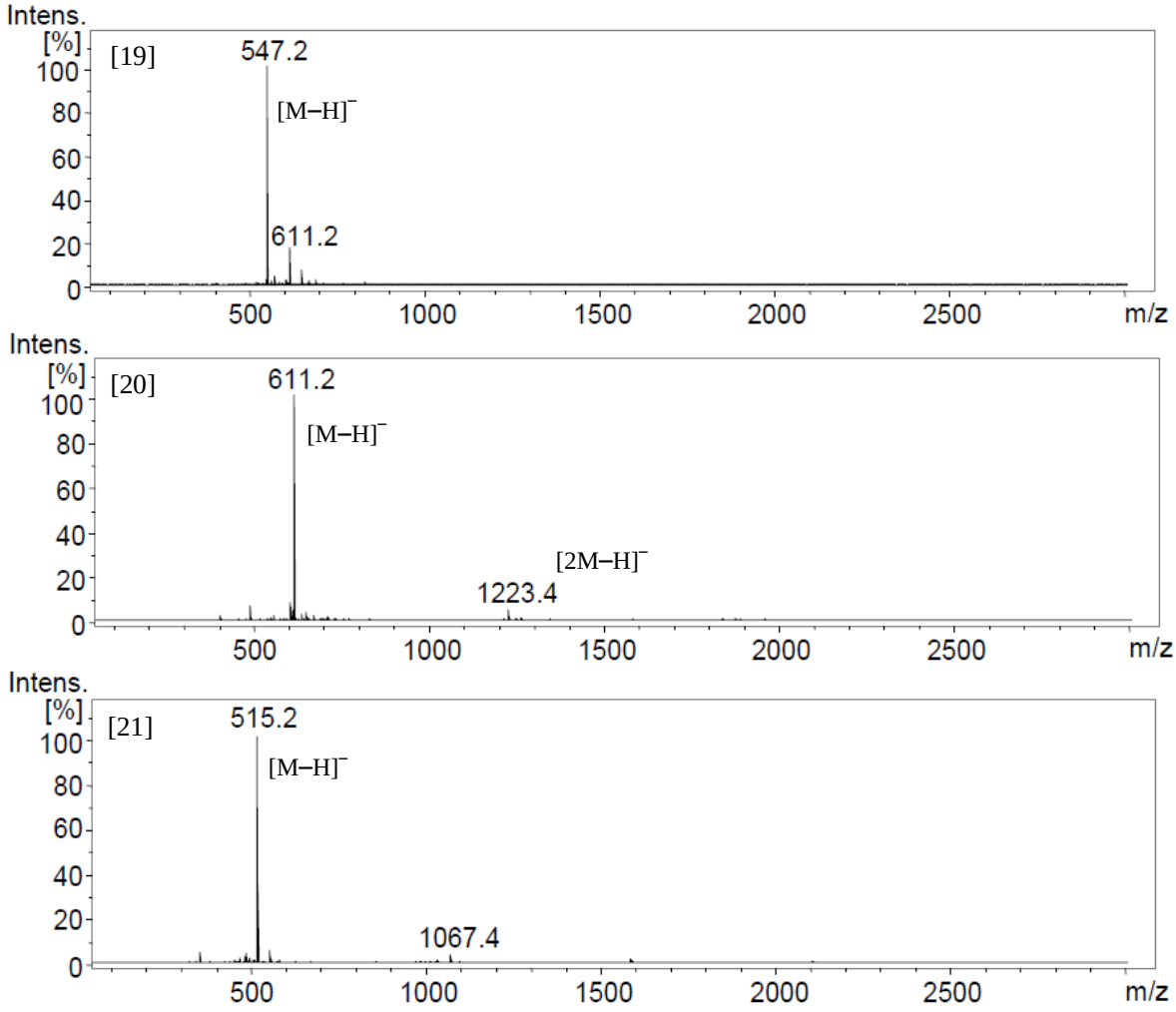

Figure 47. ESI-TOF MS of compounds (**19-21**) (DMF/CH_3CN, negative ion mode, $[M-H]^-$).

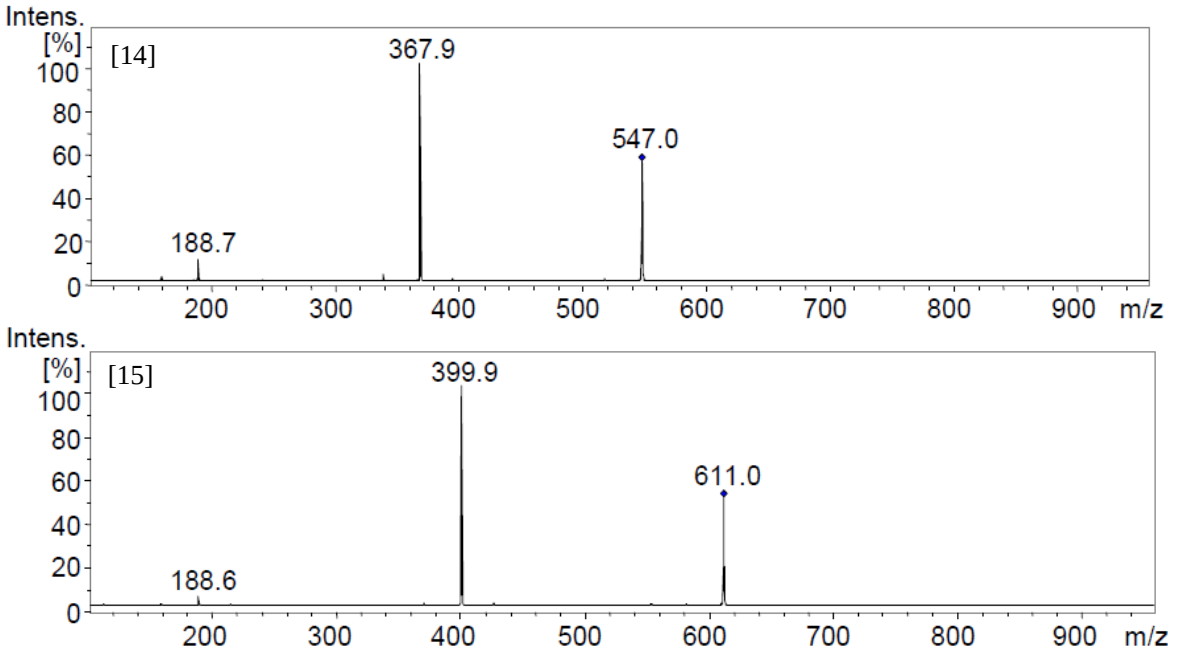

Figure 48. ESI-MS/MS of compounds (**14** and **15**) (DMF/CH_3CN, negative ion mode, $[M-H]^-$).

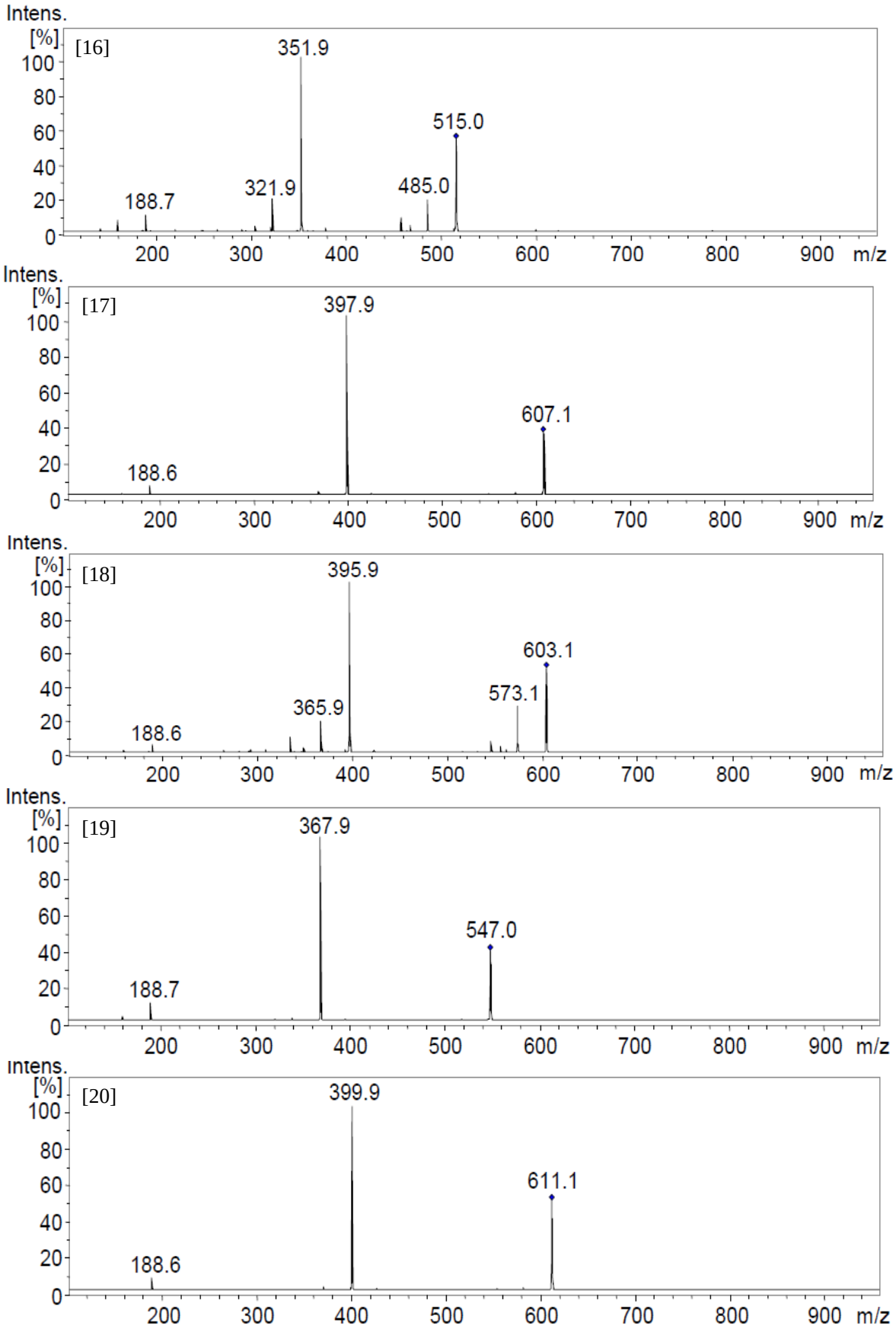

Figure 49. ESI-MS/MS of compounds (**16-20**) (DMF/CH_3CN, negative ion mode, $[M-H]^-$).

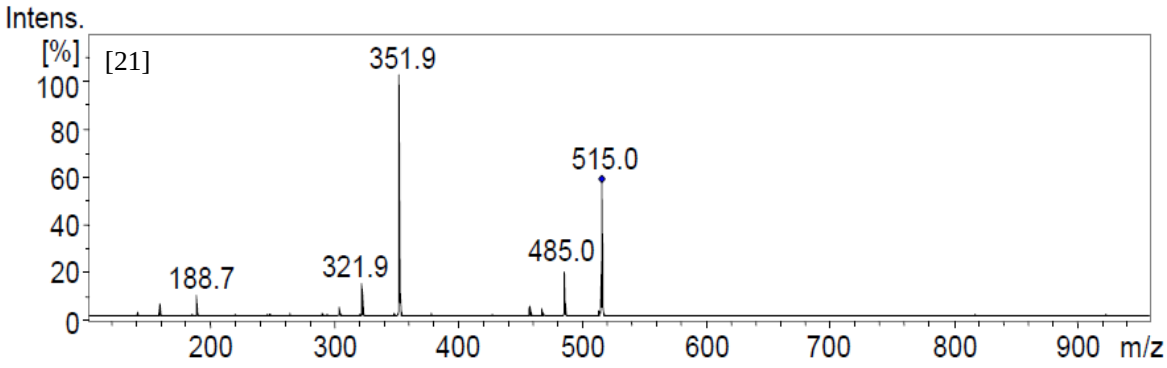

Figure 50. ESI-MS/MS of compounds (**21**) (DMF/CH_3CN, negative ion mode, $[M-H]^-$).

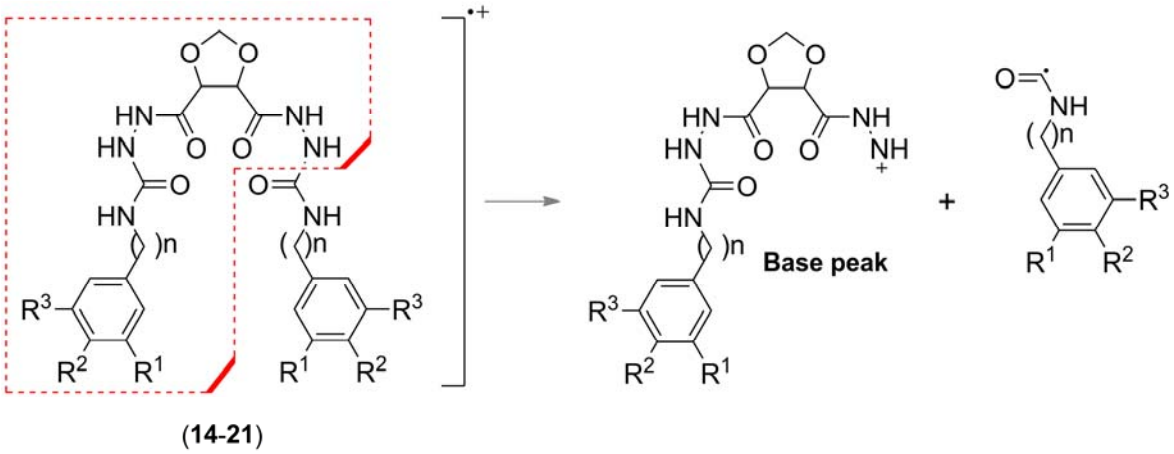

Figure 51. Proposed fragmentation mechanism of compounds (**14-21**).

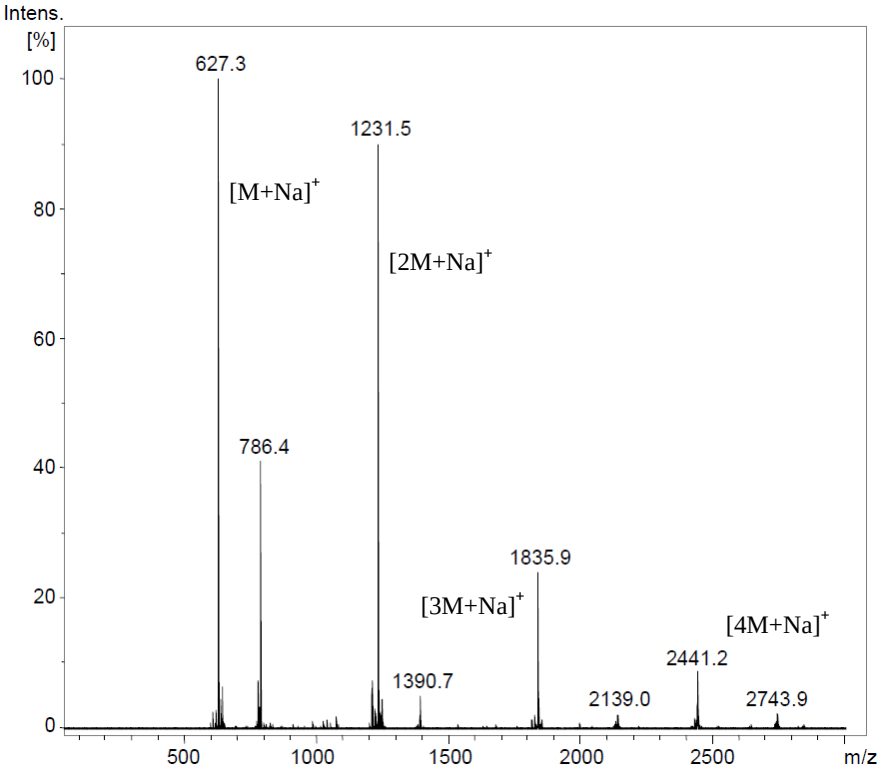

Figure 52. ESI-TOF MS for self-assembled associations of compound (**18**) (CH_3CN/DMF).

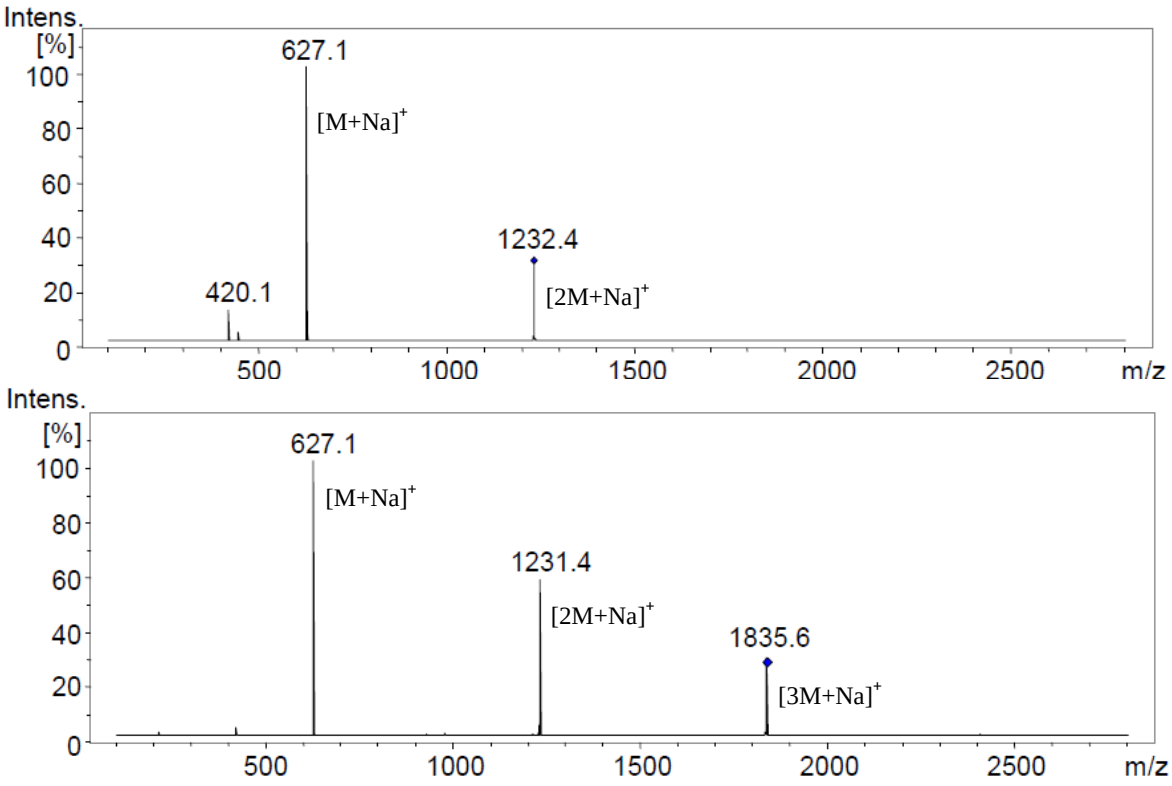

Figure 53. ESI-MS/MS of *m/z* 1231.5 and 1835.9 (DMF/CH_3CN, positive ion mode, $[M+Na]^+$).

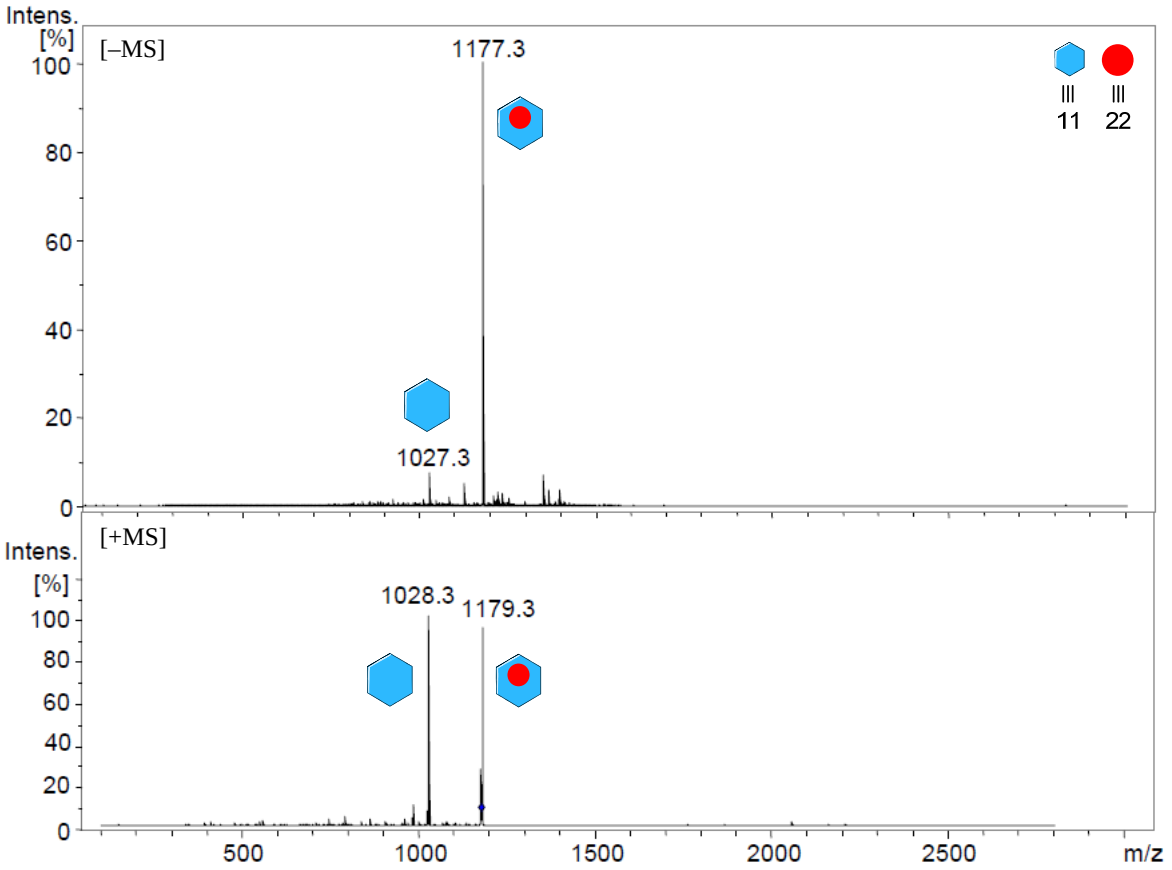

Figure 54. ESI-TOF MS and ESI-MS/MS of Ht/Gt complex **11**/**22** (DMF/CH_3CN/H_2O).

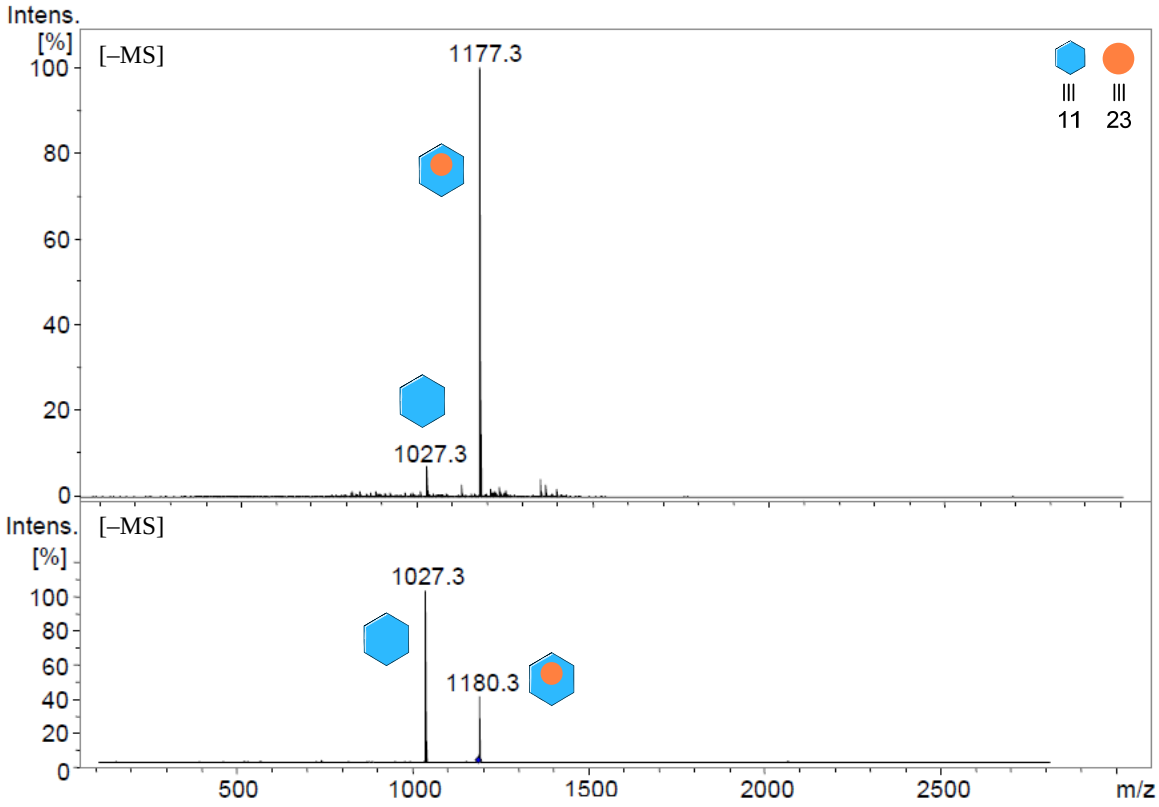

Figure 55. ESI-TOF MS and ESI-MS/MS of Ht/Gt complex **11**/**23** (DMF/CH_3CN/H_2O).

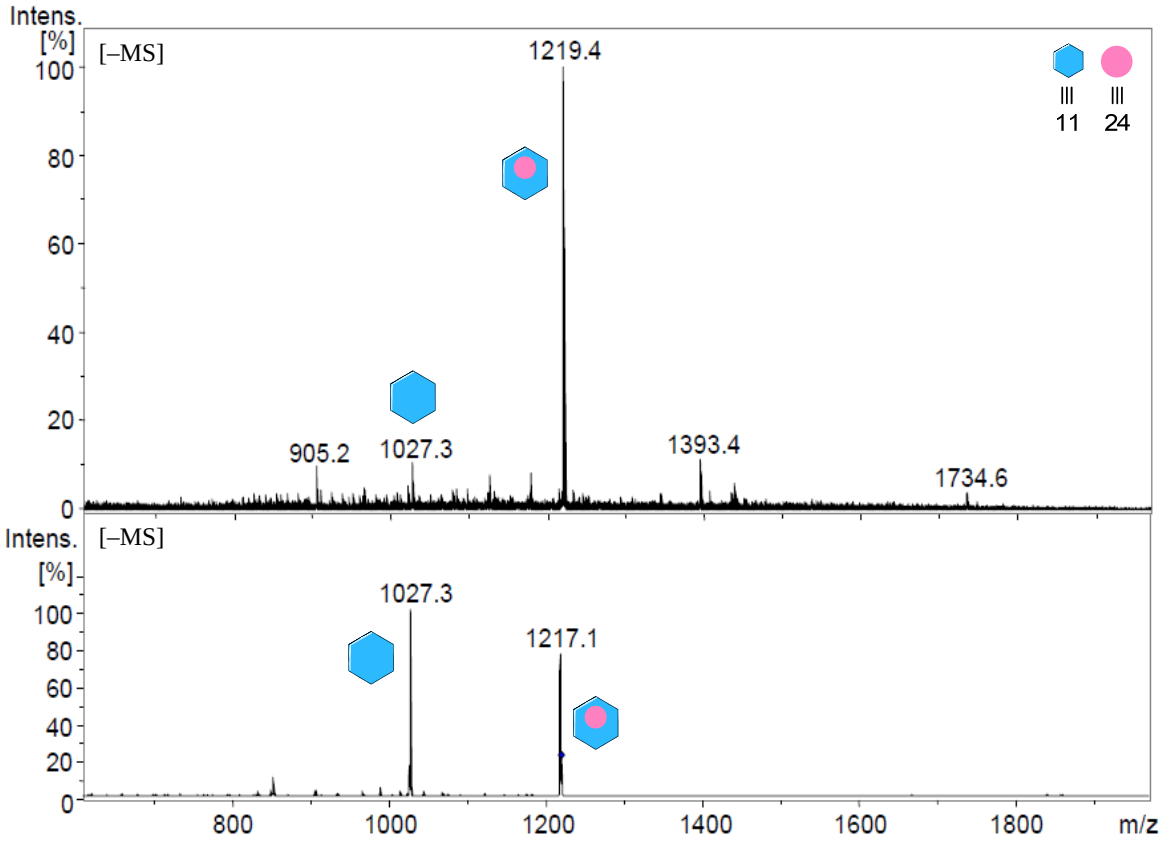

Figure 56. ESI-TOF MS and ESI-MS/MS of Ht/Gt complex **11**/**24** (DMF/CH_3CN/H_2O).

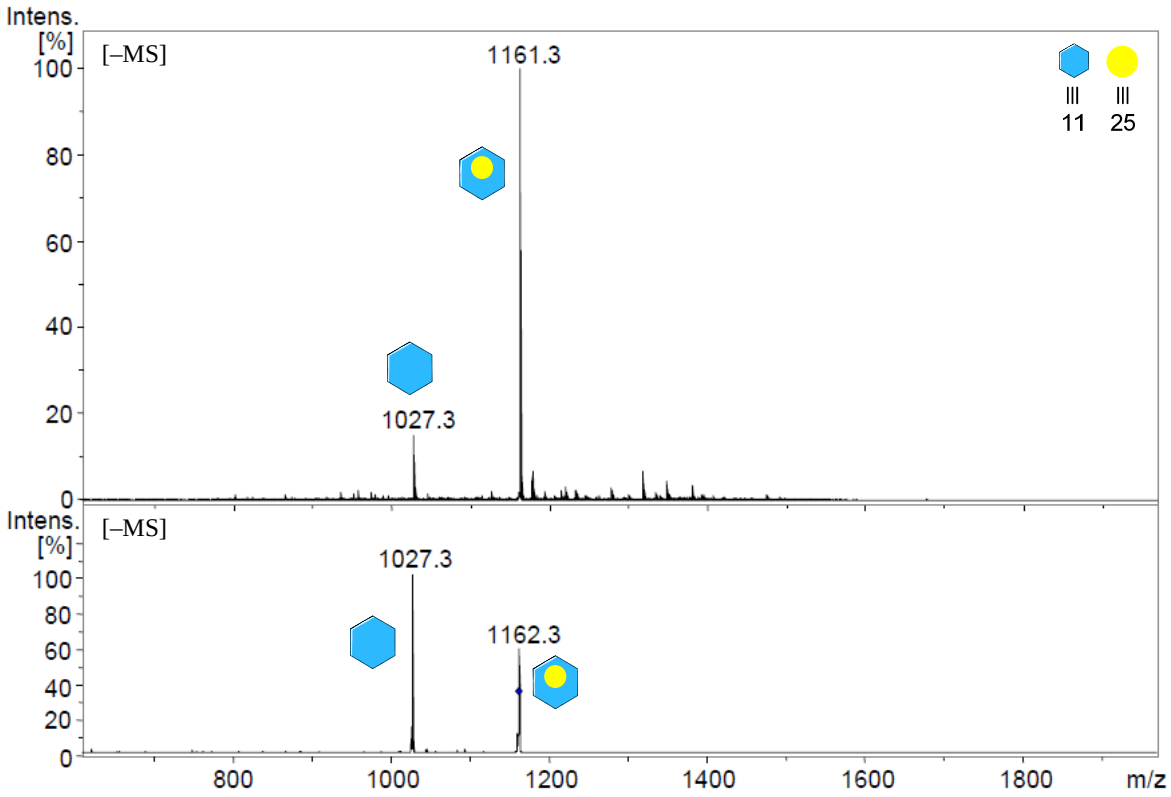

Figure 57. ESI-TOF MS and ESI-MS/MS of Ht/Gt complex **11**/**25** (DMF/CH_3CN/H_2O).

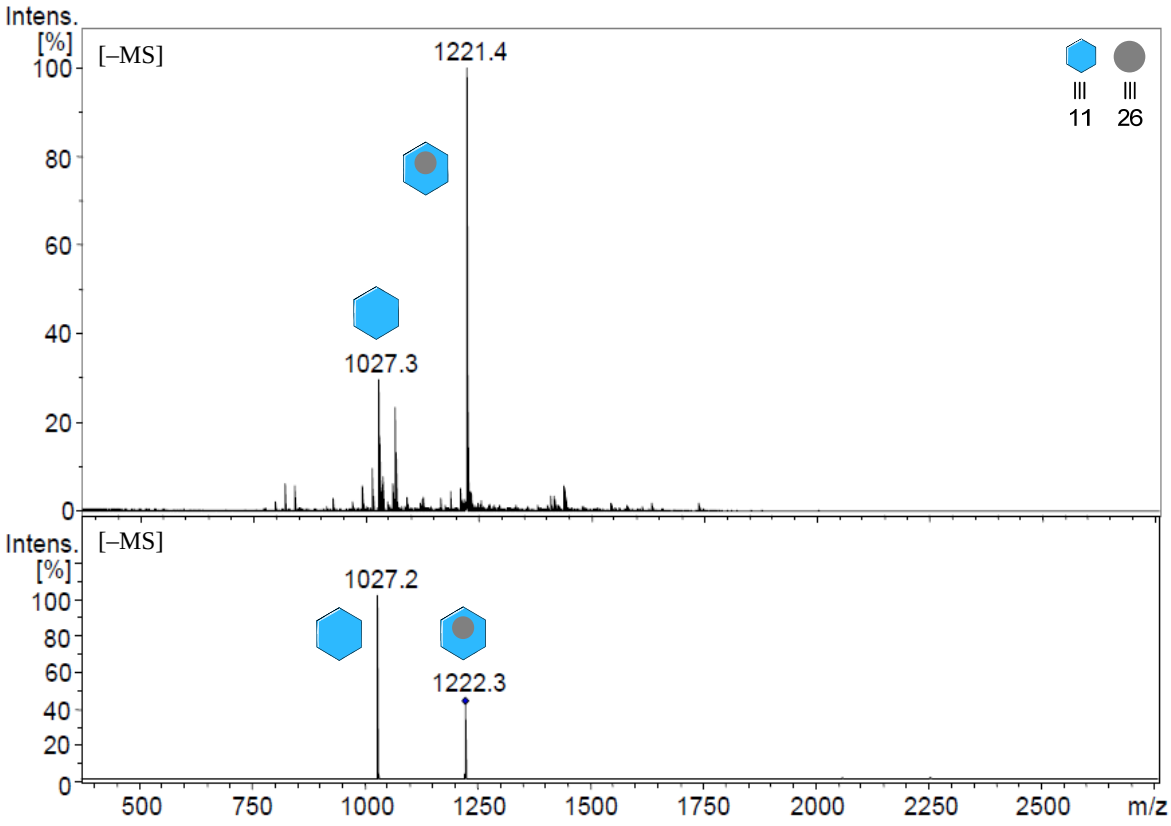

Figure 58. ESI-TOF MS and ESI-MS/MS of Ht/Gt complex **11**/**26** (DMF/CH_3CN/H_2O).

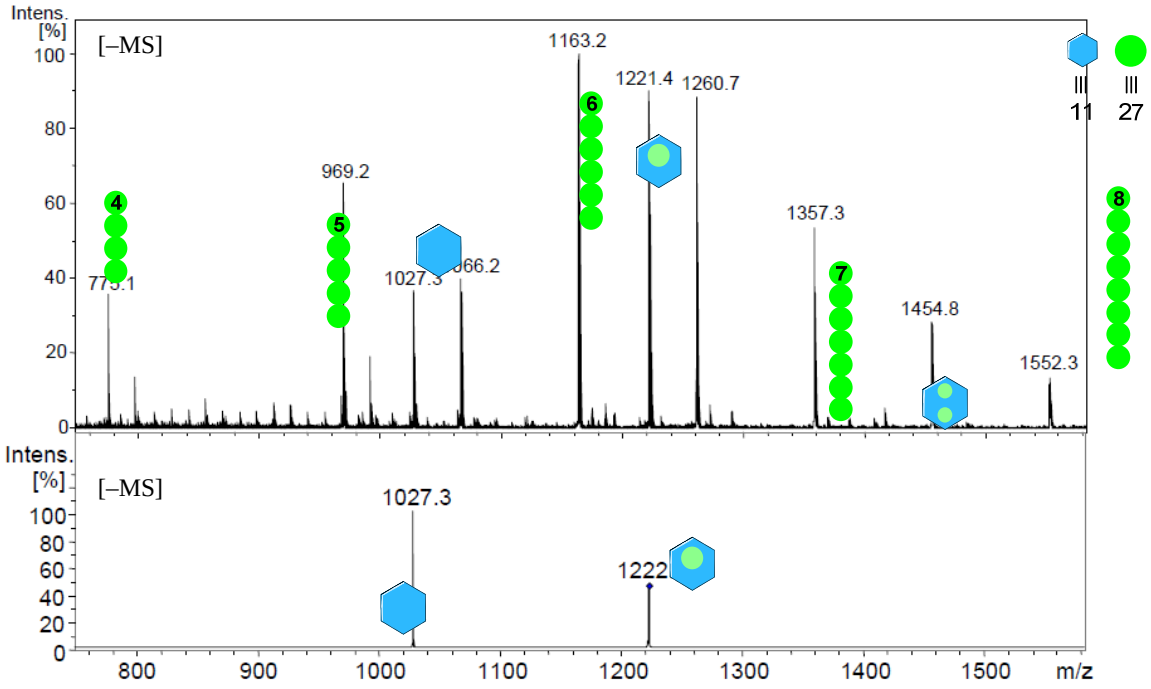

Figure 59. ESI-TOF MS and ESI-MS/MS of Ht/Gt complex **11**/**27** (DMF/CH_3CN/H_2O).

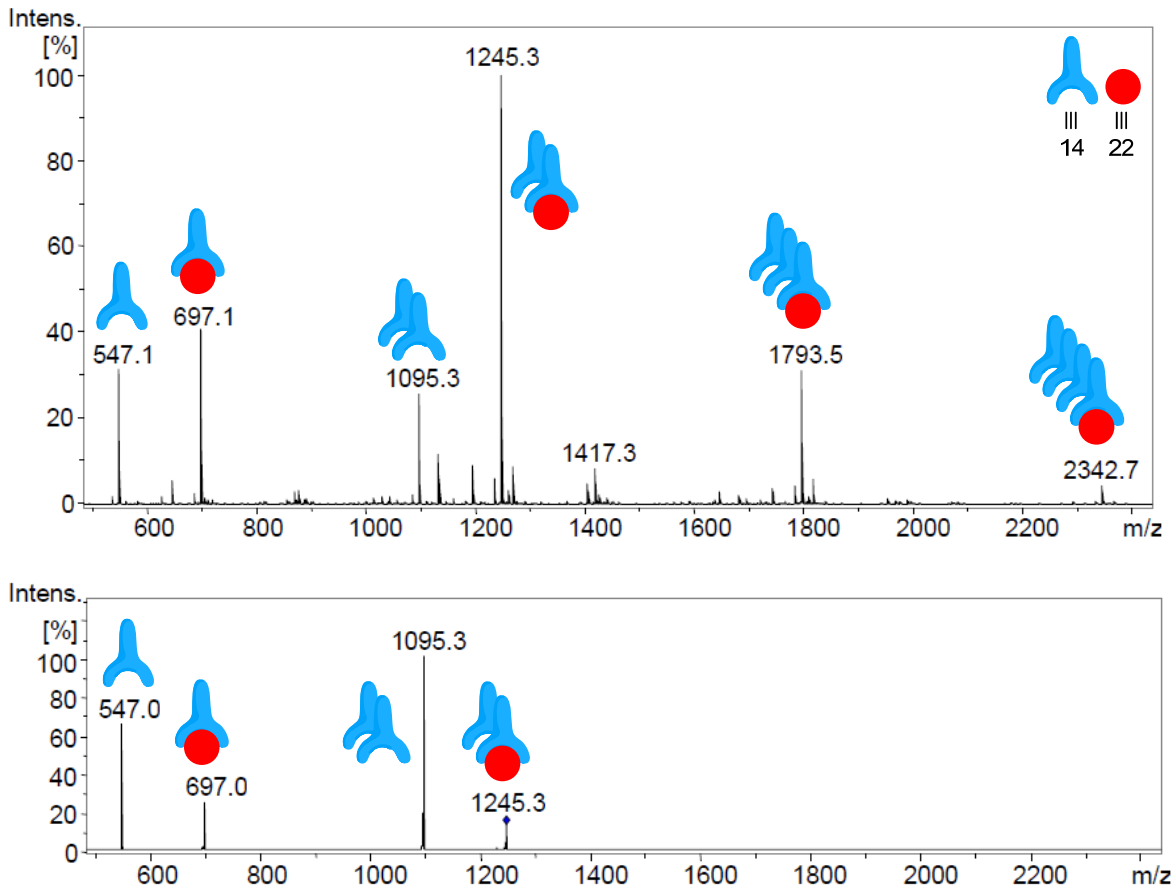

Figure 60. ESI-TOF MS and ESI-MS/MS of Ht/Gt complex **14**/**22**, DMF/CH_3CN/H_2O, negative ion mode, *m*/*z* 1245.3.

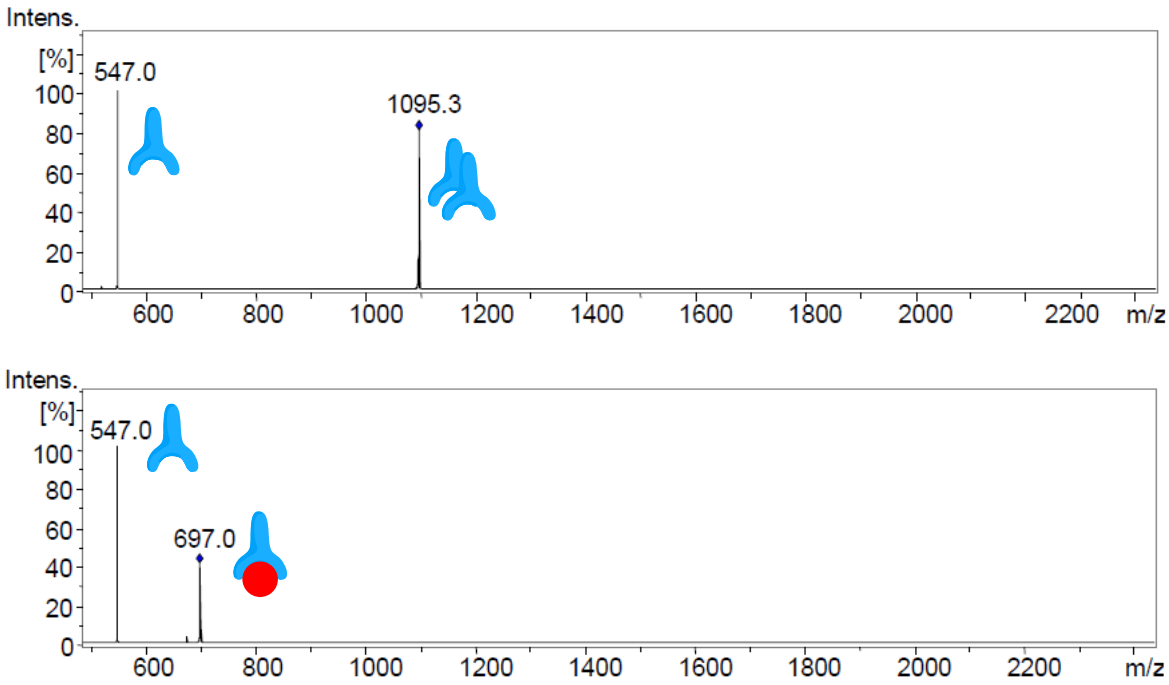

Figure 61. ESI-MS/MS of Ht/Gt complex **14**/**22** (DMF/CH_3CN/H_2O, negative ion mode, *m*/*z* 1095.3 and 697.1).

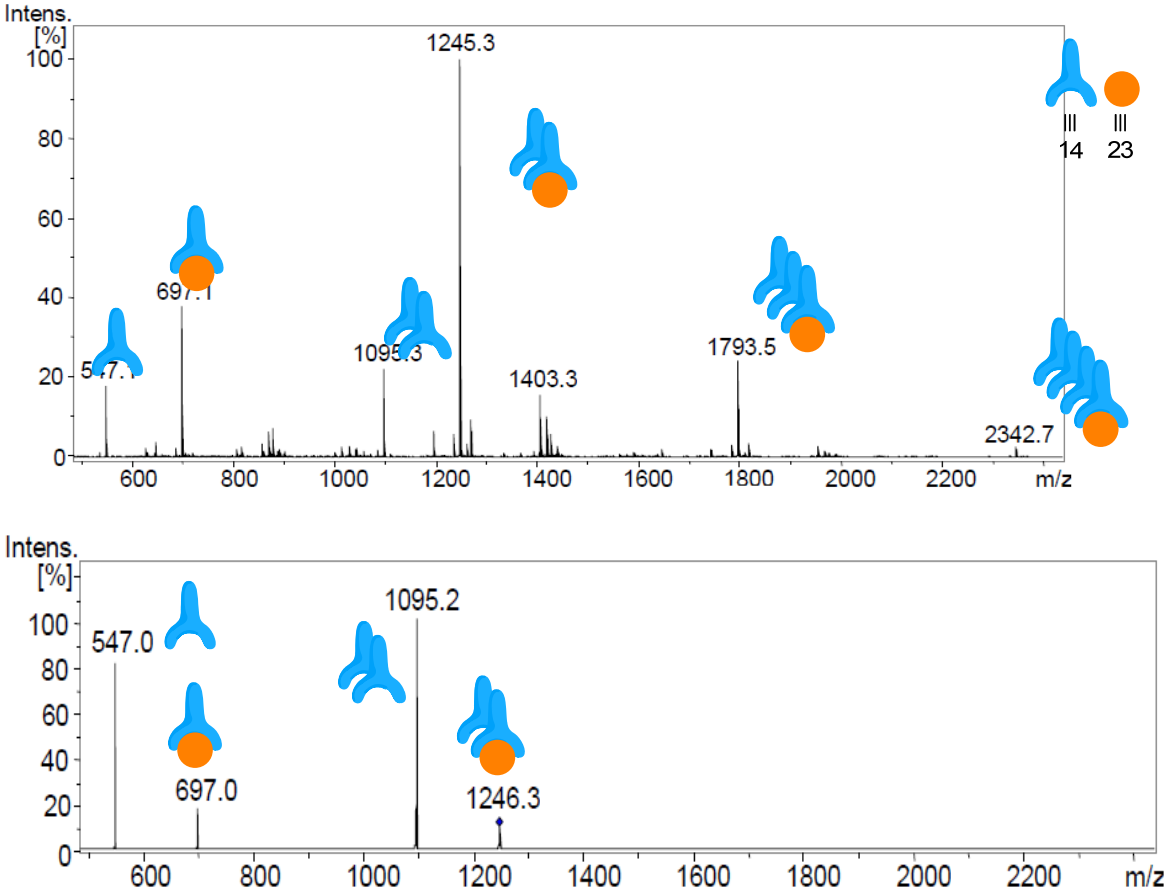

Figure 62. ESI-TOF MS and ESI-MS/MS of Ht/Gt complex **14**/**23**, DMF/CH_3CN/H_2O, negative ion mode, *m*/*z* 1245.3.

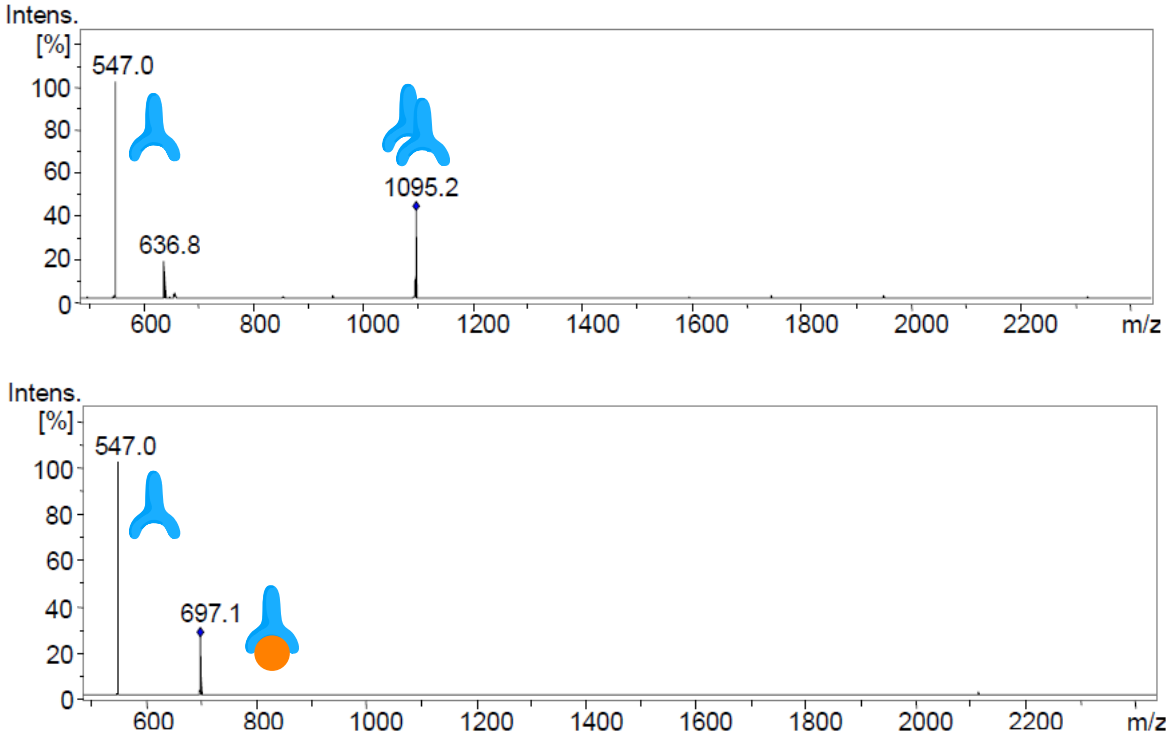

Figure 63. ESI-MS/MS of Ht/Gt complex **14**/**23** (DMF/CH_3CN/H_2O, negative ion mode, *m*/*z* 1095.3 and 697.1).

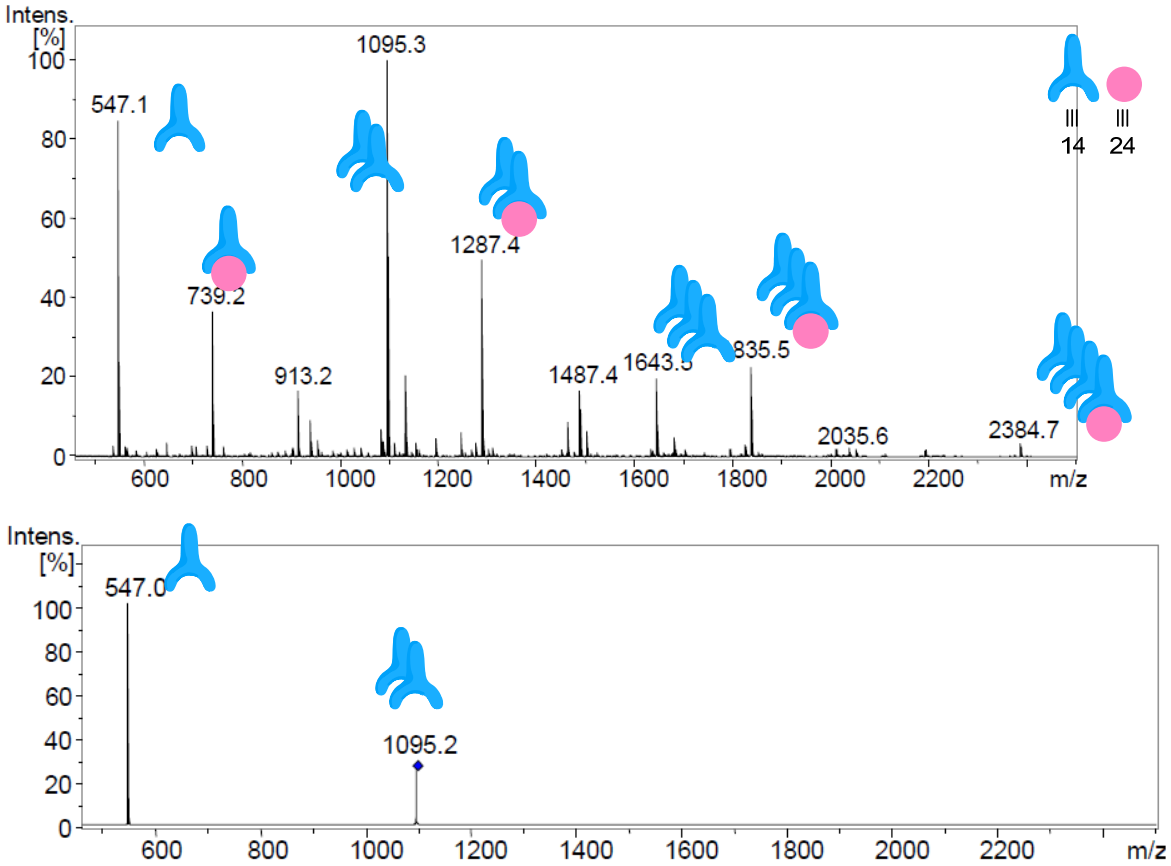

Figure 64. ESI-TOF MS and ESI-MS/MS of Ht/Gt complex **14**/**24**, DMF/CH_3CN/H_2O, negative ion mode, *m*/*z* 1095.3.

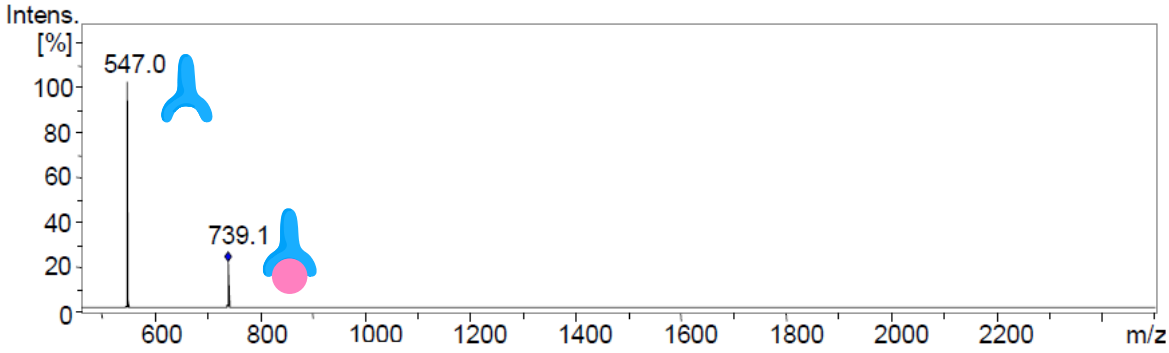

Figure 65. ESI-MS/MS of Ht/Gt complex **14**/**24** (DMF/CH_3CN/H_2O, negative ion mode, *m*/*z* 739.2).

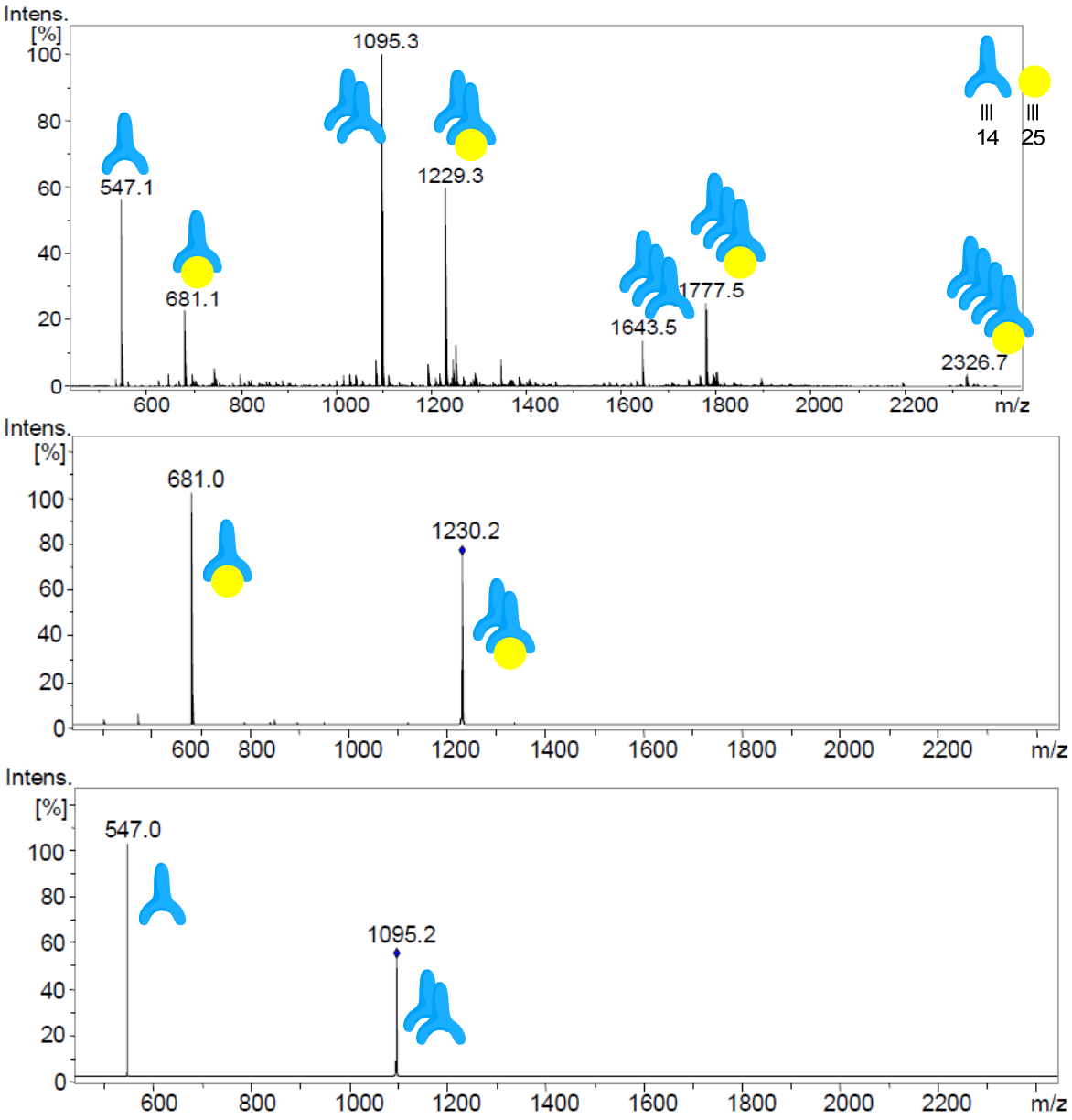

Figure 66. ESI-TOF MS and ESI-MS/MS of Ht/Gt complex **14**/**25** (DMF/CH_3CN/H_2O, negative ion mode, *m*/*z* 1229.3 and 1095.3).

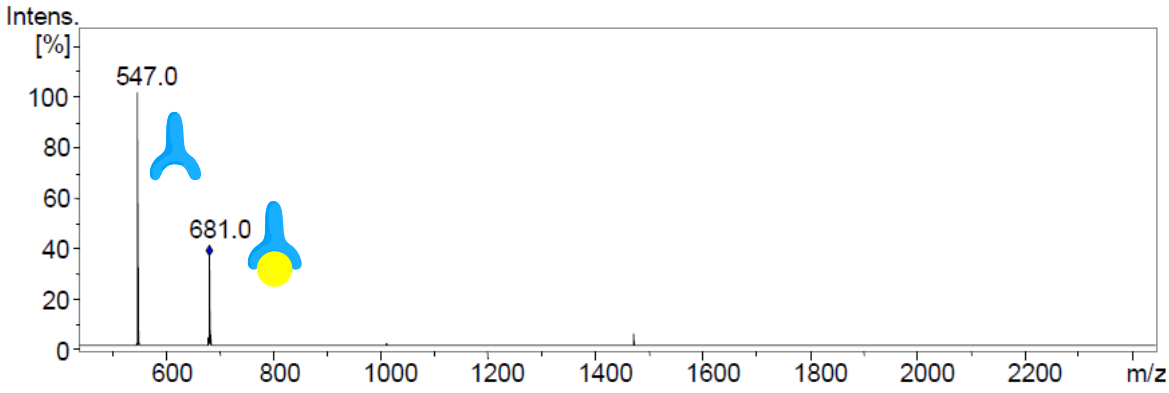

Figure 67. ESI-MS/MS of Ht/Gt complex **14**/**25** (DMF/CH_3CN/H_2O, negative ion mode, *m*/*z* 681.1).

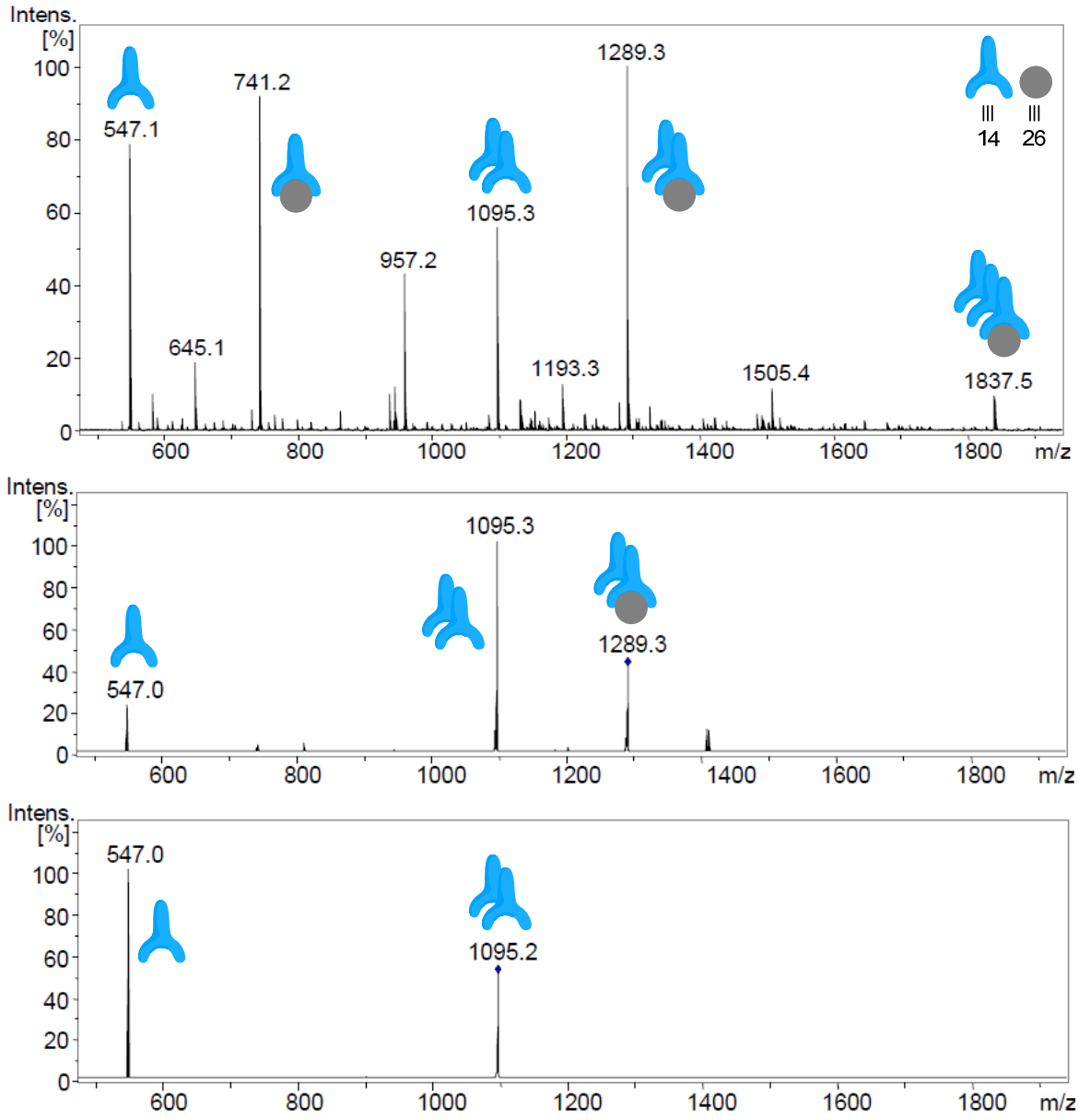

Figure 68. ESI-TOF MS and ESI-MS/MS of Ht/Gt complex **14**/**26** (DMF/CH_3CN/H_2O, negative mode, *m*/*z* 1289.3 and 1095.3).

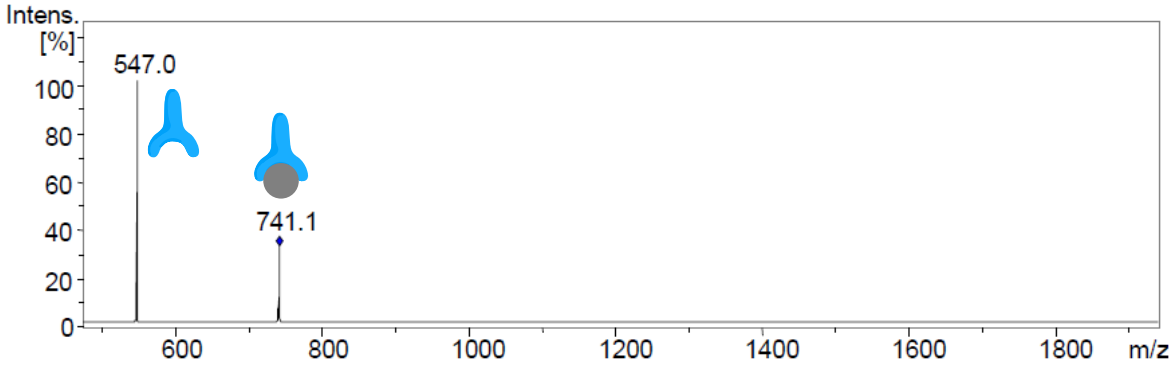

Figure 69. ESI-MS/MS of Ht/Gt complex **14**/**26** (DMF/CH_3CN/H_2O, negative ion mode, *m*/*z* 741.2).

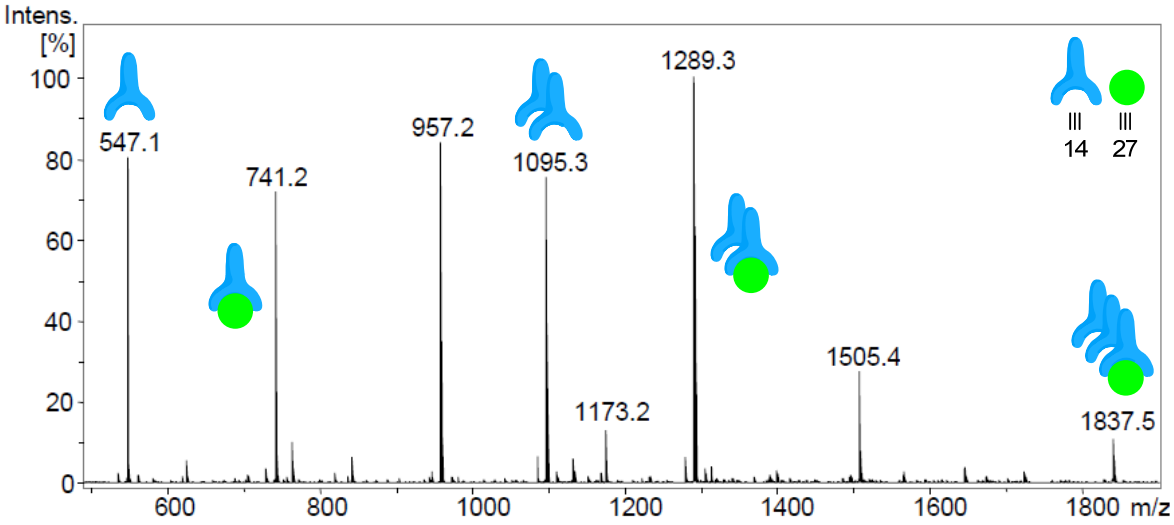

Figure 70. ESI-TOF MS and ESI-MS/MS of Ht/Gt complex **14**/**27** (DMF/CH_3CN/H_2O, negative ion mode).

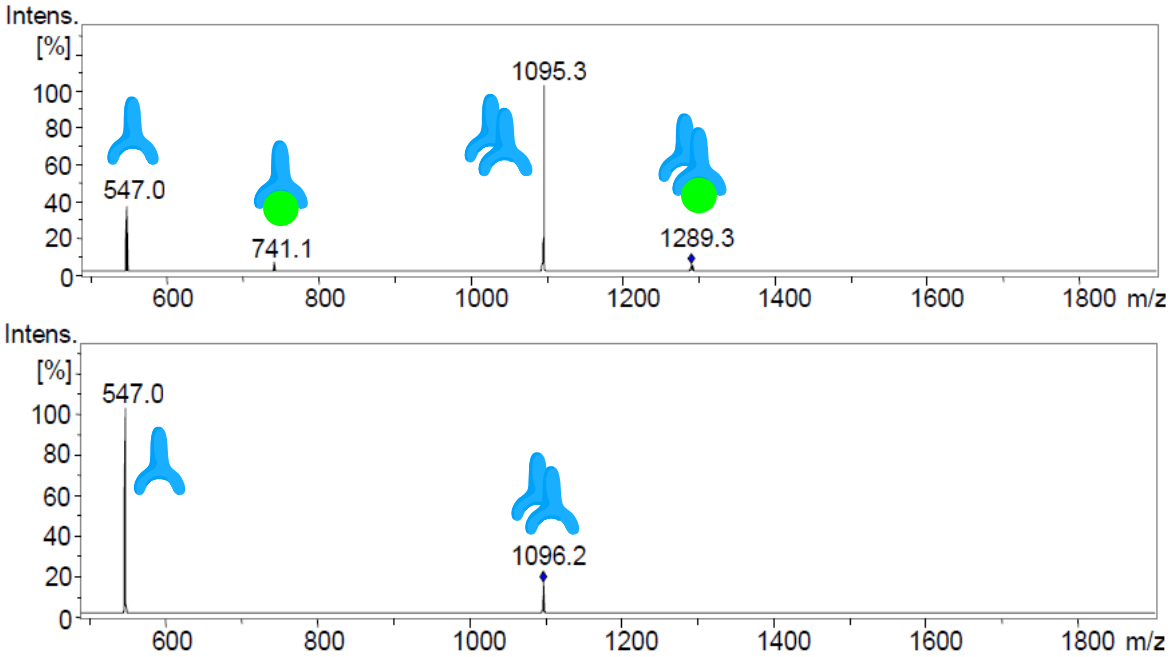

Figure 71. ESI-MS/MS of Ht/Gt complex **14**/**27** (DMF/CH_3CN/H_2O, negative ion mode, *m*/*z* 1289.3 and 1095.3).

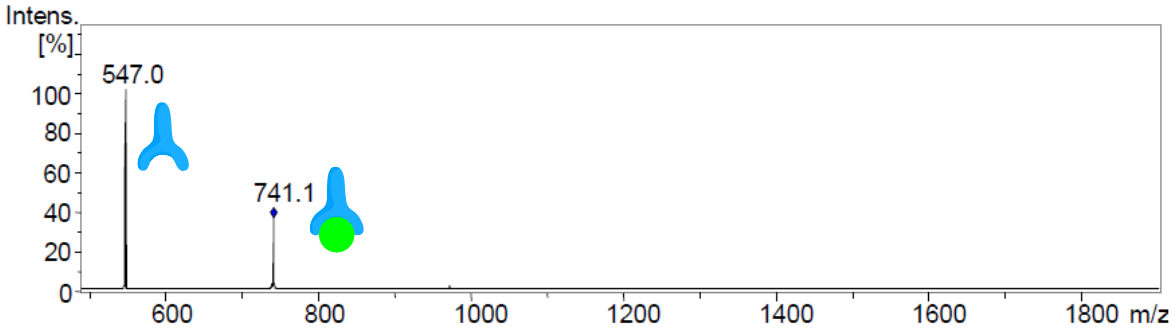

Figure 72. ESI-MS/MS of Ht/Gt complex **14**/**27** (DMF/CH_3CN/H_2O, negative ion mode, *m*/*z* 741.2).

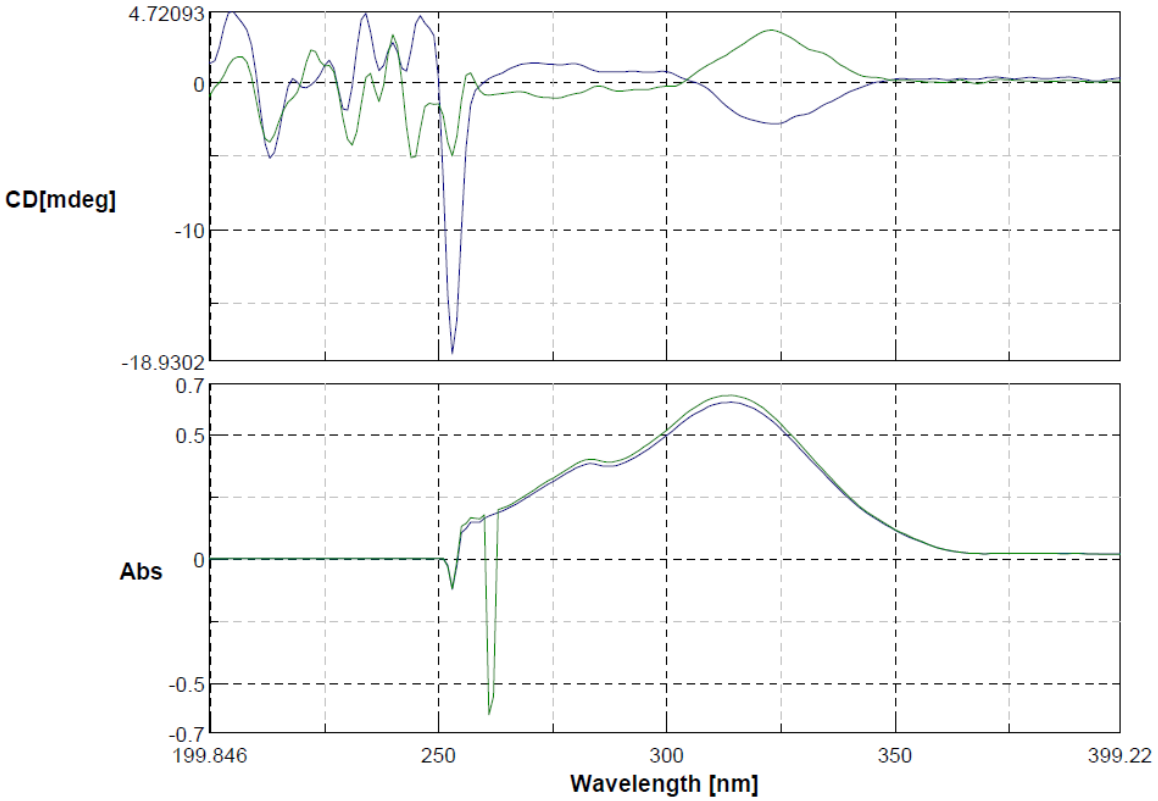

Figure 73. CD spectra of macrocycles (**9**, blue) and (**12**, green), DMSO.

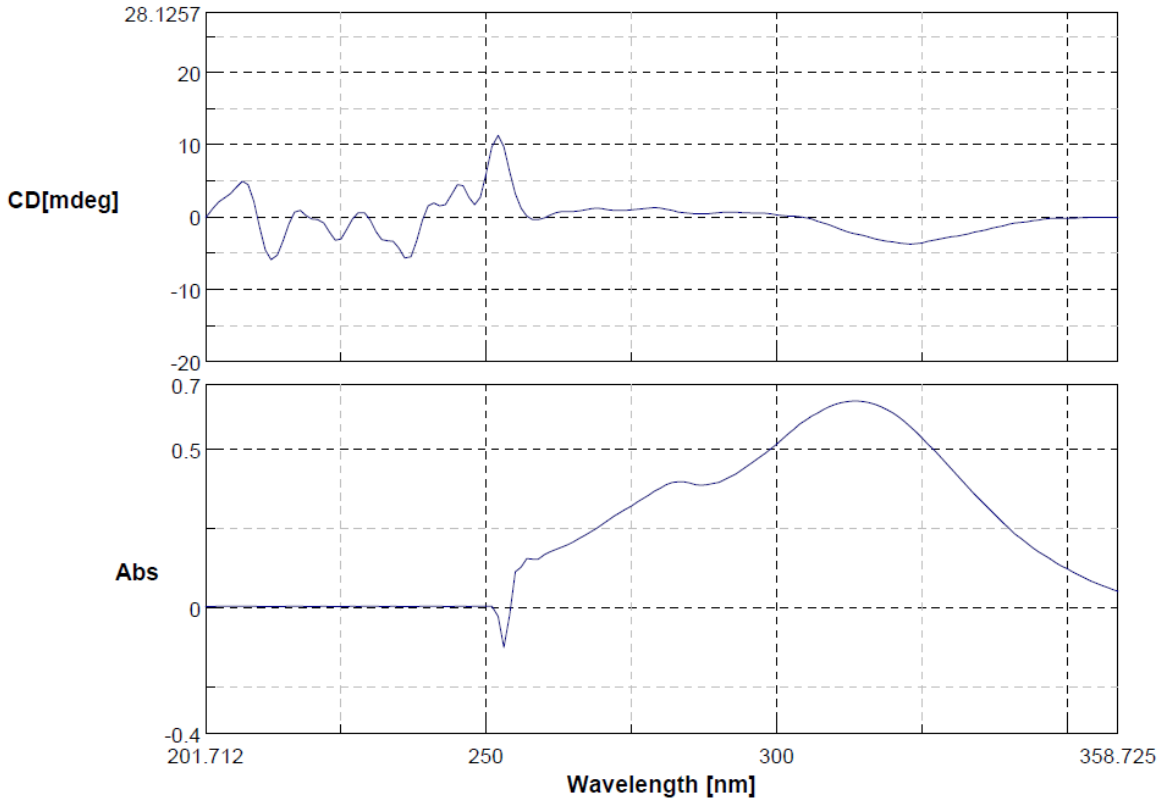

Figure 74. CD spectrum of macrocycles (**10**), DMSO.

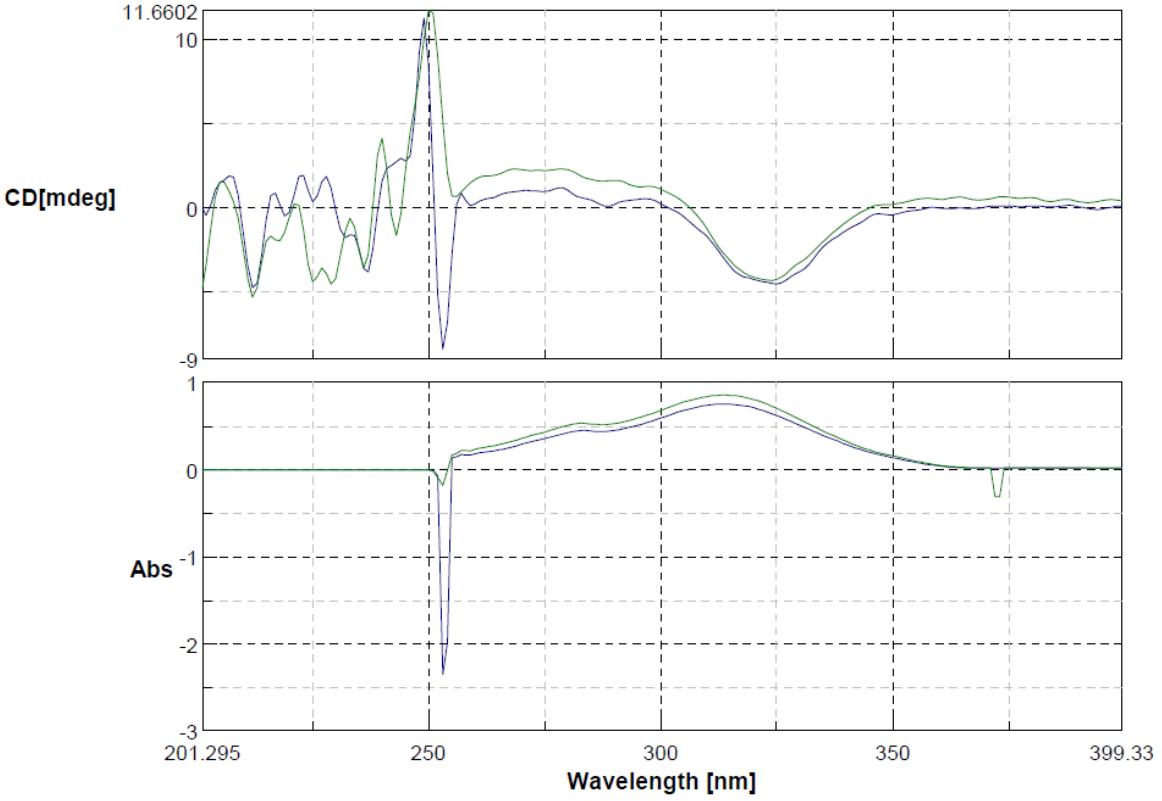

Figure 75. CD spectra of macrocycles (**11**, blue) and (**13**, green), DMSO.

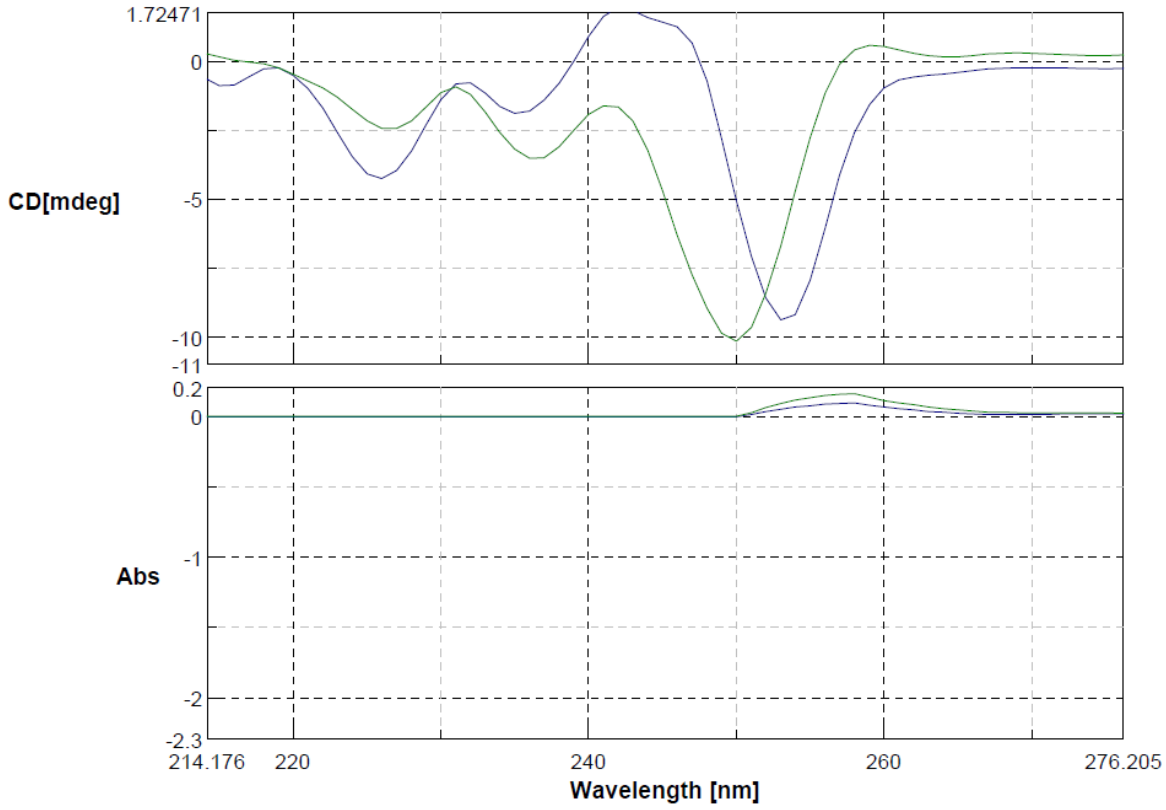

Figure 76. CD spectra of compounds (**14**, blue) and (**19**, green), DMSO.

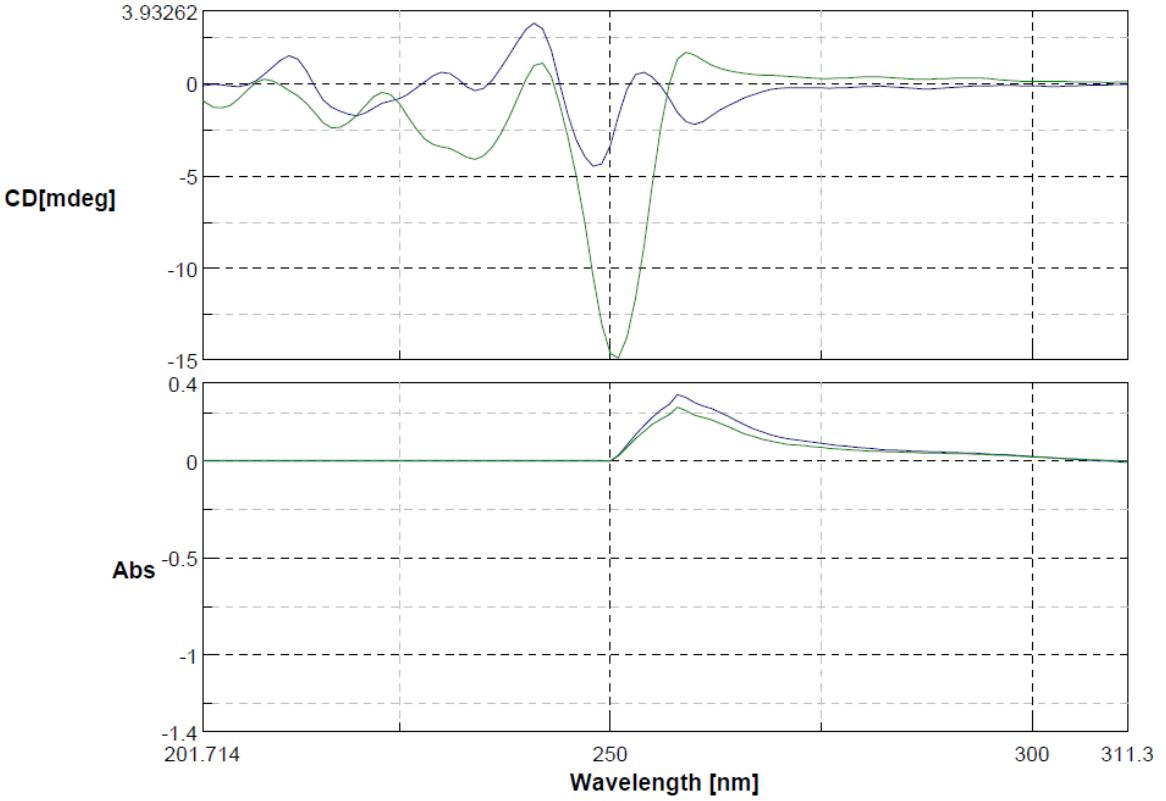

Figure 77. CD spectra of compounds (**15**, blue) and (**20**, green), DMSO.

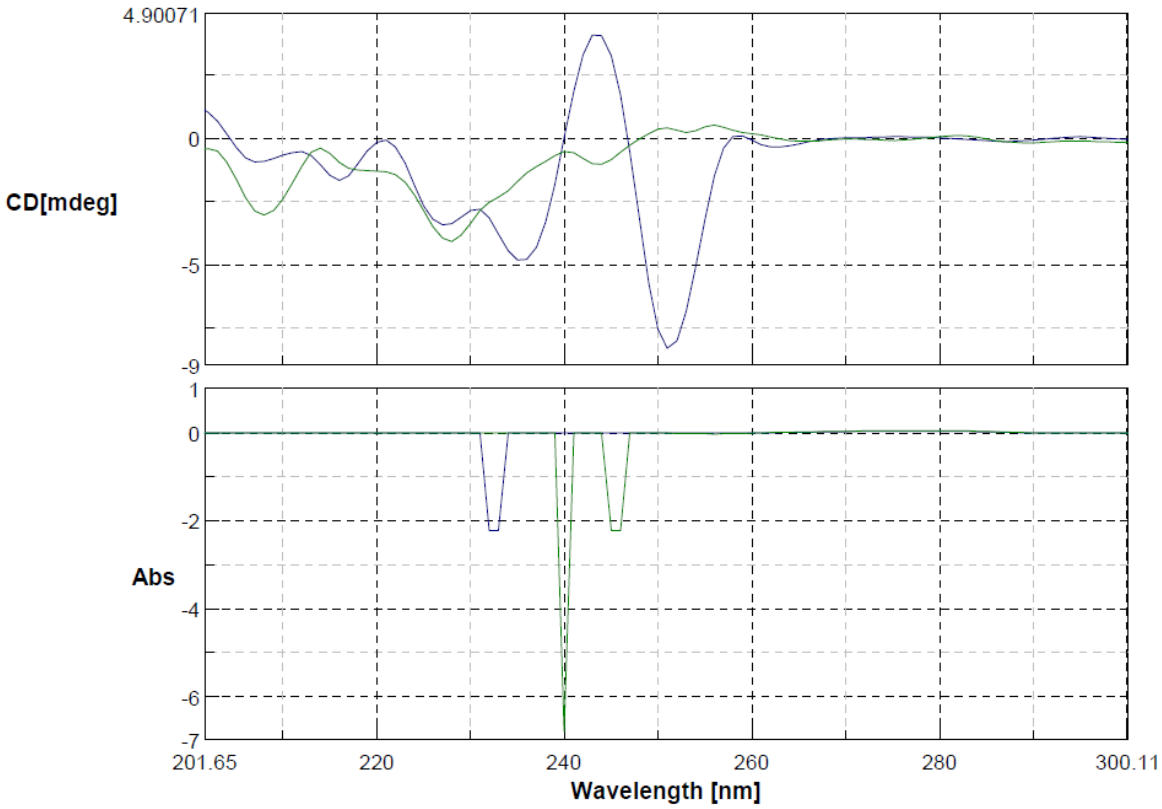

Figure 78. CD spectra of compounds (**16**, blue) and (**21**, green), DMSO.

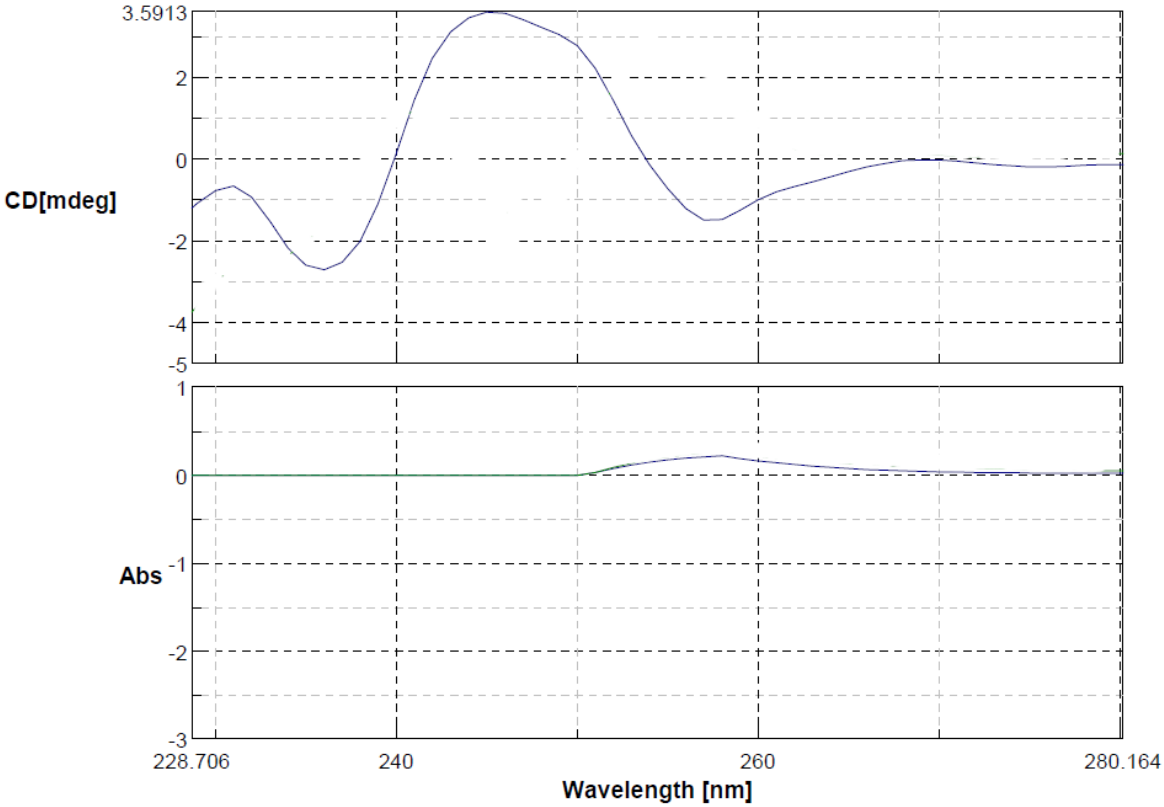

Figure 79. CD spectrum of compound (**17**), DMSO.

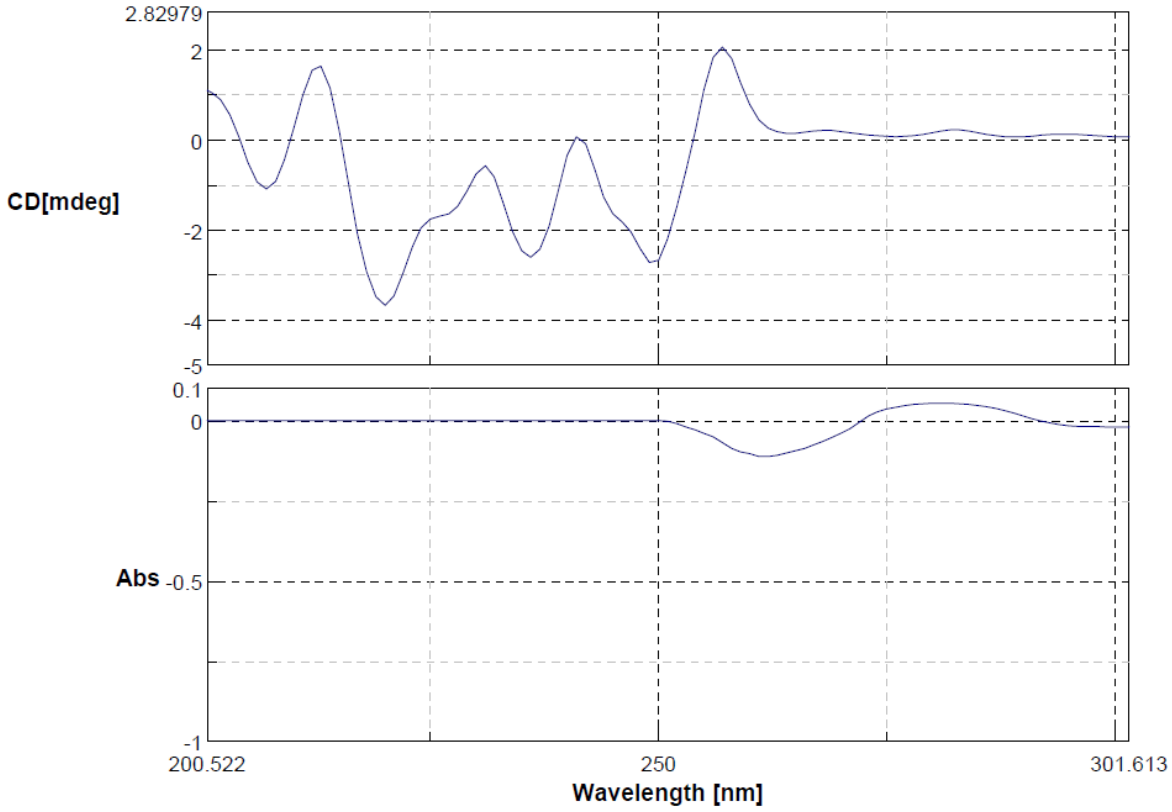

Figure 80. CD spectrum of compound (**18**), DMSO.

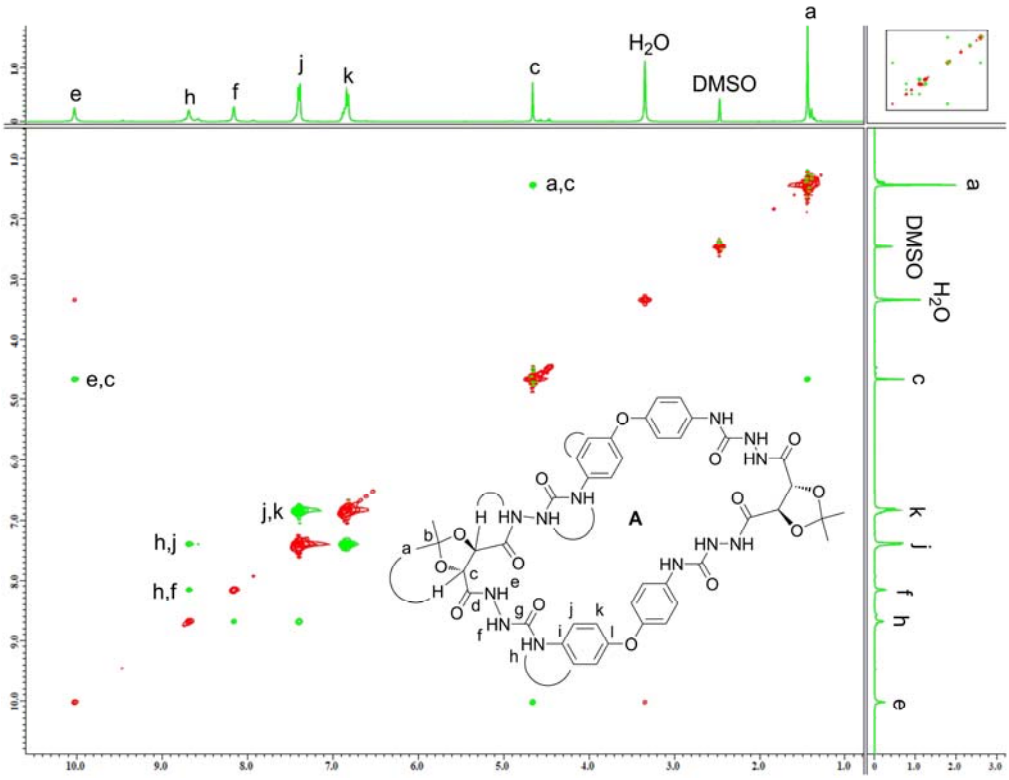

Figure 81. 2D ROESY NMR spectrum of macrocycle (**A**) showing *syn*/*anti* orientation of the N*H* moieties, (DMSO-d_6).

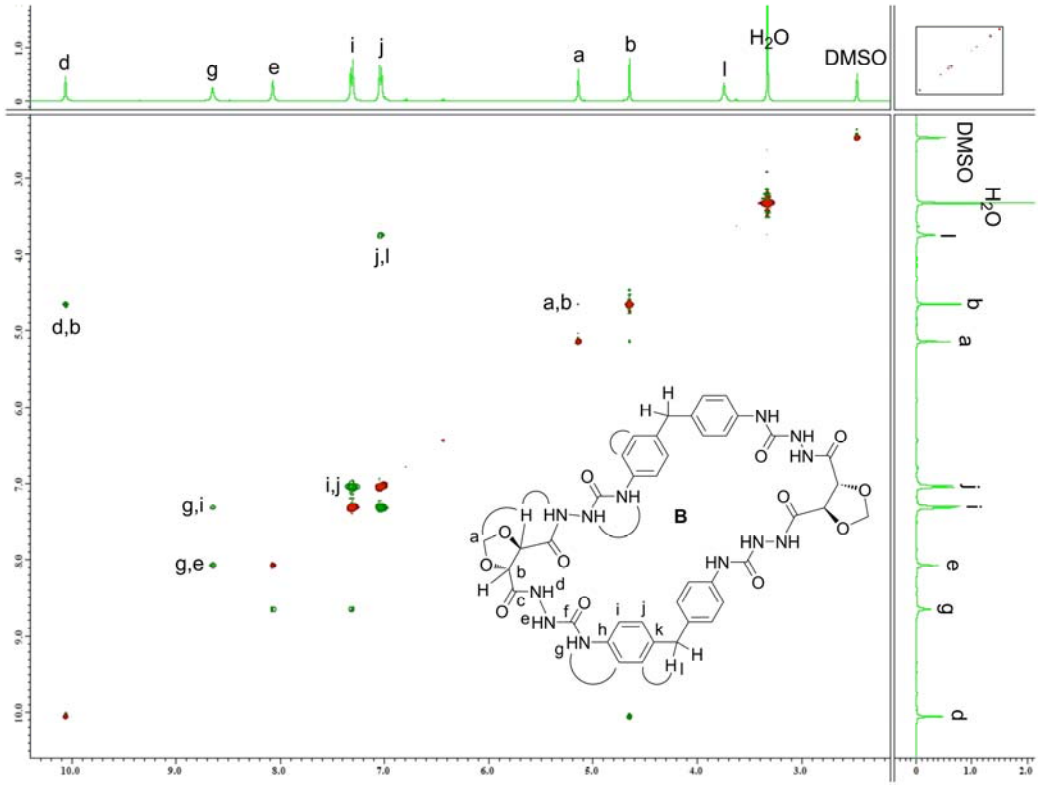

Figure 82. 2D ROESY NMR spectrum of macrocycle (**B**) showing *syn*/*anti* orientation of the N*H* moieties, (DMSO-d_6).

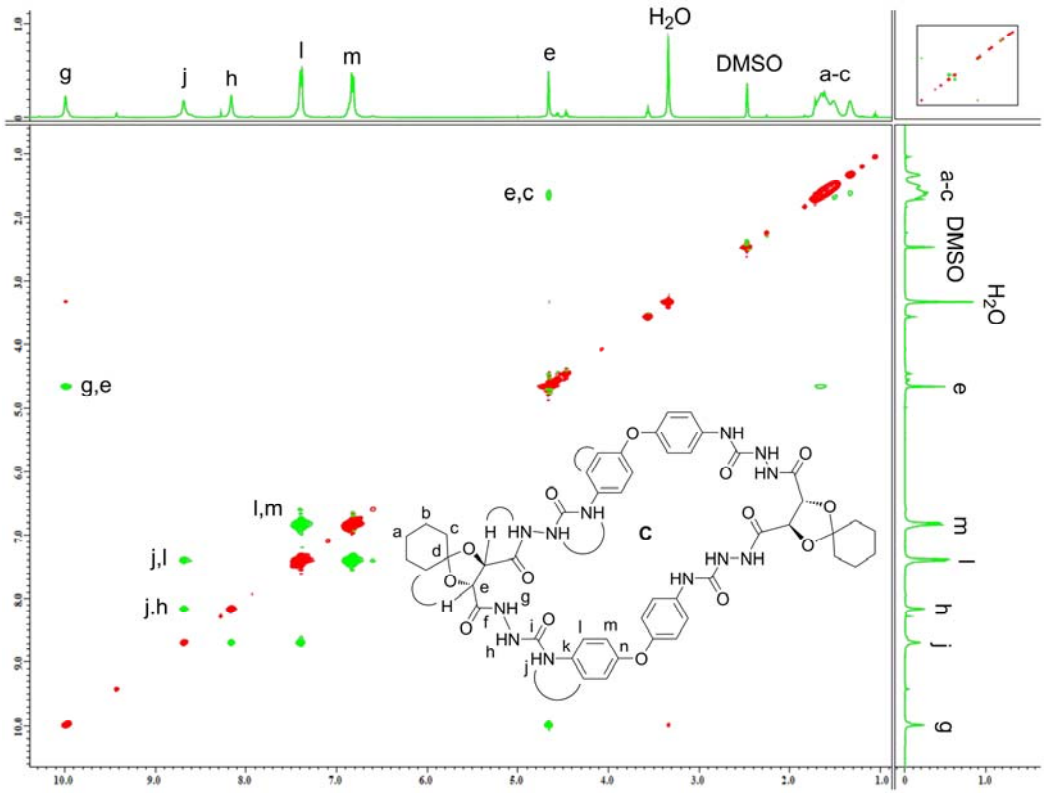

Figure 83. 2D ROESY NMR spectrum of macrocycle (**C**) showing *syn*/*anti* orientation of the N*H* moieties, (DMSO-d_6).

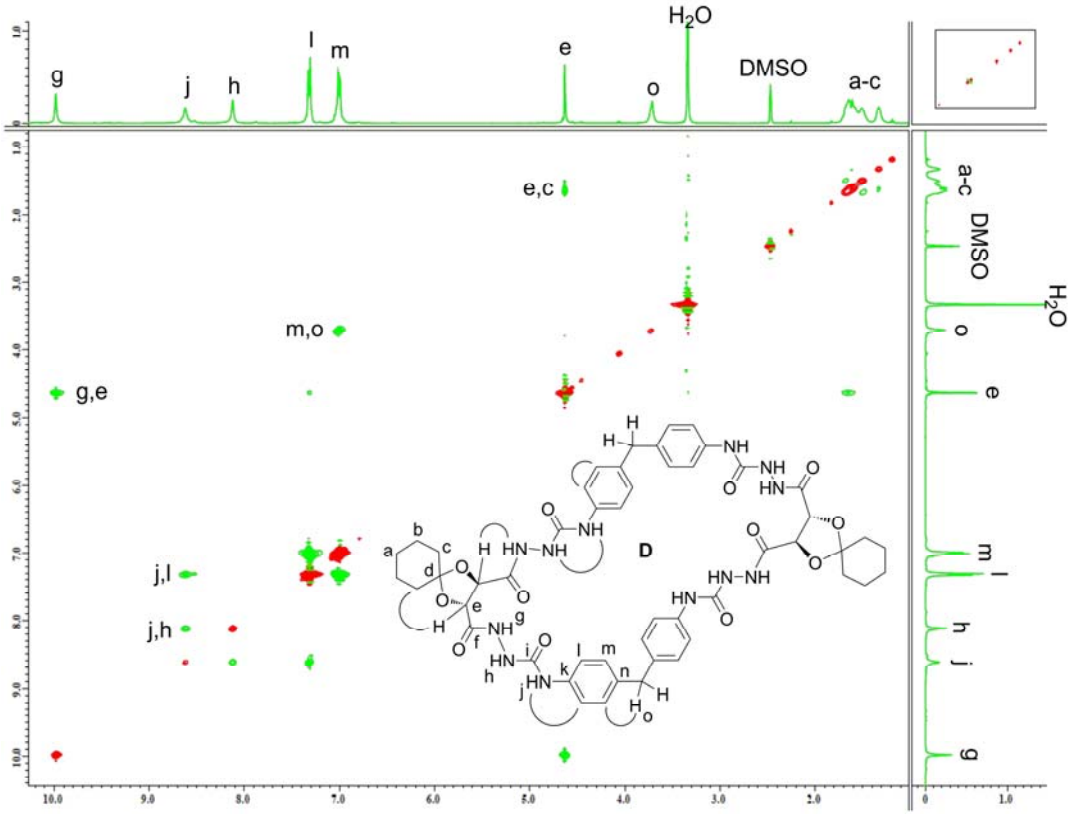

Figure 84. 2D ROESY NMR spectrum of macrocycle (**D**) showing *syn*/*anti* orientation of the N*H* moieties, (DMSO-d_6).

